

# Measurement report: Long-term measurements of ozone concentrations in semi-natural African ecosystems

5 Hagninou Elagnon Venance Donnou<sup>1</sup>, Aristide Barthélémy Akpo<sup>1</sup>, Money Ossohou<sup>2,3</sup>, Claire Delon<sup>4</sup>,  
Véronique Yoboué<sup>3</sup>, Dungall Laouali<sup>5</sup>, Marie Ouafou-Leumbe<sup>6</sup>, Pieter Gideon Van Zyl<sup>7</sup>, Ousmane  
Ndiaye<sup>8</sup>, Eric Gardrat<sup>4</sup>, Maria Dias-Alves<sup>4</sup>, and Corinne Galy-Lacaux<sup>4</sup>

<sup>1</sup>Laboratoire de Physique du Rayonnement, Faculté des Sciences et Techniques,  
Université d'Abomey-Calavi, Cotonou, 01 B.P. 526, Benin

10 <sup>2</sup>Department of Physics, University of Man, Man, Côte d'Ivoire

<sup>3</sup>Laboratoire des Sciences de la Matière, de l'Environnement et de l'Energie Solaire,  
Université Félix Houphouët-Boigny, Abidjan, Côte d'Ivoire

<sup>4</sup>Laboratoire d'Aérologie, Université Toulouse III Paul Sabatier, CNRS, Toulouse, 31400, France

15 <sup>5</sup>Laboratoire de Climat-Environnement et Matériaux-Rayonnement, Université Abdou Moumouni,  
Faculté des Sciences et Techniques, Niamey, BP 10662, Niger.

<sup>6</sup>Department of Earth Sciences, Faculty of Sciences, University of Douala, Douala, P.O. Box 2701, Cameroun

<sup>7</sup>Atmospheric Chemistry Research Group, Chemical Resource Beneficiation, North-West University,  
Potchefstroom, 2520, South Africa

<sup>8</sup>Centre de Recherches Zootechniques de Dahra, Institut Sénégalais de Recherches Agricoles, Dahra, Senegal

20

Correspondence to: H. E. Venance Donnou (donhelv@yahoo.fr) and Corinne Galy-Lacaux (corinne.galy-lacaux@aero.obs-mip.fr)

**Abstract.** In the framework of the International Network to study Deposition and Atmospheric chemistry in Africa (INDAAF) program, we present the seasonal variability of atmospheric ozone concentrations at the regional scale. The contributions correlations of local atmospheric chemistry and meteorological parameters to ozone photochemistry are investigated, as are long-term trends in ozone concentrations. Fourteen measurement sites were identified for this study, representative of the main African ecosystems: dry savannas (Banizoumbou, Niger; Katibougou and Agoufou, Mali; Bambey and Dahra, Senegal), wet savannas (Lamto, Côte d'Ivoire; Djougou, Benin), forests (Zoétélé, Cameroon; Bomassa, Republic of Congo) and semi-agricultural/arid savanna (Mbita, Kenya; Louis Trichardt, Amersfoort, Skukuza and Cape Point, South Africa). As part of several study programmes, validation and intercomparison tests of passive samplers at remote sites have been carried out to ensure controlled-quality measurements and to provide reliable long-term gases concentrations. Over the period 1995-2020, monthly ozone concentrations were measured at these sites using passive samplers. Monthly averages of surface ozone range from  $4.7 \pm 1.4$  ppb (Bomassa) to  $31.0 \pm 10.5$  ppb (Louis Trichardt). Ozone concentrations levels in the wet season (in dry savanna) are higher and in the same order of magnitude comparable to concentrations in the dry season (in wet savanna ~~and forest~~). In East Africa, ozone levels show no marked seasonality. We established a positive gradient of mean annual O<sub>3</sub> concentrations from West Central Africa to South Africa with higher levels in Southern Africa. In the dry savanna Sahel, under the influence of temperature, ozone concentrations formation is are closely linked to Bbiogenic Volatile Organic Carbon (BVOC) emissions ( $0.51 < r < 0.95$ ). It is also sensitive to nitrogen monoxide (NO) emissions in the presence of high precipitation and humidity. Biogenic VOC (BVOC) emissions, anthropogenic NO<sub>x</sub>, temperature and radiation exhibit a good correlation ( $0.49 < r < 0.92$ ) with are the dominant contributors to O<sub>3</sub> formation in wet savannas and forests. At the southern African sites, the photochemistry of O<sub>3</sub> is influenced by the most important parameters influencing surface ozone concentrations are humidity,

rainfall, temperature, ~~NO<sub>x</sub>VOC~~ emissions (anthropogenic and biogenic) and ~~VOCNO<sub>x</sub>~~. At the annual scale, from 2000 to 2020, Katibougou and Banizoumbou sites (dry savanna) experienced a ~~significant~~ decrease in ozone concentrations respectively around ~~-0.2,4 ppb decade<sup>-1</sup> (with a very high certainty)(-2.3 % yr<sup>-1</sup>)~~ and ~~-0.8 -0.15 ppb decade<sup>-1</sup> (with a medium certainty)(-1.9 % yr<sup>-1</sup>) at 95% confidence interval~~. Seasonal Kendall statistical tests revealed with a high certainty decreasing trends of ~~-0.0,7 ppb decade<sup>-1</sup>~~ in Banizoumbou and ~~-0.2,4 ppb decade<sup>-1</sup>~~ in Katibougou. These decreasing trends are consistent with those observed for nitrogen dioxide (NO<sub>2</sub>) and biogenic VOCs. ~~An significant~~ increasing trend is observed in Zoétélé (2001-2020), with the Sen slope estimated at ~~0.74 ppb yr<sup>-1</sup>~~ and at Skukuza (2000-2015; Sen slope = ~~0.3,4 ppb decade<sup>-1</sup>~~). The increasing trends are consistent with the increase in biogenic emissions at Zoétélé and NO<sub>2</sub> levels at Skukuza. Very few surface O<sub>3</sub> measurements exist in Africa, and long-term results presented in this study are the most extensive for the studied ecosystems.

## 1 Introduction

Ozone (O<sub>3</sub>) is a greenhouse gas, difficult to observe and quantify on a global scale due to its acute spatial variability resulting from its variable photochemical lifetime (between 20 and 25 days) (Cooper et al., 2020; Young et al., 2013). It has phytotoxic effects altering key plant physiological processes that can significantly reduce the productivity of agricultural crops and ecosystems (Dufour et al., 2021; Lelieveld et al., 2015; Mills et al., 2018; Monks et al., 2015). At the local scale, its presence in high concentrations in the lower troposphere is harmful to human health, notably through irritation of the upper airways (Camredon and Aumont, 2007; Schultz et al., 2017). Ozone O<sub>3</sub> is a secondary air pollutant, meaning that it is not emitted directly but formed in the troposphere as a result of oxidative chemical reactions of precursor gases such as nitrogen oxides (NO<sub>x</sub>), carbon monoxide (CO) and volatile organic compounds (VOCs) (Lu et al., 2019; Schultz et al., 2017). It is chemically lost by photodissociation or by surface deposition and uptake by plant stomata (Silva and Heald, 2018), or by heterogeneous reactions involving aerosols. Stomatal uptake of O<sub>3</sub> and subsequent damage to plants can lead to changes in biosphere-climate interactions (Sadiq et al., 2017). Mitigating its negative impacts on health requires reducing both pollutant concentrations and population exposure (Petetin et al., 2022). These changes are compounded by the variation of O<sub>3</sub> precursors, which in recent decades have shifted from high and mid-latitudes to low latitudes, where O<sub>3</sub> production efficiency is greater (Zhang et al., 2016). These variations are particularly significant in tropical regions, where seasonal cycles linked to natural and anthropogenic sources of gas and particle emissions are well marked (Adon et al., 2010). Zhang et al. (2016) indicate that both modeling and observational studies about ozone trends are not uniform regionally or seasonally, i.e. even in the tropics where a number of sites with ozonesonde profiles exhibit no trend (Thompson et al., 2021). A study with sondes over equatorial southeast Asia by Stauffer et al. (2024), shows no definite ozone trend annually but a 6-8% decade<sup>-1</sup> increase limited to 3 months.yr<sup>-1</sup>. Air quality forecasts could therefore be used to warn the population of the potential occurrence of a pollution episode (Petetin et al., 2022). Its long-term importance for atmospheric chemistry has been investigated by several studies on air quality (Monks and Leigh 2009) and atmosphere-biosphere interactions (Fowler et al., 2009; ~~Laban et al., 2018~~). International Global Atmospheric Chemistry Project (IGAC) has produced the Tropospheric Ozone Assessment Report (TOAR) on the global measures for Climate Change, Human Health and Crop/Ecosystem Research (www.igacproject.org/TOAR). This report stated that free tropospheric O<sub>3</sub> has increased during the industrial era and in recent decades (Gaudel et al., 2018; Tarasick et al., 2019). Despite these years of regional and global surface O<sub>3</sub> research and monitoring, many regions of the world such as Africa, South America, the Middle East and India, remain under sampled, leading to incomplete knowledge of the horizontal, vertical and temporal distribution of O<sub>3</sub> (Cooper et al., 2014; Lin et al., 2015; Mills et al., 2018; Oltmans et al., 2013; Sofen et al., 2016). Although Africa is considered as one of the most sensitive continents to air pollution and climate change, it is one of the least studied (Laakso et al., 2012; Swartz et al., 2020a). ~~Indeed, very little work has been done on regional atmospheric chemistry and the dominant atmospheric processes related to surface O<sub>3</sub> formation in Africa. With the exception of a few sites, O<sub>3</sub> variability is not yet sufficiently documented on this continent (Gaudel et al., 2018; Fleming et al., 2018; Mills et al., 2018).~~

From this perspective, long term measurement programs play a vital role in studies of air pollution and the various changes in the chemical composition of the atmosphere. These long-term assessments are crucial for posing the most topical research questions on atmospheric chemistry (Vet et al., 2014), in order to provide the right answers for relevant decision-making at local and global scale. In situ, satellite, O<sub>3</sub>-sonde and aircraft observations ([IAGOS research infrastructure](#)) provide a substantial amount of information on the current distribution of tropospheric O<sub>3</sub>, its variability and trends (Gaudel et al., 2018; Tarasick et al., 2019). They are well suited to improve our understanding of emissions, transport, chemical reactions, deposition processes and the impacts of atmospheric species on human health, vegetation and climate change (Lefohn et al., 2018). Numerous projects and programs [long-term](#) have therefore sprung up in several places around the world, for decades.

95 In Africa, the International Network to Study Deposition and Atmospheric Composition in AFrica (INDAAF; <https://indaaf.obs-mip.fr>), operational since 1995, is dedicated to study the evolution of the chemical composition of the atmosphere and deposition fluxes. INDAAF is a national observatory (Service National d'Observation, SNO) of the Institut National des Sciences de l'Univers (INSU) of the Centre National de Recherche Scientifique (CNRS) and of the Institut de Recherche pour le Developpement (IRD), and a labelled component of the European research infrastructure Aerosols, Clouds and Trace gases Research Infrastructure (ACTRIS). The INDAAF long term monitoring network is also labelled by Global Atmosphere Watch (GAW) program of the World Meteorological Organization (WMO) as a contributing network and is a component of the DEBITS (Deposition of Biogeochemically Important Trace Species) activity of IGAC (International Global Atmospheric Chemistry).

100 Previous ~~existing~~ studies have considered surface ozone levels in Africa. [Indeed, many large African field international campaigns \(EXPRESSO, SAFARI/TRACE-A, ORACLES, SAFARI-2000, MOZAIIC, AMMA\) have been performed over the past 30 years on African air quality and environment. The links to dynamical factors affecting ozone seasonality \(Diab et al., 2003, 2004\), the interannual variability in ozone related to ENSO and NO<sub>x</sub> \(Balashov et al., 2014\) over the South African Highveld, regional convective influence, and the ENSO transition \(Thompson et al., 2003b\) and widespread impact of biomass burning and domestic fires in southern Africa occurring several months each year are well established \(Thompson et al., 2003b\). The mean ozone profile in the lower troposphere over the coast of Gulf of Guinea \(December-February\) and over Congo \(June-August\) in the burning season is characterized by systematically high ozone \(Sauvage et al., 2005\). The combination of high NO<sub>x</sub> emissions from soil north of 13°N and northward advection by the monsoon flux of VOC-enriched air masses contributes to the ozone maximum simulated at higher latitudes \(Saunois et al., 2009\). Adon et al. \(2010\) characterized the ozone concentration levels \(together with several atmospheric pollutants\), from 2002 to 2007, at seven remote sites in West and Central Africa, while Martins et al. \(2007\) investigated O<sub>3</sub> concentrations in Southern Africa over a period of 9 to 11 years \(1995-2005\). The high ozone values recorded in southern Africa by Martins et al. \(2007\) are linked to the anthropogenic effect on the chemical species recorded in the atmosphere of the region. Biogenic emissions are the main contributor to ozone production, through the emission of NO<sub>x</sub> as precursors during the wet season in the dry savanna region \(Adon et al., 2010\). This result is consistent with the observations made by Saunois et al. \(2009\) during the AMMA programme. In the dry season \(wet savanna\), biomass burning is the dominant factor as mentioned by Sauvage et al. \(2005\). As for the tropical forests of Central Africa, they appear to be a major O<sub>3</sub> sink. In South Africa, Swartz et al. \(2020a\) assessed long-term seasonal and interannual trends of O<sub>3</sub> based on a 21-years \(1995-2015\) dataset at the Cape Point station. This work was continued at 3 historic IDAF-DEBITS sites \(Amersfoort, Louis Trichardt, Skukuza, Swartz et al., 2020b\). No trends of O<sub>3</sub> were observed at these four sites and the concentrations remained relatively constant over the sampling period. The El Niño–Southern Oscillation \(ENSO\) made a significant contribution to modelled O<sub>3</sub> levels at Amersfoort, Louis Trichardt and Skukuza confirming thus the studies of Balashov et al. \(2014\) and Thompson et al. \(2003b\). The influence of local and regional meteorological factors were also evident. Laban et al. \(2018\) reported O<sub>3</sub> levels in northeastern South Africa, and characterized the links between observed NO<sub>x</sub> and O<sub>3</sub> concentrations. These studies were completed by the effect of precursor species and meteorological conditions on ozone formation \(Laban et al., 2020\). The critical role of regional-scale O<sub>3</sub> precursors such as high anthropogenic emissions of NO<sub>x</sub> \(under a limited regime of VOC\), coupled with meteorological conditions are well](#)

105  
110  
115  
120  
125  
130

emphasised and is agreement with Swartz et al. (2020a,b). -Other works were carried out by Bencherif et al. (2020), Brown et al. (2022), Gaudel et al. (2020), Hamdun and Arakaki (2015), Ihedike et al. (2023), Josipovic et al. (2010), Khoder (2009), Lannuque et al. (2021), Lee et al. (2021), Ngoasheng et al. (2021), Tsivlidou et al. (2023) and Zunckel et al. (2004) -in different locations in Africa to characterize O<sub>3</sub> pollution levels. The conclusions of these studies reported that an increase of tropospheric column with a mean of 1.2 nmol mol<sup>-1</sup> decade<sup>-1</sup> (2.4 % decade<sup>-1</sup>) above Gulf of Guinea and +3.6% over South Africa (Bencherif et al., 2020; Gaudel et al., 2020). A strong diurnal variation of O<sub>3</sub> is observed with a maximum in the mid-day time or afternoon due to the local photochemical production (Hamdun and Arakaki, 2015; Ihedike et al., 2023; Khoder, 2009; Zunckel et al., 2004). The low surface ozone concentrations recorded at the studied sites could be caused by titration of O<sub>3</sub> by NO<sub>x</sub> (Hamdun and Arakaki, 2015; Ngoasheng et al., 2021) but the higher NO<sub>x</sub> concentrations lead to increased O<sub>3</sub> chemical production (Brown et al., 2022). The influence of local climatic as harmattan, temperature, humidity and radiation on ozone formation have been also raised (Balashov et al., 2014); Ihedike et al., 2023; Khoder, 2009). Surface emissions from biomass burning contribute of 24% to boundary layer ozone over Africa (Lee et al., 2021). In the studies of Lannuque et al. (2021), Sauvage et al. (2007), Tsivlidou et al. (2023), it appears clearly that tropical meteorology particularly impacts the O<sub>3</sub> distributions through the movement of air masses in the Intertropical Convergence Zone (ITCZ) by the north-easterly Harmattan flow (January) or the southeasterly winds and monsoon flow (July). Other projects such as POLCA (POLlution des Capitales Africaines) and DACCIWA (Interactions Dynamique-Aérosols-Chimie-Nuages en Afrique de l'Ouest), have also been implemented in African capitals such as Bamako, Dakar and Yaoundé (Adon et al., 2016), Abidjan, Cotonou (Bahino et al., 2018) and have provided O<sub>3</sub> concentration surface measurements. These studies confirmed that in cities where NO<sub>2</sub> is high, O<sub>3</sub> is less abundant than in rural areas as reported in Hamdun and Arakaki (2015) and Ngoasheng et al. (2021).

However, despite many African studies about ozone and air quality, it should be noted that these campaigns for the most part are only snapshots in time. The number of measurements publicly available is very small and INDAAF is among the few long-term datasets that are available to the scientific community. With the exception of South Africa, O<sub>3</sub> variability is not yet sufficiently documented and very little information is available on the long-term evolution of O<sub>3</sub> chemistry in Africa (Fleming et al., 2018; Gaudel et al., 2018; Mills et al., 2018). The constraints of the climate response of isoprene emissions, the temperature sensitivity of NO<sub>x</sub> and O<sub>3</sub> chemistry (Brown et al., 2022) on the one hand and on the other hand the meteorological changes meteorological changes when diagnosing regional tropospheric ozone trends and potential shifts in the timing and spatial patterns of biomass burning and ozone precursor emissions in the tropics (Stauffer et al., 2024) are recommended by these authors. The impact of meteorological parameters (temperature, humidity, rainfall, radiation) and atmospheric chemistry (NO<sub>x</sub> and VOCs concentrations) on the seasonality of O<sub>3</sub> concentrations, and the analysis of long-term O<sub>3</sub> trends are only partially explained remain unexplored. Further work is therefore needed to fill the data gaps in Africa, and better understand the mechanisms of O<sub>3</sub> formation as a function of ecosystems and their long-term evolution.

As part of the INDAAF program, this study aims to improve the long-term assessment of surface O<sub>3</sub> in the western, central, eastern and southern African regions. In the first objective, we ~~first~~ document the long-term (1995-2020 depending on the site) monthly, seasonal and interannual variability of O<sub>3</sub> concentrations on a regional scale at fourteen sites grouped by ecosystem (dry savannas, humid savannas, forests and agricultural/semi-arid savannas), followed by a comparative study with existing references. The study goes further by discussing the seasonal architecture of anthropogenic and biogenic O<sub>3</sub> precursors based on meteorological parameters and emission inventories. ~~and In the second objective, we study the impact of meteorological parameters (temperature, humidity, precipitation, radiation) and atmospheric chemistry precursors (NO<sub>x</sub> and VOC) on photochemical O<sub>3</sub> production, using principal component analysis. In this section, we establish the correlation matrix between O<sub>3</sub>, and these factors, its gaseous precursors and meteorological parameters. An attempt is made to assess their different contributions to photochemical O<sub>3</sub> production in each ecosystem.~~ In the third objective, we use non-parametric statistical tests to assess long-term seasonal and annual trends in O<sub>3</sub>, and discuss the results according to trends in anthropogenic and biogenic emissions of precursors and several new trend studies that include African data. For the first time, the chemical evolution of

175 tropospheric O<sub>3</sub> is examined over the long term at all INDAAF and companion sites. This study provides a robust regional mapping of the long-term seasonal cycle O<sub>3</sub> formation at the continental scale.

## 2. Materials and methods

### 2.1 Sampling sites

180 Fourteen O<sub>3</sub> measurement sites located in different African ecosystems have been selected for this long-term study of tropospheric O<sub>3</sub> chemistry (Fig. 1), among which 8 stations of the INDAAF long-term monitoring network located in 7 West and Central Africa countries (Mali, Niger, Ivory Coast, Senegal, Benin, Congo and Cameroon). These sites are characteristic of dry savanna, ~~wet~~ wet ~~humid~~ humid savanna, ~~and~~ forest, agricultural and semi-arid ecosystems (Table 1). A detailed description of INDAAF monitoring stations and land use classes is available in Adon et al. (2010, 2013). Other sites implemented through INDAAF's companion projects and using the same O<sub>3</sub> measurements protocols were also selected for this study. The site of Dahra in Senegal, part of the 'Cycle de l'Azote entre la Surface et l'Atmosphère en afriQUE" (CASAQUE) project is located in dry savanna and used for grazing (Bigaignon et al., 2020). The site of Mbita, part of the Integrated Nitrogen Management system (INMS) is located in East Africa. In South Africa, four long-term DEBITS sites (Louis Trichardt, Skukuza, Cape Point and Amersfoort) are considered. They are regionally representative of the specific ecosystems of southern Africa. Full descriptions of these South African sites can be found in the works of Conradie et al. (2016), Laakso et al. (2012) and Swartz et al. (2020a,b). All study sites are representative of semi natural rural sites in remote regions. Table 1 presents geographical coordinates and some ecological and climatological characteristics of the sites. In the remainder of the text, the measuring stations will be referred to using the following abbreviations: Banizoumbou (Ba), Katibougou (Ka), Agoufou (Ag), Bambe (Bb), Dahra (Da), Lamto (La), Djougou (Dj), Zoetele (Zo), Bomassa (Bo), Mbita (Mb), Louis Trichardt (LT), Skukuza (Sk), Cape Point (CP) and Amersfoort (Af).

195 **Table 1.** Geographical, ecological and climatic characteristics of the study sites

Ecosystem	Station	Latitude, Longitude	Country	Land cover classes	Climate
Dry savanna	Banizoumbou (Ba)	13°18' N, 02°22' E	Niger	Open grassland with sparse shrub and culture	Sahelian
	Katibougou (Ka)	12°56' N, 07°32' W	Mali	Deciduous shrubland with sparse trees	Sudano-Sahelian
	Agoufou (Ag)	15°20' N, 01°29' W	Mali	Open grassland with sparse shrub and trees	Sahelian
	Bambe (Bb)	14°42' N, 16°28' W	Senegal	Cultivated grass land with sparse trees	Sahelian
	Dahra (Da)	15°24' N, 15°26' W	Senegal	Open grassland with sparse shrub and trees, sylvopastoral area	Sahelian
Wet savanna	Lamto (La)	06°13' N, 05°02' W	Cote d'Ivoire	Mosaic forest/savanna	Guinean
	Djougou (Dj)	09°39' N, 01°44' E	Benin	Deciduous open woodland	Sudano-Guinean
Forest	Zoetele (Zo)	03°10' N, 11°49' E	Cameroun	Dense evergreen	Guinean
	Bomassa (Bo)	02°12' N, 16°20' E	Congo	lowland forest	Guinean

Agricultural field	Mbita (Mb)	0°25' S, 34°12' E	Kenya	Tropical agricultural area	Subtropical
Regional savanna/ Semi-arid	Louis Trichardt (LT)	22°59' S, 30°01' E	South Africa	Cultivated/Semi-arid regional savanna	Subtropical
	Skukuza (Sk)	24°59' S, 31°35' E		Semi-arid regional background site surrounded by natural bushveld in a protected area	Subtropical
	Cape Point (CP)	34°21' S, 18°29' E		Southern Hemispherical marine background site, rocky and sparsely vegetated, Fynbos biome	Mediterranean
	Amersfoort (Af)	27°04' S, 29°52' E		Semi-arid regional savanna, impacted by anthropogenic activities	Warmtemperate

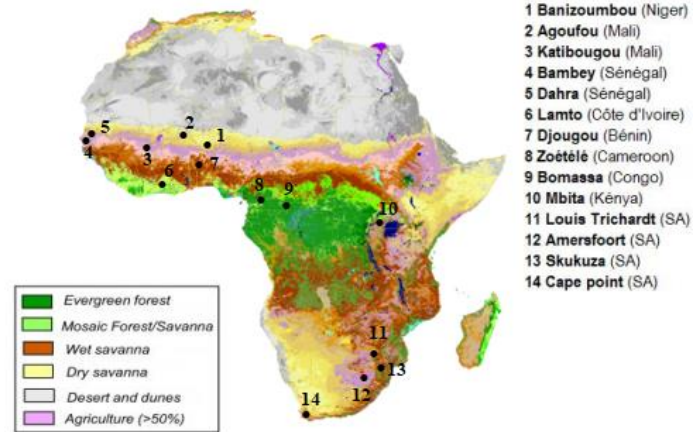


**Figure 1.** Location of the 14 measurement studied sites in Africa on a vegetation map (adapted from Mayaux et al., 2004)

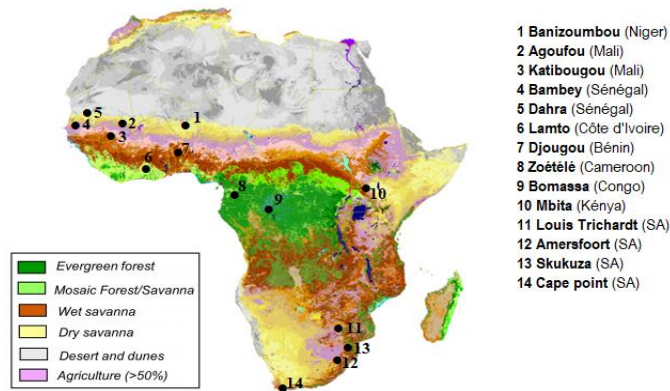


**Figure 1.** Location of the 14 measurement studied sites in Africa on a vegetation map (adapted from Mayaux et al., 2004)

## 205 2.2 Passive sampling and chemical analysis

### 2.2.1 Sampling procedure

O<sub>3</sub> concentrations were measured using passive samplers developed at the Laboratoire d'Aérodologie (LAERO) in Toulouse in the framework of the INDAAF program, and at the North West University in Potchefstroom in South Africa. They are based on the passive sampling technique, which relies on laminar diffusion and the chemical reaction of the atmospheric pollutant under consideration (Adon et al., 2010; Ferm, 1991 and Martins et al., 2007). ~~These sensors have been tested and validated in different tropical and subtropical regions (Carmichael et al., 2003; Martins et al., 2007).~~ The measurement protocols including passive samplers deployment, analysis by Ionic chromatography and the calculation method of concentrations have been widely described in previous studies (Adon et al., 2010; Bahino et al., 2018; Carmichael et al., 2003; Ferm and Rodhe, 1997; Galy-Lacaux et al., 2009; Galy-Lacaux and Modi, 1998; Osohou et al., 2019; Swartz et al., 2020b).

215 Sampling periods at the measurement sites were coordinated and passive samplers are exposed on a monthly basis using the calendar months. One blank dedicated to ozone is included in the expedition of samplers each two months on sites. In this way, the delay between field deployment and analysis are the same both blanks and exposed samples. All data presented in this paper are blank corrected. A total of 1,317 blanks were assessed at the 14 sites over the studied period. In this paper, we use monthly database of O<sub>3</sub> concentrations. The concentration measurement period runs from the start date of measurements at each site to 2015-2020 (Table 2). O<sub>3</sub> concentration collection efficiency (%) on the sampling period (ratio of the number of valid concentrations to the number of filters analysed) was assessed at each of the 14 sites (Table 2). All wet and dry seasons duration are indicated in Table 2. These proportions are fairly representative of high quality measurements as indicated in the work of Laakso et al. (2008, 2012), Laban et al. (2018) and Petäjä et al. (2013). Measurements of O<sub>3</sub> concentrations are continuing at the most of various sites and are referenced in the INDAAF website (<https://indaaf.obs-mip.fr>).

225

**Table 2.** Sampling period and concentration data collection efficiency

Ecosystem	Station	Sampling period	Detection limit (ppb)	Data collection efficiency (%)	Total of samplers	Season	Measurement altitude (m)
Dry savanna	Ba	2000-2020	0.1	<del>93.5</del> <sup>232</sup> / <del>248</del>	<u>248</u>	Dry season: Oct-May Wet season: Jun-Sep	1.5
	Ka	2001-2020		<del>86.7</del> <sup>208</sup> / <del>240</del>	<u>240</u>		
	Ag	2005-2018		<del>82.6</del> <sup>109</sup> / <del>132</del>	<u>132</u>		
	Bb	2016-2020		<del>94</del> <sup>47</sup> / <del>50</del>	<u>50</u>		
	Da	2012-2020		<del>83.7</del> <sup>87</sup> / <del>104</del>	<u>104</u>		
Wet savanna	La	2001-2020		<del>94.2</del> <sup>226</sup> / <del>240</del>	<u>240</u>	Dry season: Nov-Mar Wet season: Apr-Oct	1.5
	Dj	2005-2020		<del>92.5</del> <sup>172</sup> / <del>186</del>	<u>186</u>		
Forest	Zo	2001-2020		<del>86.7</del> <sup>208</sup> / <del>240</del>	<u>240</u>	Dry season: Dec-Feb and July-Aug Wet season: Mar-Jun and Sep-Nov	3

	Bo	2001-2020		<del>68.3</del> 64/240	<del>240</del>	Dry season: Dec-Feb Wet season: Mar-Nov	
Agricultural field	Mb	2017-2020		<del>95.34</del> 43	<del>43</del>	Dry season: Jun-Oct and Jan-Feb Wet season: Mar-May and Nov-Dec	1.5
Regional savanna/semi-arid	LT Sk Af	1995-2015 2000-2015 1997-2015	0.02	<del>95.22</del> 36/248 <del>86.4</del> 65/192 <del>85.5</del> 189/221	<del>248</del> <del>192</del> <del>221</del>	Dry season: Apr-Sep Wet season: Oct-Mar	1.5
	CP	1995-2020		<del>90.7</del> 225/248	<del>248</del>	Dry season: Oct-Mar Wet season: Apr-Sep	

### 230 2.2.2 Validation and quality control of INDAAF passive samplers

235 To ensure the reliability of the ozone concentrations measurements carried out by the passive sampling monitoring network in West, Central, East and Southern Africa, several validation and quality control tests were carried out as part of the IGAC-DEBITS program and other collaborations with the Swedish Environmental Research Institute (IVL), the AMMA program, the pilot program for measuring urban meteorology and the environment (GURME) launched by the WMO/GAW and the National University of Singapore. These various performance tests were carried out in Africa at the Banizoumbou (Niger), Zoetele (Cameroon), Lamto (Côte d'Ivoire), Djougou (Benin) and Cape Point (South Africa) sites, in France at Toulouse and in Asia (Singapore). In this assessment, the precision and accuracy of the passive samplers used for O<sub>3</sub> monitoring by the various institutions were determined. O<sub>3</sub> detection limits were calculated on the basis of laboratory blank samples. Comparison of gas concentrations measured by passive samplers (integrated over 15 days) and active analysers was carried out at various sites in Toulouse (1998-2020). The test results indicated a good correlation between the two measurement methods, with an average comparative ratio of 1:0.8 for ozone and a correlation coefficient R<sup>2</sup>=0.8 (Adon et al., 2010). During the 2007 AMMA campaign in Djougou, an intercomparison between measurements from passive samplers and active analysers during the wet season from April to September 2006 revealed that the maximum difference observed between the two techniques (passive/active) was around 6% (Adon et al., 2010). In Banizoumbou, Zoétéélé, Lamto and Cape Point, INDAAF and IVL passive samplers were co-located and exposed for a period of one year. The correlation was good between the two types of measurements (Adon et al., 2010; Carmichael et al., 2003). The most recent evaluation of the University of the North West passive samplers used at the South African sites was an international comparison study organised by the National University of Singapore in 2008 (Swartz et al., 2020b). Results indicated that the passive sensors used and operated in INDAAF compared very well with active samplers and had better accuracies. Data quality of the analytical facilities is also ensured through participation in the World Meteorological Organization (WMO) bi-annual Laboratory Intercomparison Study (LIS) (Swartz et al., 2020a,b). The recovery of each ion in standard samples was between 95 % and 105 % (Conradie et al., 2016) and the analysed data were also subjected to the Q test, with a 95 % confidence threshold to identify, evaluate and reject outliers in the datasets (Swartz et al., 2020a). Diffusive samplers have many advantages in the field, including no need for calibration, sampling tubing, electricity or technicians and are small, light, reusable, costefficient and soundless (Adon et al., 2010).



### 2.3 Meteorological parameters and leaf area index

In order to characterize each measurement site, classical meteorological parameters are used such relative humidity, ambient air temperature, rainfall, radiation and leaf area index (LAI). At Ba, Bb, La, Dj and Zo sites, the data on ambient air temperature, relative humidity and rainfall are extracted from the AMMA-CATCH database (Analyse Multidisciplinaire de la Mousson Africaine - Couplage de l'Atmosphère Tropicale et du Cycle Hydrologique; [www.amma-catch.org/](http://www.amma-catch.org/)) and the Observatoire de recherche en environnement "Bassins versants tropicaux expérimentaux" (SO BVET; [bvet.obs-mip.fr/](http://bvet.obs-mip.fr/)) (Ossohou et al., 2019). The measuring devices used at Ka, La and Bo is described in the same work (Ossohou et al., 2019). At Bb site, relative humidity, temperature and rainfall are collected in the INDAAF database (<https://indaaf.obs-mip.fr>). At Da site, measurements of meteorological parameters come from a measuring station installed by the University of Copenhagen (Bigaignon et al., 2020). In Ka, Ag, Bo, Mb, LT, Af, Sk and CP, the meteorological data are provided by the intermediate reanalysis archive (ERA 5) of the European Center for Medium-Range Weather Forecasts (ECMWF). The time series of global solar radiation used in this study at all sites except Dahra are also ERA 5 reanalysis data obtained from ECMWF. To ensure the reliability of the ERA5 data on the study sites, we determined the estimation errors (RMSE) and the correlation between the reanalysis data and those measured in situ. We chose the Banizoumbou site in Niger (2000-2020), which hosts a meteorological station that provides temperature, humidity and rainfall data, and the Dahra site, where radiation data are measured. We obtained a low error estimate (RMSE) of the order of  $9.9 \times 10^{-3} \text{ }^\circ\text{C}$  for temperature,  $4.8 \times 10^{-3} \%$  for humidity and  $2.3 \times 10^{-1} \text{ mm}$  for rainfall in Niger. At the Bambey site in Senegal, the estimated errors are of the order of  $6.4 \times 10^{-2} \text{ J/m}^2$  for radiation. The correlation between in situ and ERA5 data for these two sites is very good and is about of 0.96 for rainfall, 0.99 for humidity, 0.80 for radiation and 0.99 for temperature. LAI data are obtained from MODIS (Moderate Resolution Imaging Spectroradiometer) with a resolution of  $0.25 \text{ km}^2$  for an 8-day time scale centred around each station (Ossohou et al., 2019). All these parameters are collected at the same sampling period as  $\text{O}_3$  concentrations, with the exception of LAI measurements, which began in 2000 (<https://modis.ornl.gov/data.html>).

### 2.4 $\text{NO}_x$ and VOC emissions

The emissions of volatile organic compounds (VOCs) and nitrogen oxides ( $\text{NO}_x$ ) from biomass combustion were downloaded from the ECCAD (Emissions of atmospheric Compounds and Compilation of Ancillary Data) database in the GFED4 inventories for  $0.25^\circ \times 0.25^\circ$  grid cells. BVOC emissions are extracted from the MEGAN-MACC inventory in the ECCAD database ([eccad.aeris-data.fr](http://eccad.aeris-data.fr)). The biogenic  $\text{NO}$  fluxes used are model outputs in reference to the work of Delon et al. (2010, 2012). They were filtered in the eastern grid from  $5^\circ \text{ S}$  to  $20^\circ \text{ N}$  in latitude, and  $20^\circ \text{ W}$  to  $30^\circ \text{ E}$  in longitude over the period from 2002 to 2007 and cover only the Ba, Ka, Ag, La, Dj, Zo and Bo sites. ECCAD platform is the emissions database of the international GEIA project (Global Emission Initiative: [geiacenter.org](http://geiacenter.org)) has been developed within the framework of the French atmospheric data center AERIS (<http://www.aeris-data.fr>) (Darras et al., 2022). The GFED4 inventory is based on satellite data of fire activities and vegetation productivity observed since 1997 ([eccad.aeris-data.fr](http://eccad.aeris-data.fr)). MEGAN (Model of Emissions of Gases and Aerosols from Nature) inventory quantifies net biogenic emissions of isoprene and other gases emitted by vegetation into the atmosphere (Guenther et al., 2006; Sindelarova et al., 2014). The determining variables of MEGAN are derived from models and satellite and ground observations, enabling simulations to be carried out on a regional and global scale. They take into account the emission factor, which represents the emission of a compound in the canopy under standard conditions, the emission activity factor, which included changes in emission due to deviations from standard conditions, and the factor that explains production and losses within the plant canopy (Guenther et al., 2006). Isoprene,  $\alpha$ -pinene and  $\beta$ -pinene, which account for the largest proportion of BVOCs emitted by vegetation in Africa (Ferreira et al., 2010; Jaars et al. 2016; Liu et al., 2021; Saxton et al., 2007; Serça et al., 2001), were identified and used in this study. A more detailed description of these emission inventories is discussed in the work of García-Lázaro et al. (2018), Guenther et al. (2006) and Vitolo et al. (2018). For each emission category,  $\text{NO}_x$  ( $\text{kg m}^{-2} \text{ s}^{-1}$ ) and VOC ( $\text{kg m}^{-2} \text{ s}^{-1}$ ), we use the sum of fluxes from all biomass combustion sources (agricultural, waste combustion, savanna, grassland, scrubland, boreal forest, temperate forest, tropical deforestation,

peat degradation and peat fires) at a monthly scale and over the study period for each site. These inventories emissions are widely used and Global Fire Emissions Database GFED have been recommended by Stauffer et al. (2024) to study potential shifts in the timing and spatial patterns of biomass burning and ozone precursor emissions in the tropics.

## 305 2.5 Statistical analysis

~~We use Principal Component Analysis (PCA) and Mann-Kendall test to investigate respectively the different contributions of O<sub>3</sub>-precursors from photochemical formation and the monotonic trends in the time series of each site. PCA multivariate analysis method (Jolliffe, 1986), is often used in air quality analyses to identify the major sources of pollutants emitted into the atmosphere (Bruno et al., 2001; Lanz et al., 2007). It specifies the relationships between variables, the phenomena behind these relationships and the similarities between individuals (Mouissi and Alayat, 2016). In this study, the statistical analysis of meteorological data and atmospheric chemical pollutants was carried out on a data matrix made up of ten to eleven variables depending on the site, and 12 individuals representing the months of the year. For PCA implementation, R programming software was used. More detailed information on the calculation of PCA can be found in the literature (Ait-Sahalia and Xiu, 2019; Baglama et al., 2021; Duriš et al., 2021; Tsuyuzaki et al., 2020).~~ The Mann-Kendall and seasonal Kendall tests, associated with the calculation of Sen's slope (Sen, 1968) is applied to all sites with at least 10 years of measure using XLSTAT 2022.2.1.1313 software at 95% confidence intervals. ~~The trend is said to be statistically significant when the p-value of the test is less than 5%.~~ In the case of Kendall's seasonal test, the seasonal nature of the series is taken into account. The literature provides extensive information on Mann-Kendall trends calculations (Frimpong et al., 2022; Hirsch et al., 1982; Kendall, 1975; Merabtene et al., 2016). Vectors with p-values less than 0.05 exhibit a very high certainty to obtain the trend, while vectors with p-values in the range of 0.05–0.10 give an indication of a trend (Gaudel et al., 2018). Vectors with p-values in the range of 0.10–0.34 provide a weak indication of change, and p-values greater than 0.34 indicate weak or no change. The vectors with p-values in the range of 0.05–0.34 are very useful for understanding regional trends as they typically follow the same pattern as the very high certainty vectors (Chang et al., 2017; Gaudel et al., 2018). Another non-parametric breakpoint test (Pettitt test) is carried out using Khronostat 1.01 software to assess possible breaks in homogeneity in the O<sub>3</sub> concentration series and for optimal application of the trend test.

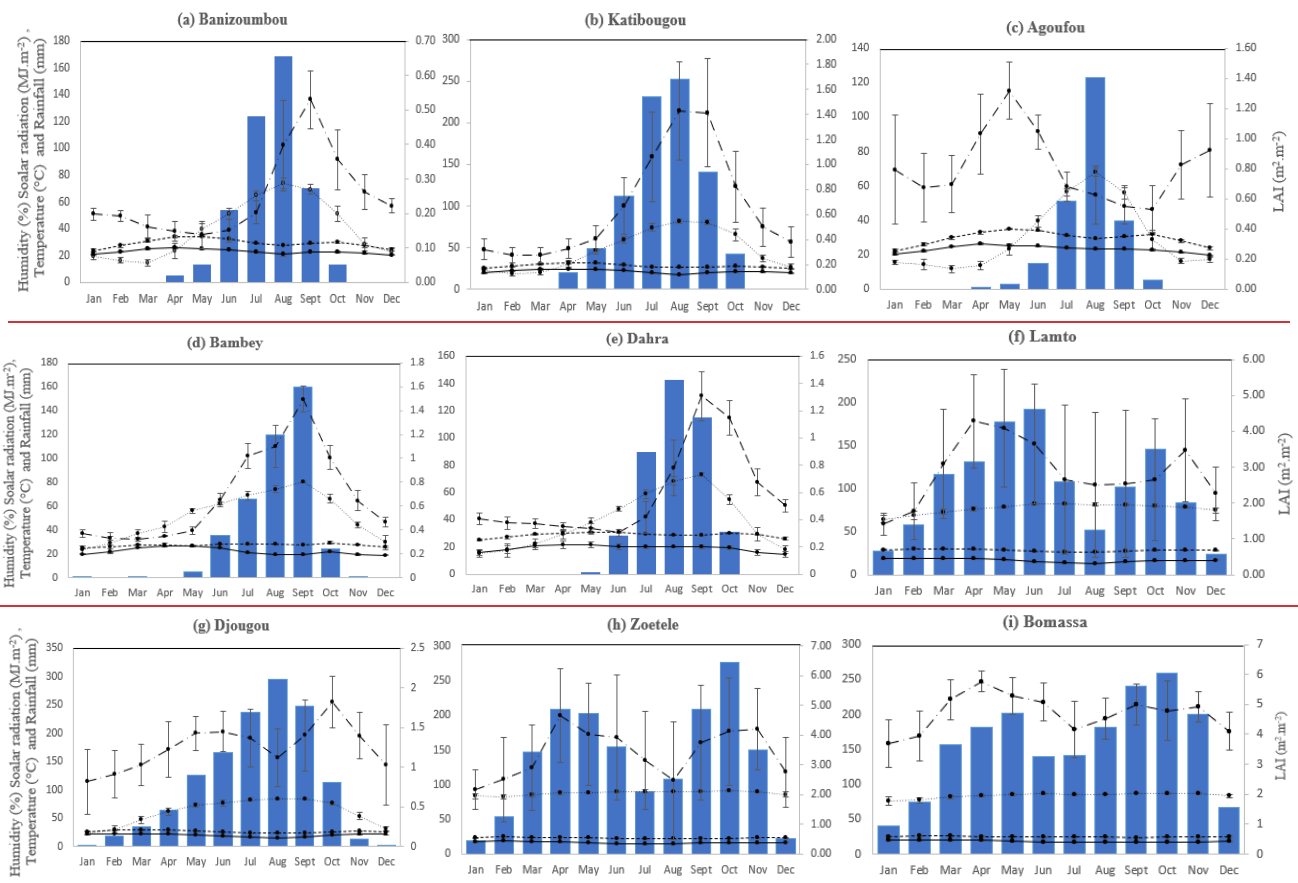
## 3. Results and discussion

### 3.1 Meteorological and biophysical parameters variation

The monthly variations of meteorological parameters and leaf area indexes (LAI) are shown in Fig. 2 for all sites. In dry savanna, the rainfall regime is unimodal, with the greatest amounts of rain recorded from July to September corresponding at the maxima of LAI. Mean air temperature ranged from  $22.1 \pm 0.9^\circ\text{C}$  to  $34.9 \pm 0.4^\circ\text{C}$ , with air relative humidity from 68% to 82%. The most elevated solar radiation is found at Ag ( $23.1 \pm 0.5 \text{ MJ}\cdot\text{m}^{-2}$ ). In wet savanna and forest sites, the rainfall pattern and LAI follow a quasi-bimodal distribution. The mean annual LAI varies from  $1.2 \pm 0.3 \text{ m}^2\cdot\text{m}^{-2}$  (Dj) to  $4.7 \pm 0.7 \text{ m}^2\cdot\text{m}^{-2}$  (Bo). The most significant monthly variations in relative humidity are found in Dj (23.2 - 84.1%). At Mb site, the maximum rainfall occurs between March and May, reaching 255 mm in April. The vegetation cover is denser at the end of the first wet season ( $1.3 \pm 0.3 \text{ m}^2\cdot\text{m}^{-2}$  in May) with an average value of humidity around 70%. In Southern Africa, the humidity varies from 13% to 22% year-round except at CP where variations are very low. The maximum of rain is collected between December and January (432 mm on average) at LT, Af and Sk sites and in August at CP (343 mm). LAI maxima are of the order of  $1.6 \pm 0.2 \text{ m}^2\cdot\text{m}^{-2}$  at Af ;  $3.1 \pm 0.6 \text{ m}^2\cdot\text{m}^{-2}$  at LT;  $4.0 \pm 0.1 \text{ m}^2\cdot\text{m}^{-2}$  at CP and  $1.7 \pm 0.2 \text{ m}^2\cdot\text{m}^{-2}$  at Sk in wet season. In wet savanna and forest, the temperature variations are low, as well as in Mb ( $23.6 \pm 0.5^\circ\text{C}$ ). On the other hand, at the South African sites, the temperature reaches amplitudes ranging from  $6^\circ\text{C}$  to  $10^\circ\text{C}$ . From wet savanna to semi-arid savanna (South Africa), the average solar radiation is below at  $22 \text{ MJ}\cdot\text{m}^{-2}$ . Along the north-south transect for the study sites, the gradient of humidity, leaf area index and rainfall are positive, whereas it is negative for temperature and radiation. The variations in meteorological parameters are strongly influenced by the alternating seasons. These characteristics are dependent on the type of climate. Indeed, in West

345 and Central African climate (and its variability) is a function of the position of the Inter Tropical Convergence Zone (ITCZ),  
 which is a band separating the hot and dry continental air coming from the Sahara desert (Harmattan) from the cooler, humid  
 350 maritime air masses (Monsoon) originating from the equatorial Atlantic Ocean (Adon et al., 2010; Lannuque et al., 2021;  
 Sauvage et al., 2005). Its geographical shift from the Northern Hemisphere during the boreal summer to the Southern  
 Hemisphere during the boreal winter with different positions throughout the year (for example in January, around 5° N and in  
 August, around 22° N) define the seasons in this region of Africa and explain the marked seasonal variations observed in West  
 and Central Africa (Sauvage et al., 2005). The position of the convergence zone gives rise to the “wet” seasons. Compared  
 with West Africa, East Africa exhibits slightly different regimes due to the topography and the proximity of the Indian Ocean.  
 355 The climate of southern Africa is characterized by alternating wet and dry periods which are also modified by the position of  
 the ITCZ (Lannuque et al., 2021). Within the ITCZ warm and humid surface air masses converge and are convectively uplifted  
 into the upper troposphere. The uplifted air masses are then advected polewards in the upper branches of the Hadley cells. The  
 dry air in the descending branches of these cells creates the conditions for wildfires and the resulting emission of ozone  
 precursors (Lannuque et al., 2021).

360



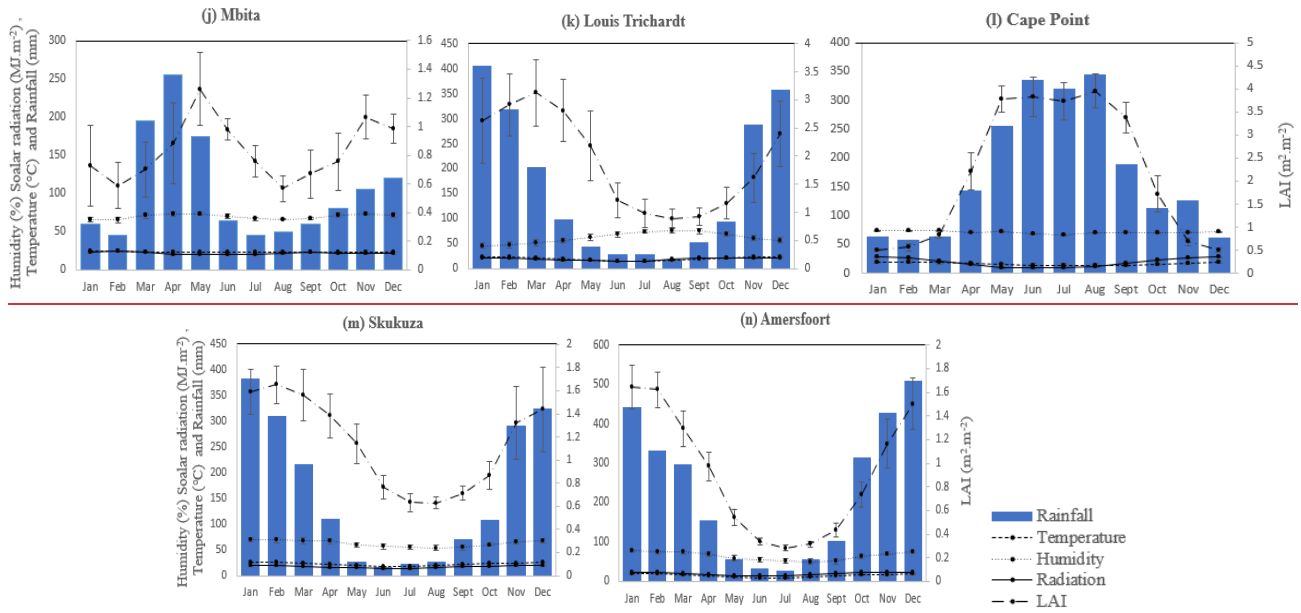
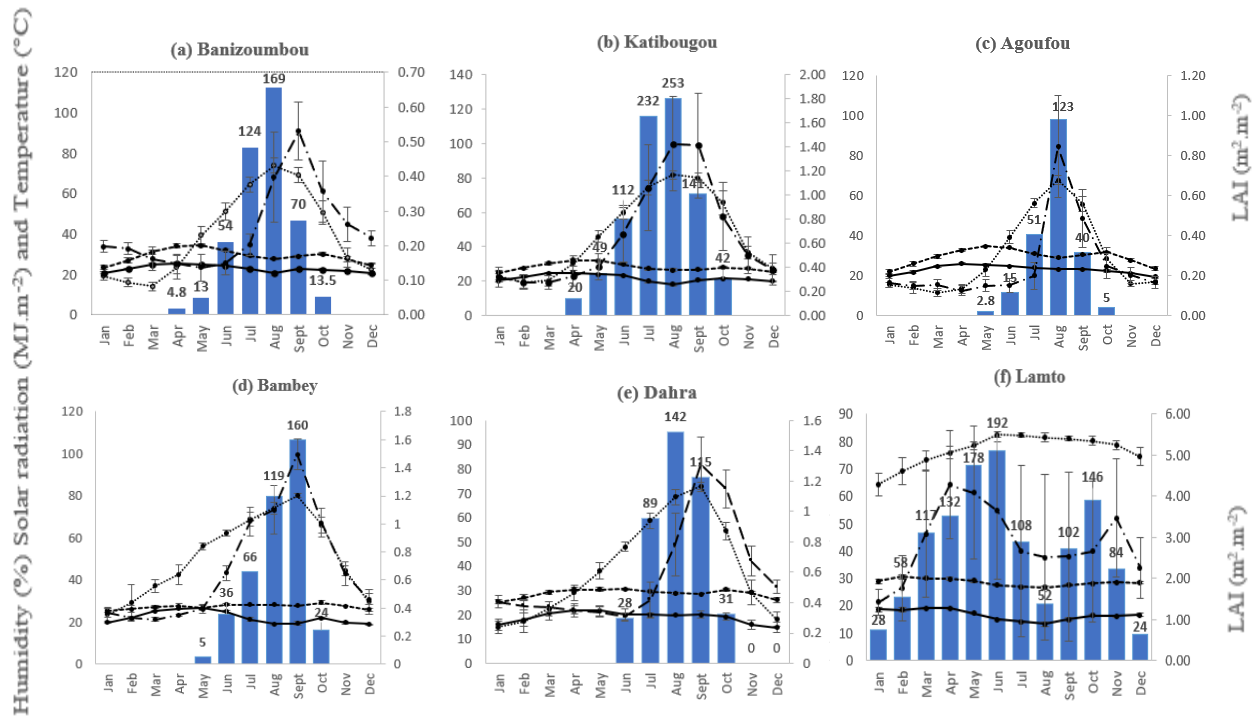
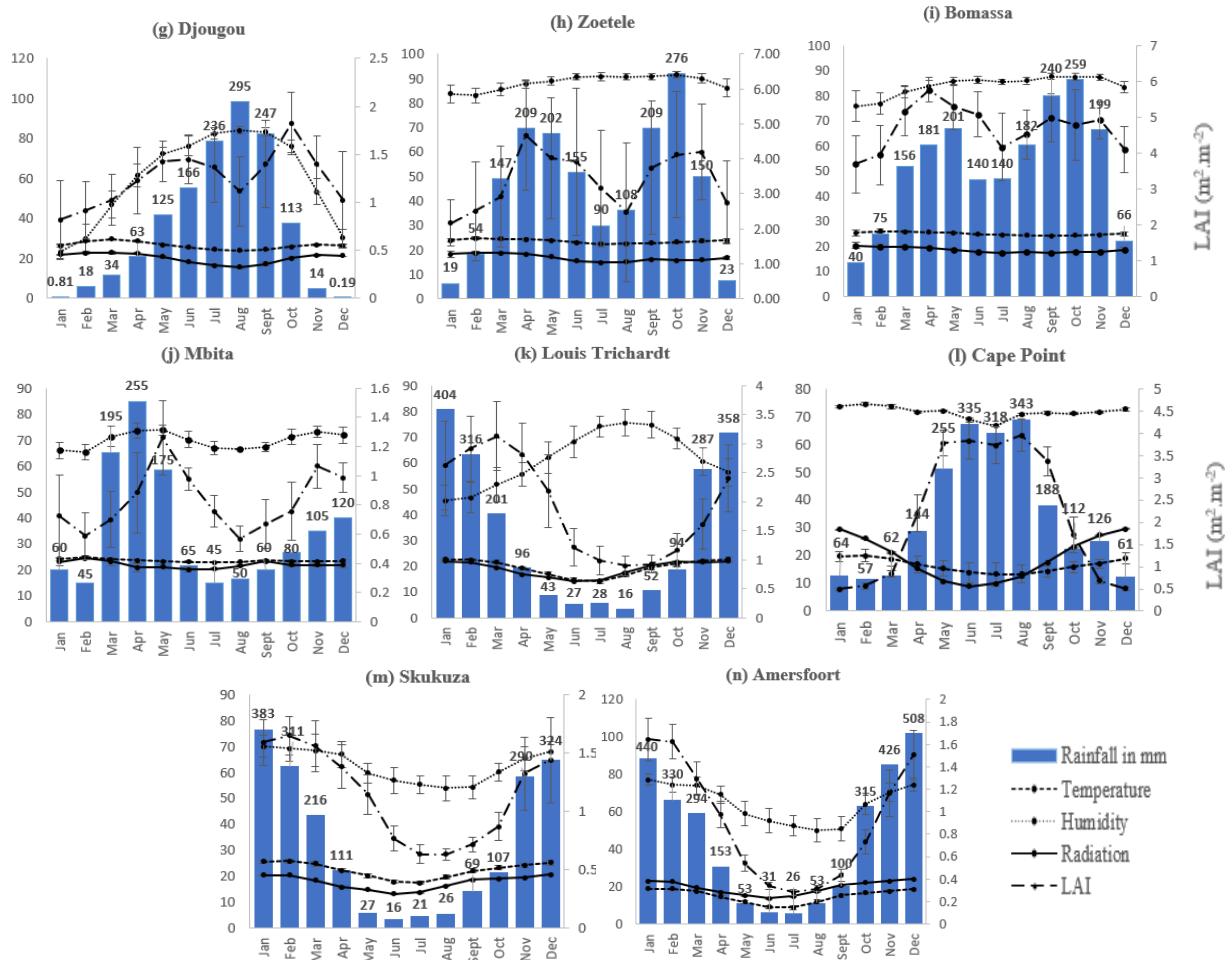


**Figure 2.** Mean monthly variation in air temperature ( $^{\circ}\text{C}$ ), rainfall (mm), relative humidity (%), solar radiation ( $\text{MJ}\cdot\text{m}^{-2}$ ) and leaf area index ( $\text{m}^2\cdot\text{m}^{-2}$ ). The mean absolute deviation is represented by the vertical bars.

365



370



375 **Figure 2.** Mean monthly variation in air temperature ( $^{\circ}\text{C}$ ), rainfall (mm), relative humidity (%), solar radiation ( $\text{MJ}\cdot\text{m}^{-2}$ ) and  
 380 leaf area index ( $\text{m}^2\cdot\text{m}^{-2}$ ). The mean absolute deviation is represented by the vertical bars.

### 3.2 Characterization of $\text{O}_3$ levels

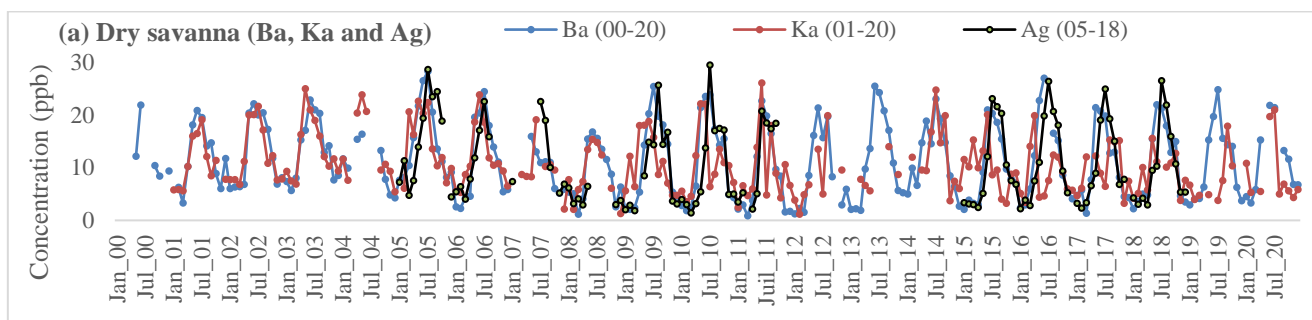
#### 380 3.2.1 Seasonal and annual variation in $\text{O}_3$ levels

##### 3.2.1.1 Dry savanna

Figure 3 presents monthly  $\text{O}_3$  surface concentrations measured in Ba, Ka, Ag (Fig. 3a), Bb and Da (Fig. 3b) representative of dry savannas in Niger, Mali and Senegal. The seasonal variability of  $\text{O}_3$  is well marked:  $\text{O}_3$  levels during the wet season are higher than in the dry season (Table 3). On most sites, from January to May, the  $\text{O}_3$  concentrations gradually increase to finally reach annual peaks at the start of the wet season (May-June-July). The mean annual cycle of monthly  $\text{O}_3$  concentrations at Ba, Ka, Ag (Fig. 4a), Bb and Da (Fig. 4b) are obtained from averages of monthly in situ measurements over the whole studied period. The annual distribution is similar to the regional rainfall pattern.  $\text{O}_3$  concentrations decrease as the rainy season progresses, but remain at higher levels compared to the dry season. At dry savanna sites, monthly average surface  $\text{O}_3$  concentrations range from  $6.1\pm 2.4$  ppb to  $14.5\pm 2.6$  ppb during the dry season, and from  $13.9\pm 5.1$  ppb to  $19.4\pm 3.9$  ppb during the rainy season (Table 3). From dry to wet season,  $\text{O}_3$  levels increased from 18.7% to 68.5%. The annual  $\text{O}_3$  concentrations ranged from  $10.5\pm 5.4$  ppb at Ka to  $14.8\pm 4.3$  ppb at Bb (Table 3).

The high O<sub>3</sub> concentrations observed at the start of the rainy season are due to soil humidification during this period, which generates biogenic NO emissions pulses in the region. Indeed, the accumulated nitrogen in soils (in the form of ammonium and nitrate ions) from traditional agricultural practices, such as grazing, manure spreading and decomposition of crop residues (Delon et al., 2015; Laville et al., 2005) is released to the atmosphere when the first rains fall on dry soils. Bacterial nitrification is thus activated, leading to nitrogen consumption and consequent release of large pulses of NO (Adon et al. 2010; Delon et al., 2015; Jaegle et al., 2004; Laville et al., 2005; Ludwig et al., 2001; Ossouhou et al., 2019). During the wet season, the decrease in O<sub>3</sub> levels may be attributed to a decrease in NO<sub>x</sub> concentrations. Indeed, soil mineral N is used by plants during their root growth phase, and is therefore less available for the production of NO to be released to the atmosphere (Homyak et al., 2014). On the Fig. 5, which presents the monthly variation of NO<sub>x</sub> and VOCs (natural and anthropogenic emissions) in dry savanna, biogenic NO fluxes (Fig 5e, f and g) in dry savanna show a bell-shaped variation, peaking in August (wet season). We observe a good dependence of O<sub>3</sub> with NO (0.73 < r < 0.92) at Ba, Ka and Ag in the presence of high relative humidity and precipitation (0.64 < r < 0.95) (Table 4), that is agreement with the high values of O<sub>3</sub> observed in wet season over these sites. Monthly profile of BVOC fluxes (isoprene, α pinene and β pinene) in dry savanna (Fig. 5) shows a maximum at the end of the dry season/beginning of wet season at Ba, Ka and Ag (Fig. 5e, f and g), or during the wet season at Bb and Da (Fig. 5h and i). Isoprene fluxes are more obvious at Da (214.2 ± 30) ng.m<sup>-2</sup>.s<sup>-1</sup> whereas α pinene, and β pinene exhibit larger values at Ka site (11.2 ± 1.8; 5.2 ± 0.8 ng.m<sup>-2</sup>.s<sup>-1</sup> respectively). The fluxes of β pinene (0.70 < r < 0.79) and isoprene (r = 0.79) correlates well with O<sub>3</sub> respectively at (Ba, Ka, Ag) and (Bb, Da) under the influence of the humidity, rainfall in Mali and Niger and the temperature, radiation and humidity (0.50 < r < 0.76) in Senegal (Table 4).

These observations in dry savanna are confirmed by Stewart et al. (2008) who correlated O<sub>3</sub> production in the Sahel during the wet season with high NO<sub>x</sub> concentrations attributed to biogenic emissions during the AMMA (Analyse Multidisciplinaire de la Mousson Africaine) campaign. In dry savanna, Oluleye et al. (2013) estimated that rain was responsible for 62% of the O<sub>3</sub> distribution in the West African region, excluding the precursors NO, CO and hydrocarbons, as also illustrated in our results. Saunois et al. (2009) have shown that soil NO<sub>x</sub> emissions, combined with the northward advection of volatile organic compounds (VOCs), play a key role in O<sub>3</sub> production in dry savanna regions. This large-scale impact of biogenic emissions has also been verified by Williams et al. (2009), who estimate that 2-45% of tropospheric O<sub>3</sub> over equatorial Africa may originate from NO<sub>x</sub> emissions from African soils. All these works are in agreement with the results of this study. Monthly variation in anthropogenic NO<sub>x</sub> and VOC emissions (Fig. 5a, b, c and d) indicates during the wet season, NO<sub>x</sub> and VOC fluxes are very low. On the other hand, maxima are observed in the dry season with the highest emissions found in Ka and could be the cause of ozone production in the dry season. Indeed, the monthly averaged biomass combustion emissions (GFED4) over the 18-year period (1998-2015) in the Sahel show that Ka is significantly affected by the biomass combustion source in November (Ossouhou et al., 2019).



425

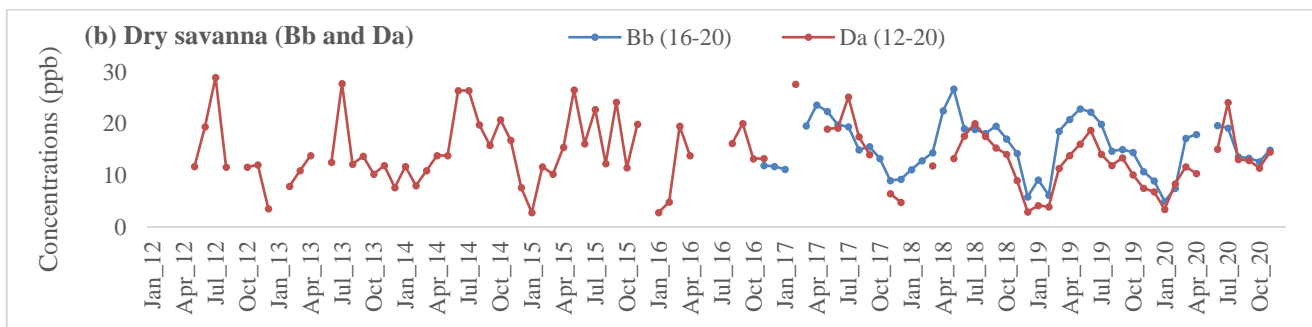
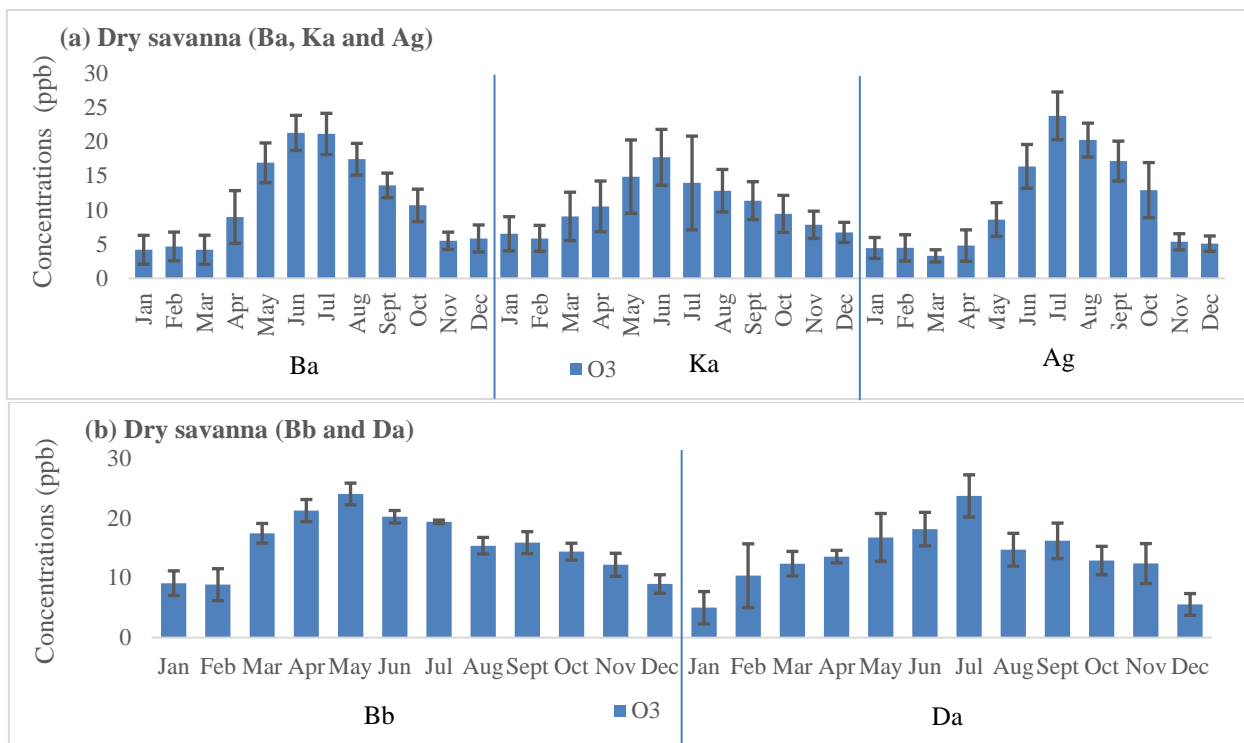


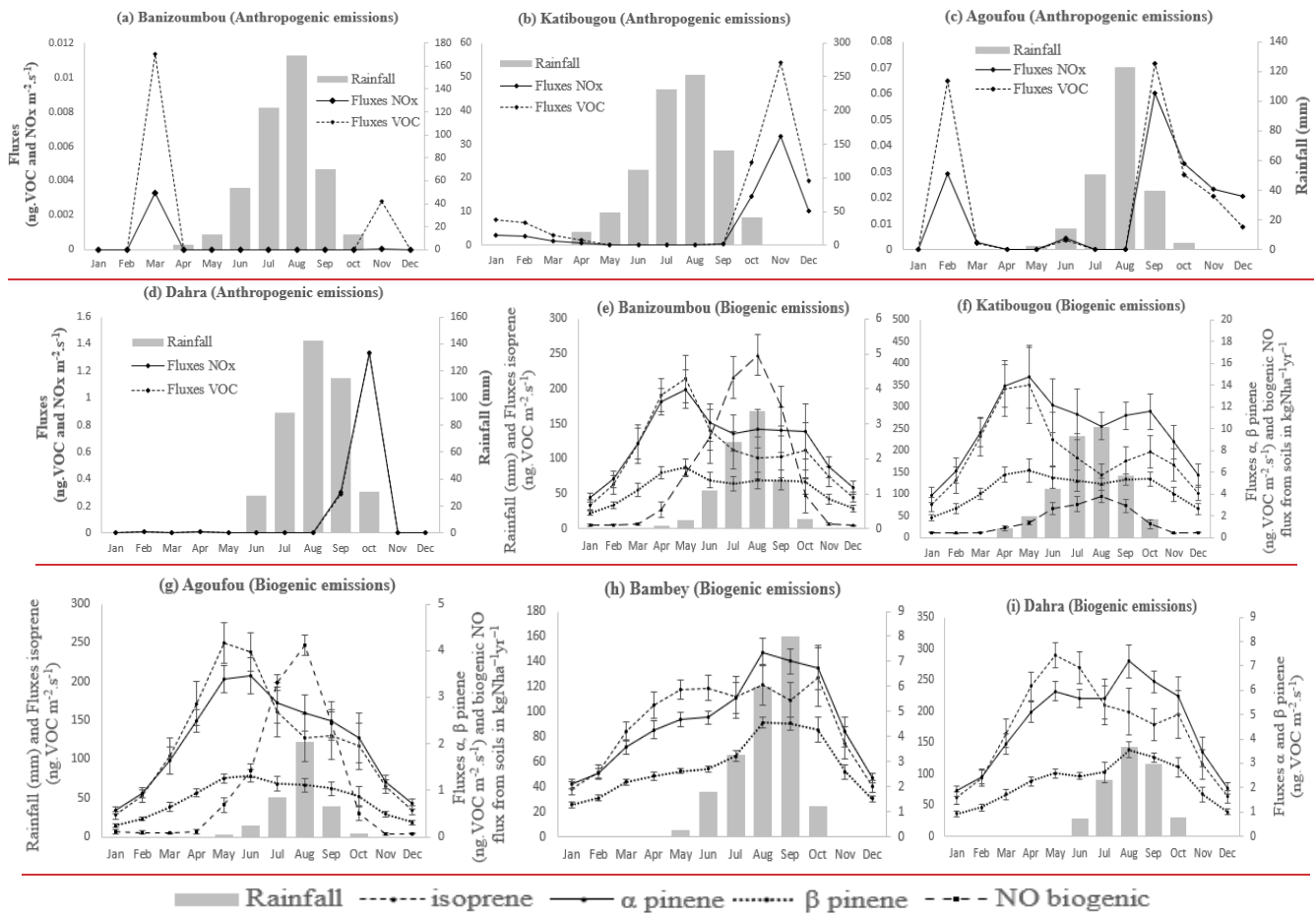
**Figure 3.** Monthly evolution of O<sub>3</sub> concentrations (ppb) in dry savanna (a) Ba (Niger), Ka, Ag (Mali) and (b) Bb, Da (Senegal).



430

**Figure 4.** Mean monthly averages of O<sub>3</sub> concentrations (ppb) in dry savanna (a) Ba (Niger), Ka, Ag (Mali) and (b) Bb, Da (Senegal). Mean monthly averages are calculated from the long ozone data series of Fig. 3. Bars represent mean absolute deviation.

435



440

Figure 5. Mean monthly fluxes of natural and anthropogenic NO<sub>x</sub> and VOC estimated by the MEGAN and GFED4 inventories for 0.25° x 0.25° grid cells centered on each of dry savanna

Table 3. Minimum, maximum and average of monthly, annual and seasonal O<sub>3</sub> concentrations at all sites (1995-2020)

Ecosystem		Monthly		Annual	Dry season			Wet season		
		min	max	moyAvg	min	max	moyAvg	min	max	moyAvg
Dry savanna	Ba	0.9	28.3	11.2±6.9	4.2±2.7	16.9±3.7	7.6±2.9	13.6±2.5	21.2±3.5	18.3±3.2
	Ka	1.2	26.1	10.5±5.4	5.8±2.6	14.9±6.6	8.8±3.7	11.3±3.8	17.7±5.4	13.9±5.1
	Ag	1.4	29.5	10.5±7.3	3.3±1.1	12.9±4.6	6.1±2.4	16.4±3.8	23.7±4.6	19.4±3.9
	Bb	4.96	26.7	14.8±4.3	8.8±3.5	24.0±2.4	14.5±2.6	15.4±1.9	20.2±1.4	17.7±1.6
	Da	2.8	29.0	13.9±6.3	5.0±3.8	16.7±5.4	11.1±4.0	14.7±3.1	23.7±4.8	18.2±4.0
Wet savanna	La	4.25	20.6	10.8±3.3	9.9±1.4	15.1±2.3	13.5±2.3	6.7±1.1	12.2±1.9	9.0±1.5
	Dj	3.3	24.8	13.5±4.8	10.8±4.5	18.7±2.7	14.1±4.0	9.0±2.0	18.4±2.4	13.2±2.8
Forest	Zo	1.2	11.1	5.2±2.1	7.1±2.1	7.8±1.6	7.5±2.1	3.5±1.3	6.6±1.9	4.6±1.6
	Bo	1.5	8.3	3.9±1.1	4.0±1.0	5.2±1.2	4.7±1.4	2.8±1.0	5.4±1.0	3.7±1.0



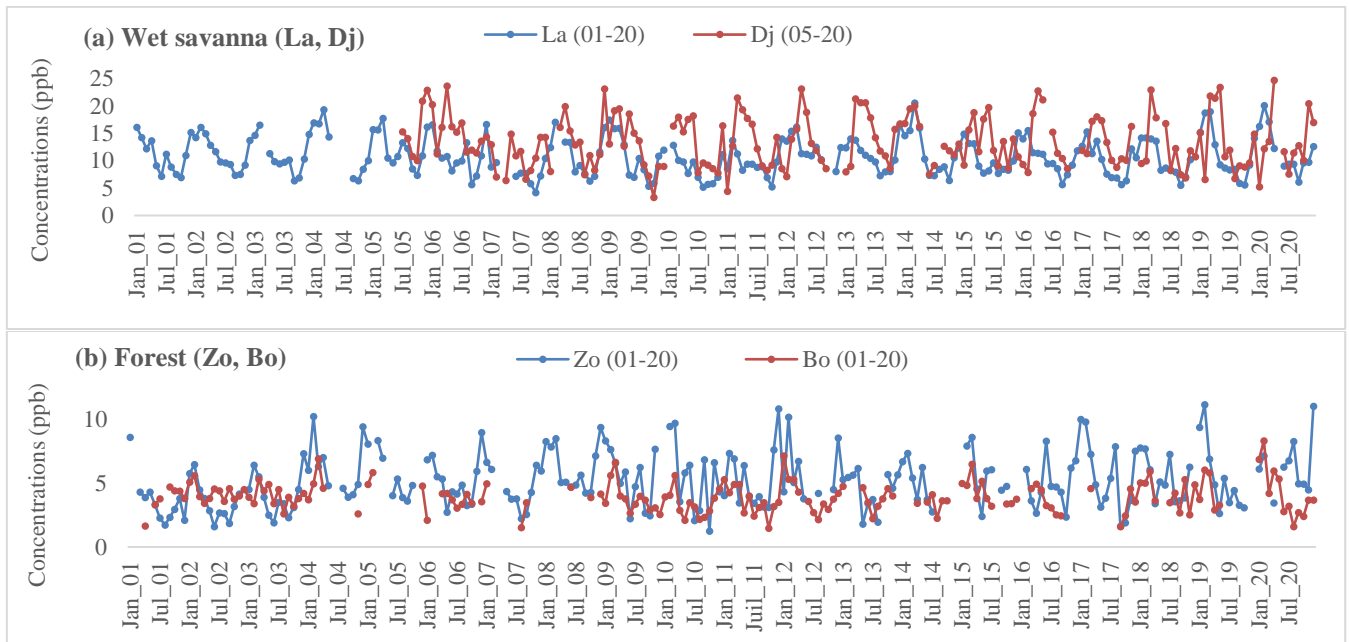
Agricultural or semi-arid savanna	Mb	10.5	30.2	19.9±4.7	13.8±3.4	25.7±5.7	20.9±4.0	14.1±5.0	22.5±2.7	18.5±3.9
	Sk	6.3	64.1	22.8±7.3	23.0±9.6	30.2±6.0	25.9±7.3	14.5±1.9	29.2±5.6	20.3±5.4
	Af	3.2	55.5	26.9±6.3	19.9±6.2	31.2±7.6	24.5±6.3	23.8±4.9	34.4±7.4	29.0±7.3
	CP	3.3	67.4	26.8±6.2	17.3±5.3	30.4±6.0	23.4±5.6	25.9±6.3	32.1±5.7	29.8±6.1
	LT	9.0	86.6	30.8±8.0	24.7±7.9	40.1±10.8	32.0±8.9	21.3±5.2	36.0±9.1	28.3±8.2

### 445 3.2.1.2 Wet savanna and forest

Figure 65 presents the mean monthly surface O<sub>3</sub> concentrations in Dj, La (Fig. 65a), Zo and Bo (Fig. 65b). O<sub>3</sub> concentrations present a seasonality during the year. The maximum of the data series in La is 20.6 ppb in March (dry season) and the minimum is 4.3 ppb in October (wet season). In Dj, the O<sub>3</sub> levels are higher than in La. The monthly highest value recorded in Dj is 24.8 ppb in April (start of the wet season). At the forested ecosystems sites, O<sub>3</sub> concentrations are lower than in dry, wet and semi-agricultural/semi-arid savannas (Table 3). In Zo and Bo, the highest annual peaks are found in February (11.1 ppb and 8.3 ppb respectively). Monthly averages in the dry season ranged from 4.7±1.4 ppb (Bo) to 14.1±4.0 ppb (Dj), and in the wet season from 3.7±1.0 ppb (Bo) to 13.2±2.8 ppb (Dj) (Table 3). The O<sub>3</sub> mean annual cycle is shown in Fig. 76.

The high O<sub>3</sub> concentrations in dry season in these two ecosystems could be related to the biomass burning source, which is generally recorded during the months of December-February in rural tropical environments and BVOC emissions. Indeed, in wet savannas (La, Dj), and forest (Zo) (Fig. 8), NO<sub>x</sub> and VOC anthropogenic fluxes reach their maxima during the dry season. The mean flux estimates are respectively 14.5; 24.2; 4.9 —ng.m<sup>-2</sup>.s<sup>-1</sup> for NO<sub>x</sub> and 26.8; 29.4; 5.5 ng.m<sup>-2</sup>.s<sup>-1</sup> for anthropogenic VOCs at La, Dj and Zo (Fig 8a, b and c). In La, Dj, Zo, Bo and Mb, BVOC maxima fluxes are also obtained at the end of the dry season/beginning of the wet season (Fig. 8e, f, g and h). A drop in these fluxes is then observed during the wet season. Strong Pearson correlations are observed between O<sub>3</sub>, NO<sub>x</sub> and the VOCs (0.49 < r < 0.92) (Table 45). Temperature and radiation are also well correlated with O<sub>3</sub> (0.54 < r < 0.89) in these two ecosystems. These results are corroborated by the literature. Indeed, radiation and humidity facilitate the propagation of radical chain reactions and the production of hydroxyl radicals (OH) at these sites (Graedel and Crutzen, 1993). According to several authors, O<sub>3</sub> levels tend to increase under warm, sunny conditions favorable to photochemical O<sub>3</sub> production (Hamdun and Arakaki, 2015; Morakinyo et al., 2020). Moreover, Aghedo et al. (2007), Mari et al. (2011), Saunois et al. (2009) and Saxton et al. (2007) have reported that vegetated areas emit large quantities of biogenic organic compounds that influence O<sub>3</sub> production in the presence of light and temperature. Others authors such as Abbadie (2006), Adon et al. (2010), and Galanter et al. (2000) and Tsvilidou et al. (2023) have linked the high O<sub>3</sub> concentrations recorded in the dry season to the presence of NO<sub>x</sub> emitted by biomass combustion in the wet savanna (Gulf of Guinea). According to Adon et al. (2010), Baldy et al. (1996), Clain et al. (2009), Cros et al. (1992), Hamdun and Arakaki (2015), Martins et al. (2007), Oluleye et al. (2013) the biomass burning is likely to contribute significantly to O<sub>3</sub> production through precursor emissions (NO<sub>x</sub> and CO) in the dry season (wet savanna) with nearly 30% to 80% of the savanna ground surface burnt annually between December and February. The high O<sub>3</sub> concentrations measured in Tranquebar (India) have been linked to increased emissions of NO<sub>x</sub> and other precursors from various sources (Debaje et al., 2003). Compared to wet and dry savannas, forest sites recorded the lowest O<sub>3</sub> amounts due to significant dry deposition of O<sub>3</sub> on the ground, on foliage and trees (Mari et al., 2011; Rummel et al., 2007; Saunois et al., 2009). Tropical forests are shown to be important O<sub>3</sub> sinks. A strong gradient of O<sub>3</sub> between forest and dry savanna in West Africa has been observed from aircraft measurements (Saunois et al., 2009).

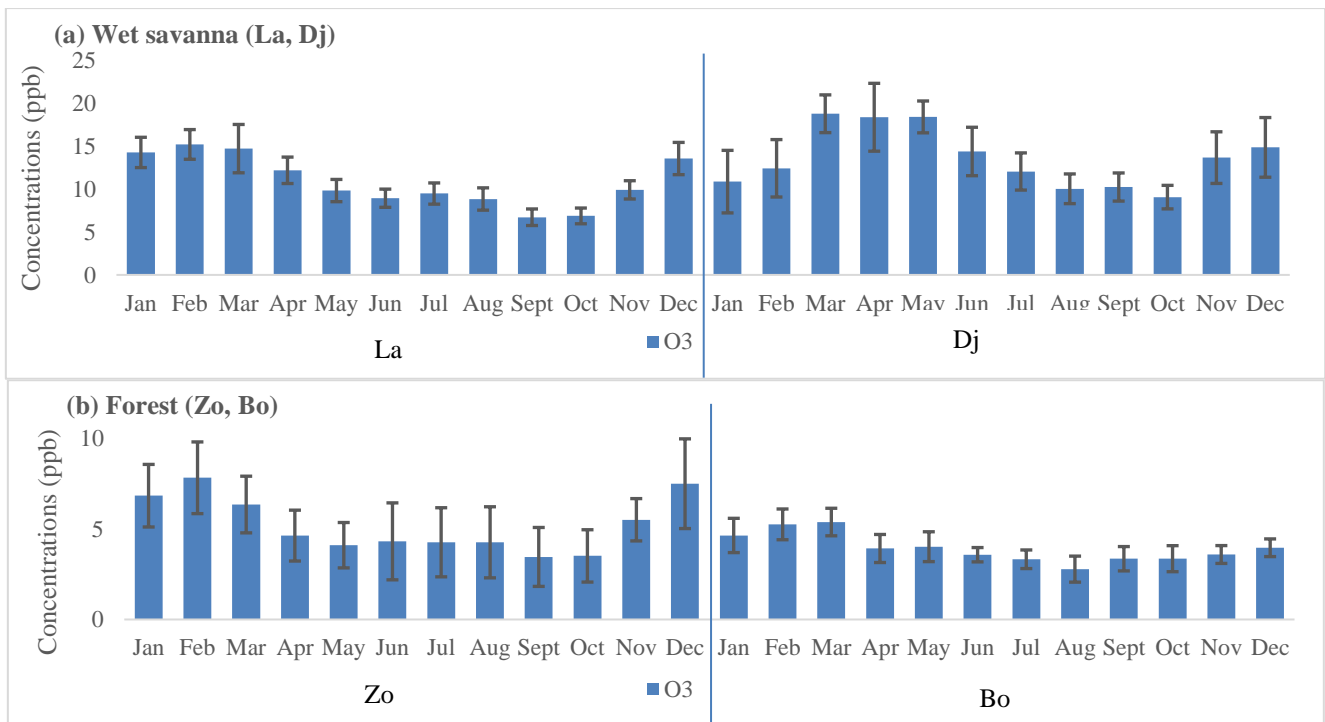
In Bo, high NO<sub>x</sub> and VOC fluxes are observed in the wet season (Fig. 8d), unlike in Zo (Fig. 8c) and, corroborated by Ossohou et al. (2019) over the period 1998-2015. The source of these recorded anthropogenic during this period of year at Bo emissions could be biomass combustion. Indeed, according to the work of Sauvage et al. (2005), the period from August to September corresponds to a peak in biomass burning activity in the southern African countries (Mozambique, Zimbabwe, South Africa). Moving air masses over Central Africa via the northern edge of the continental anticyclone could explain such high emissions at Bo in August-September.



485

**Figure 65.** Monthly evolution of O<sub>3</sub> concentrations (ppb) in (a) humid savanna, La (Cote d'Ivoire) and Dj (Benin) and (b) in forest, Zo (Cameroon) and Bo (Congo).

|



490

**Figure 76.** Mean monthly averages of O<sub>3</sub> concentrations (ppb) a) in humid savanna, La (Cote d'Ivoire) and Dj (Benin) and b) in forest, Zo (Cameroon) and Bo (Congo). Mean monthly averages are calculated from the long ozone data series of Fig. 6. Bars represent mean absolute deviation.

495

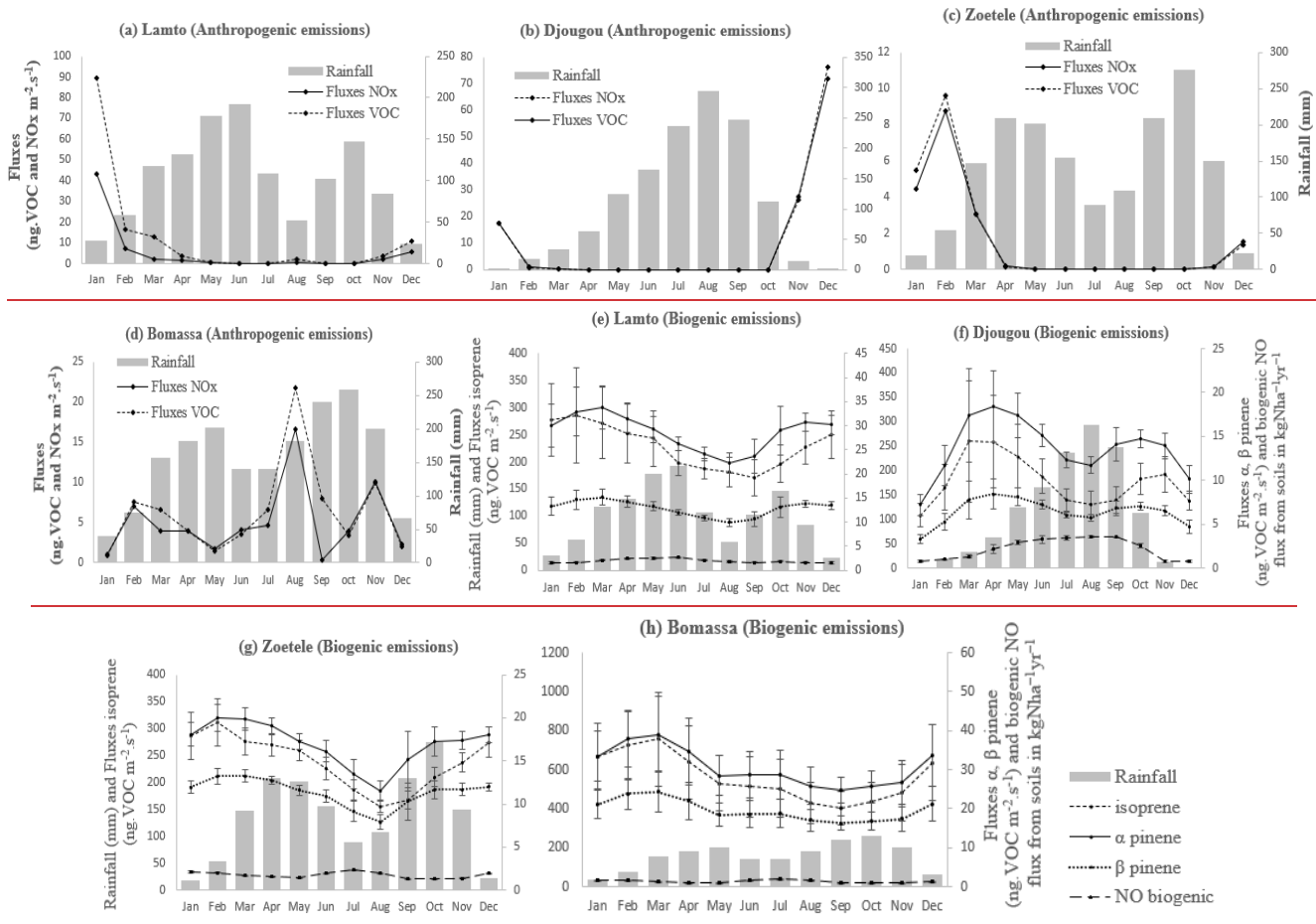


**Figure 8.** Mean monthly fluxes of natural and anthropogenic NO<sub>x</sub> and VOC estimated by the MEGAN and GFED4 inventories for 0.25° x 0.25° grid cells centered on each of wet savanna and forests

**Table 45.** Correlation *r* between O<sub>3</sub>, its precursors and meteorological variables at different sites. Blank spaces in the table indicate the absence of data on this site for the precursor concerned over the study period.

505

Ecosystem	Dry savanna					Wet savanna		Forest		Agricultural/semi-arid savanna				
	Ba	Ka	Ag	Bb	Da	La	Dj	Zo	Bo	Mb	LT	CP	Af	Sk
	<u>O<sub>3</sub></u>													
<u>NO biogenic</u>	0.85	0.73	0.92	=	=	-0.15	-0.24	0.43	-10 <sup>-3</sup>	=	=	=	=	=
<u>NO<sub>x</sub> C</u>	-0.33	-0.43	0.04	=	0.001	0.49	0.059	0.80	-0.33	0.31	0.37	-0.67	0.62	0.61
<u>VOC C</u>	-0.40	-0.47	-0.003	=	-5.10 <sup>-4</sup>	0.54	0.05	0.79	-0.40	0.31	0.60	-0.87	0.52	0.65

<u>isoprene</u>	<u>0.51</u>	<u>0.54</u>	<u>0.46</u>	<u>0.79</u>	<u>0.78</u>	<u>0.92</u>	<u>0.81</u>	<u>0.80</u>	<u>0.92</u>	<u>0.42</u>	<u>-0.39</u>	<u>-0.91</u>	<u>0.29</u>	<u>-0.64</u>
<u><math>\alpha</math> pinene</u>	<u>0.67</u>	<u>0.76</u>	<u>0.66</u>	<u>0.45</u>	<u>0.77</u>	<u>0.74</u>	<u>0.64</u>	<u>0.63</u>	<u>0.90</u>	<u>0.36</u>	<u>-0.45</u>	<u>-0.86</u>	<u>0.29</u>	<u>-0.67</u>
<u><math>\beta</math> pinene</u>	<u>0.70</u>	<u>0.79</u>	<u>0.72</u>	<u>0.34</u>	<u>0.72</u>	<u>0.70</u>	<u>0.56</u>	<u>0.60</u>	<u>0.89</u>	<u>0.33</u>	<u>-0.48</u>	<u>-0.85</u>	<u>0.27</u>	<u>-0.71</u>
<u>Temperature</u>	<u>0.45</u>	<u>0.47</u>	<u>0.42</u>	<u>0.51</u>	<u>0.76</u>	<u>0.72</u>	<u>0.69</u>	<u>0.68</u>	<u>0.89</u>	<u>0.47</u>	<u>-0.46</u>	<u>-0.90</u>	<u>0.49</u>	<u>-0.62</u>
<u>Humidity</u>	<u>0.82</u>	<u>0.64</u>	<u>0.95</u>	<u>0.52</u>	<u>0.70</u>	<u>-0.85</u>	<u>-0.19</u>	<u>-0.89</u>	<u>-0.79</u>	<u>-0.61</u>	<u>-0.79</u>	<u>-0.68</u>	<u>0.1</u>	<u>-0.80</u>
<u>Rainfall</u>	<u>0.74</u>	<u>0.64</u>	<u>0.75</u>	<u>0.15</u>	<u>0.51</u>	<u>-0.48</u>	<u>-0.39</u>	<u>-0.76</u>	<u>-0.54</u>	<u>-0.18</u>	<u>-0.49</u>	<u>0.74</u>	<u>0.53</u>	<u>-0.69</u>
<u>Radiation</u>	<u>0.16</u>	<u>0.15</u>	<u>0.26</u>	<u>0.75</u>	<u>0.69</u>	<u>0.73</u>	<u>0.54</u>	<u>0.65</u>	<u>0.87</u>	<u>0.21</u>	<u>-0.19</u>	<u>-0.76</u>	<u>0.71</u>	<u>-0.43</u>

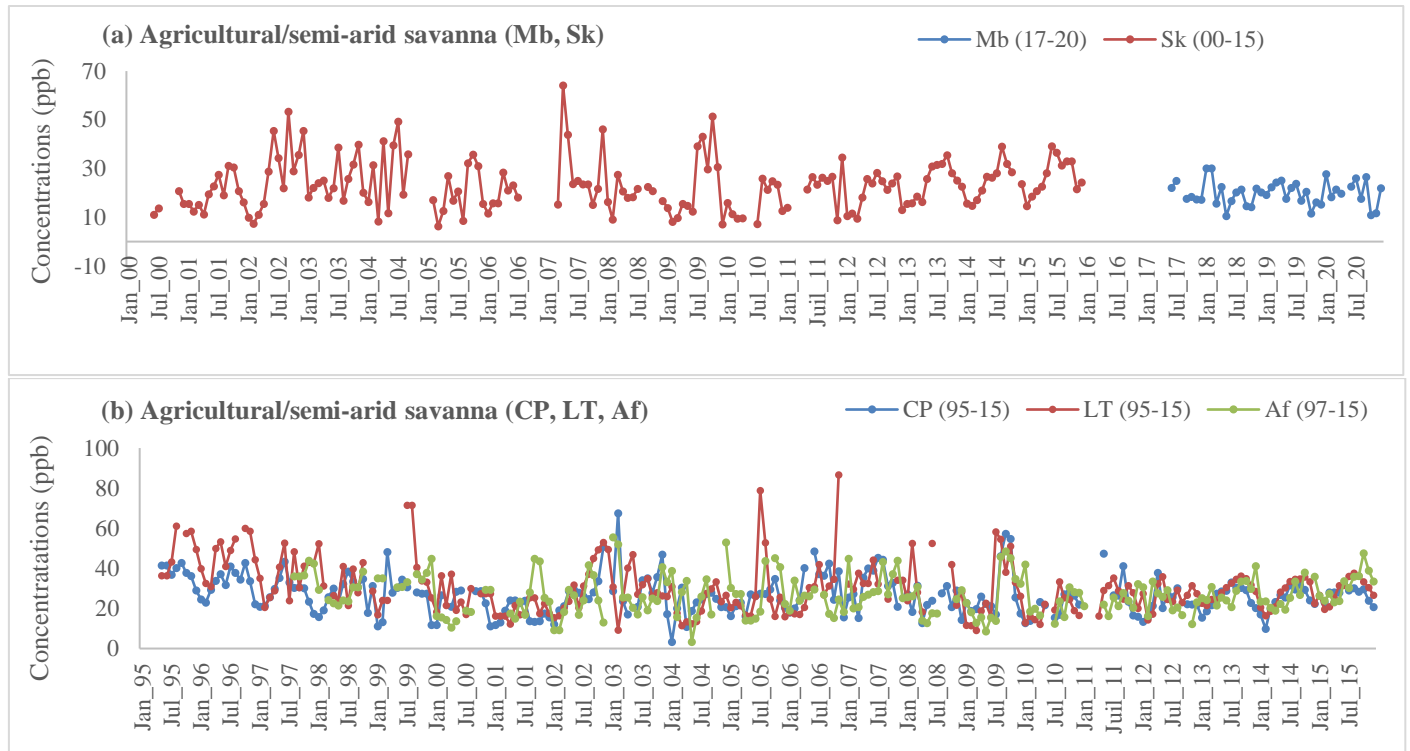
### 3.2.1.3 Agricultural and semi-arid savanna

Figure 97 presents the monthly evolution of surface O<sub>3</sub> concentration in agricultural site (Mb) and semi-arid savanna sites (LT, CP, Sk and Af). At Mb site, monthly O<sub>3</sub> concentrations do not exceed 30.2 ppb (Table 3). At the CP, LT, Sk and Af sites, O<sub>3</sub> levels are almost twice as high as in West African sites. The mean annual cycle of O<sub>3</sub> concentrations (Fig. 108a and b) shows that at Mb, O<sub>3</sub> levels are almost similar between seasons (Table 3). In southern African ecosystems, dry-season O<sub>3</sub> concentrations are the highest at LT and Sk. The annual averages are around 19.9±4.7 ppb at Mb; 22.8±7.3 ppb at Sk; 26.9±6.3 ppb at Af; 26.8±6.2ppb at CP and 30.8±8.0ppb at LT (Table 3).

These O<sub>3</sub> levels observed in Mb during the dry season could be associated with at the combustion sources biomass burning and natural emissions. Indeed, on the Fig. 11a, we observe NO<sub>x</sub> and VOC fluxes are quantifiable in February (dry season) at Mbita. Based on the analysis of burned surface areas, Bakayoko et al. (2021) indicated that Mb is strongly influenced by biomass burning from northern and southern sides during both dry seasons. High O<sub>3</sub> levels measured at Mb site during the dry season show similar values as in Nairobi, Kenya, during the same months (Kimayu et al., 2017). At the South African sites, the Fig. 11b, c, d and e shows the mean fluxes of anthropogenic emissions vary from 0.3 ng.m<sup>-2</sup>.s<sup>-1</sup> (LT) to 10.2 ng.m<sup>-2</sup>.s<sup>-1</sup> (Sk) for NO<sub>x</sub> and from 2.9 ng.m<sup>-2</sup>.s<sup>-1</sup> to 11.8 ng.m<sup>-2</sup>.s<sup>-1</sup> (Sk) for VOCs with the maxima recorded in dry season. As for the BVOC emissions (Fig. 11 g, i and j) At Southern African sites, more specifically at LT, Af and Sk, the highest values of BVOC are reached in the wet season: 189.6 ± 46.8 ng.m<sup>-2</sup>.s<sup>-1</sup> (isoprene), 14.2 ± 2.7 ng.m<sup>-2</sup>.s<sup>-1</sup> ( $\alpha$  pinene) and 5.6 ± 1.0 ng.m<sup>-2</sup>.s<sup>-1</sup> ( $\beta$  pinene). At CP (Fig. 11h), the maximum emissions are measured in the dry months of January/February. The calculations of correlation indicate ozone is linked to anthropogenic combustion sources at LT, Af and Sk and are anti-correlated with temperature, humidity, and radiation (-0.90 < r < -0.43) at LT, CP and Sk (Table 4). High O<sub>3</sub> concentrations are therefore measured at these sites during the driest and coldest months (Swartz et al., 2020b). Except at Af where O<sub>3</sub> has a weak link with BVOC, the increase of isoprene,  $\alpha$  pinene,  $\beta$  pinene emissions rate is positively correlated with O<sub>3</sub> decrease at the others sites. At the CP and Af sites, rainfall and O<sub>3</sub> are correlated (0.53 < r < 0.74) and ozone production could therefore also be linked to microbial activity of soils on these two sites. At CP site during the same study period, Swartz et al. (2020b) emphasised higher NO<sub>2</sub> concentrations were attributed to increased microbial activity in the wet season and O<sub>3</sub> seasonal pattern corresponded to the NO<sub>2</sub> seasonality, which was attributed to their related chemistry. The importance of humidity and temperature in O<sub>3</sub> photochemistry observed at almost all South African sites has been highlighted by Balashov et al. (2014) and Laban et al. (2018, 2020).

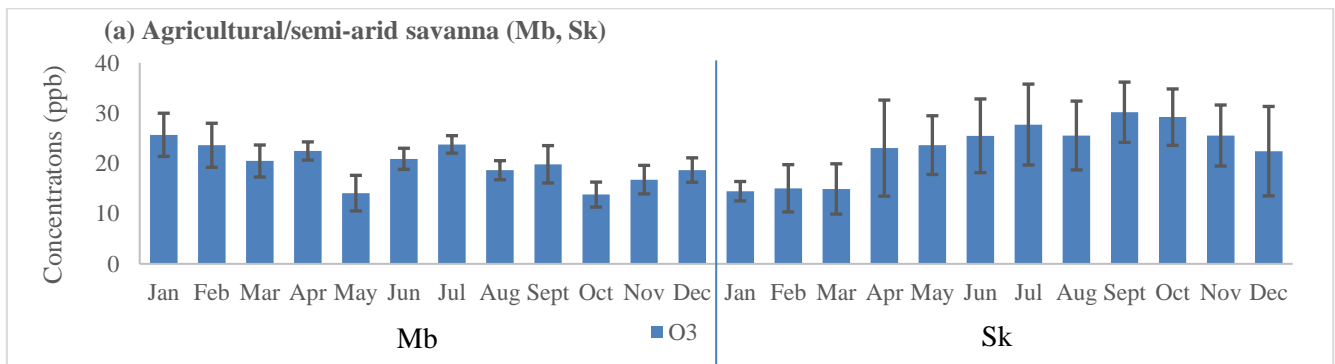
At southern African sites, O<sub>3</sub> levels could be also attributed to a combination of regional and local influences, including emissions from industrial, vehicular and domestic biomass combustion to biomass combustion events in sub-Saharan Africa (Mozambique, Zambia, Zimbabwe and Angola) recirculated by anticyclonic air mass processes (Baldy et al., 1996; Laban et al., 2018; Martins et al., 2007; Swap et al., 2003; Tiitta et al., 2014). Biomass combustion is considered as a major source of O<sub>3</sub> precursors in South Africa (Ngoasheng et al., 2021; Vakkari et al., 2013) and in Southern Africa (Heue et al., 2016) and may explain the O<sub>3</sub> levels observed in dry season at LT and Sk. The high O<sub>3</sub> levels in the wet season (at Af and CP) are thought to be due to soil microbial activity (Swartz et al., 2020a) could be also explained by as well as long-range transport of air pollutants emitted from the industrialized Highveld region (Abiodun et al., 2014; Ojumu, 2013). During the austral winter,

545 O<sub>3</sub> concentrations in the boundary layer are higher (e.g. at CP and Af) due to a systematic increase in O<sub>3</sub> precursors from households, combustion for space heating (Bencherif et al., 2020; Laban et al., 2018; Lourens et al., 2011; Oltmans et al., 2013; Swartz et al., 2020b). The high concentrations measured at Af could also be due to industrial activities located near this site (Lourens et al., 2011).

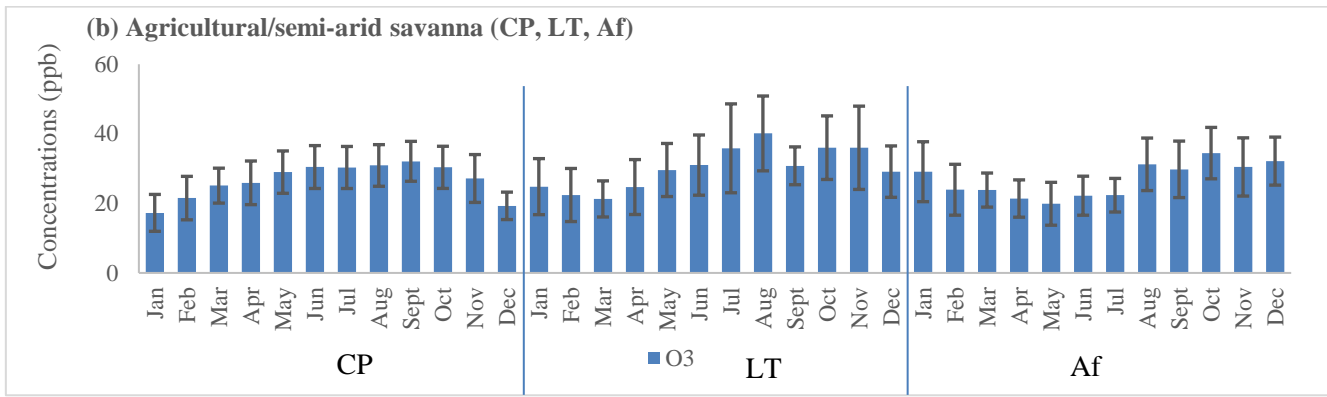


550

**Figure 27.** Monthly evolution of O<sub>3</sub> concentrations (ppb) in Agricultural/semi-arid savanna (a) Mb (Kenya) and Sk (South Africa) and (b) CP, LT and Af (South Africa).

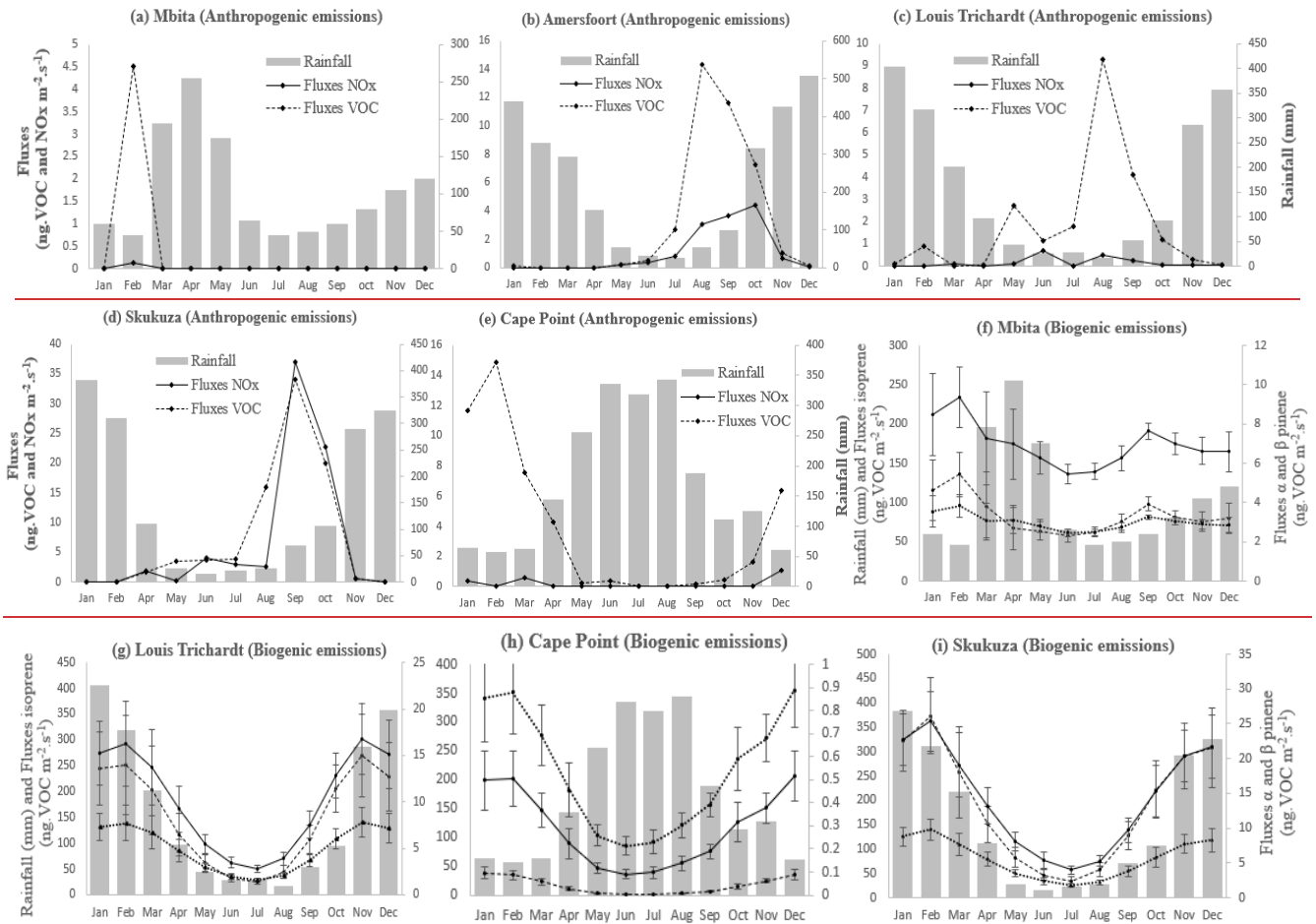


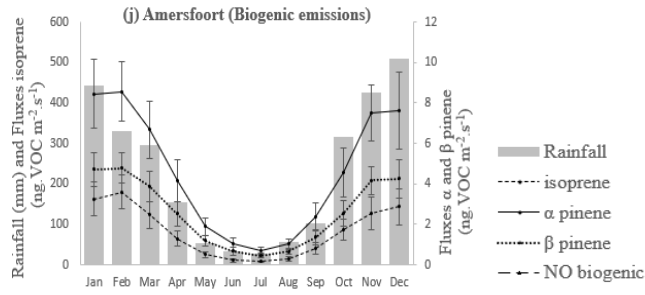
555



**Figure 108.** Mean monthly averages of O<sub>3</sub> concentrations (ppb) in Agricultural/semi-arid savanna (a) Mb (Kenya) and Sk (South Africa) and (b) CP, LT and Af (South Africa). Mean monthly averages are calculated from the long ozone data series of Fig. 9. Bars represent mean absolute deviation.

560



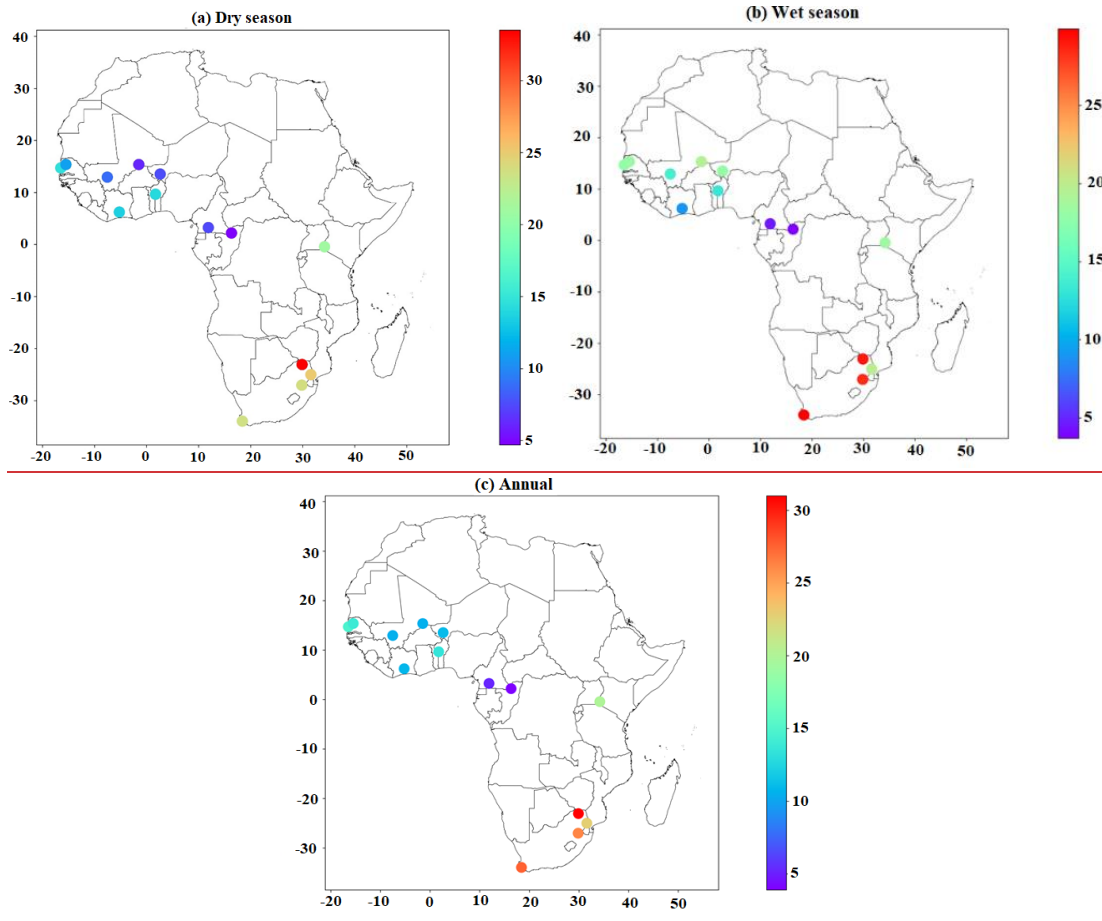


565

**Figure 11.** Mean monthly fluxes of natural and anthropogenic NO<sub>x</sub> and VOC estimated by the MEGAN and GFED4 inventories for 0.25° x 0.25° grid cells centered on each of agricultural/semi-arid savanna sites

### 3.2.2 O<sub>3</sub> levels in Africa, set in a global context

570 O<sub>3</sub> concentrations measured at the 14 studied site are mapped on a seasonal and annual scale (Fig. 129).



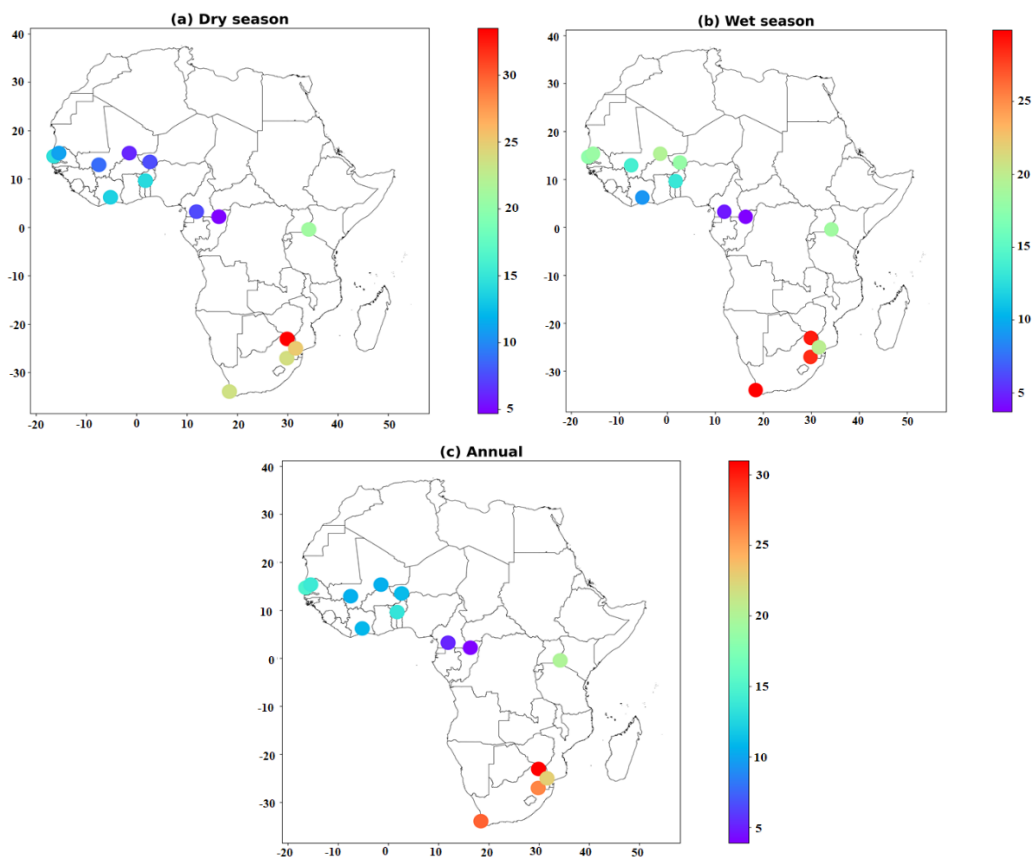


**Figure 129.** Seasonal and annual mapping of O<sub>3</sub> concentration levels in (a) Dry season (Ba, Ka, Ag, Da and Bb: October to May ; La and Dj: November to March ; Zo : December to February and July to August ; Bo: December to February ; Mb: June to October and January to February ; LT, Sk and Af : April to September; CP: October to March), (b) Wet season (Ba, Ka, Ag, Da and Bb: June to September; La and Dj: April to October ; Zo : March to June and September to November ; Bo: March to November ; Mb: March to May and November to December ; LT, Sk and Af : October to March ; CP : April to September) and (c) Annual over the 14 studied sites.

We compared African ozone levels related in this study with studies carried out in Africa and around the world over the last 20 years (Table 54, Fig. 130). The bibliographical synthesis takes into account studies where data measurement methodology has been clearly described. Sites where concentrations have been measured by passive samplers are listed. We have identified among others, sites in Nepal, North America, North-Eastern Europe, Asia and Africa. Figure 130 focuses more on O<sub>3</sub> monitoring studies in Africa.

**Table 54.** O<sub>3</sub> concentrations at various sites worldwide as reported in literature

Sites	Type	Period	O <sub>3</sub> (ppb)	References
India, Tranquebar	Rural	May 1997 -Oct 2000	17±7 - 23 ± 9	Debaje et al. (2003)
Sweden, Malmö (20 sites)	Rural		37.0±5.4	
	Urban		35.0±3.9	



Sweden, Umeå (20 sites)	Traffic	(16–24 Apr 2012 ; 28 May–4 Jun; 20– 27 Aug 2012	33.6±3.5	Hagenbjörk et al. (2017)
	Rural		27.7±8.4	
	Urban		26.7±7.3	
	Traffic		25.2±6.9	
China, Waliguan mountain	Rural	Sept 99-May 2001	44.9	Carmichael et al. (2003)
Taiwan, Shui-Li	Rural		25.0	
Malaysia, Tanah Rata	Rural		16.0	
Indonesia, Bukit Kototabang	Rural		10.7	
Inde, Agra	Rural		30.8	
Argentina, Isla Redonda	Rural		15.9	
Brazil, Arembepe	Rural		19.2	
Turkey, Camkoru	Rural		35.4	
Arab Emirates, Al-Ain	Rural	Apr 2005-Apr 2006	8.7	Salem et al. (2009)
	Industrial		5.9	
	Traffic		4.4	
	Commercial		5.9	
	Residential		7.3	
American Samoa Island, Tutuila	Urban and Rural	1990-2015	13.7 ± 1.0	Lu et al. (2018)
Chili, El Tololo			32.0 ± 1.3	
South Africa, Cape point			24.3 ± 1.1	
Australia, Cape grim			24.9 ± 0.8	
New Zealand, Baring head			21.4 ± 1.6	
Syowa			25.2 ± 0.9	
Neumayer-G			24.3 ± 1.5	
Arrival heights			25.9 ± 1.5	
South Pole			28.4 ± 1.7	
Nepal, Bode			Urban	
Nepal, Indrachowk	37.9 ± 6.2			
Nepal, Maharajgunj	46.4 ± 12.0			
Nepal, Mangal Bazaar	40.3 ± 8.0			
Nepal, Suryabinayak	41.3 ± 5.4			
Nepal, Bhaisepati	Suburban	47.7 ± 9.1		
Nepal, Budhanilkantha		50.3 ± 11.3		
Nepal, Kirtipur		46.9 ± 9.8		
Nepal, Lubhu		50.7 ± 8.6		
Nepal, Bhimdhunga		59.7 ± 11.9		
Nepal, Nagarkot	Rural	70.1 ± 9.7		
Nepal, Naikhandi		53.5 ± 13.0		
Nepal, Nala Pass		43.6 ± 10.5		
Nepal, Sankhu		57.6 ± 11.9		
Nepal, Timpiple		54.4 ± 13.4		
Barrow Atmospheric Baseline Observatory		Remote site	1973-2015	15-44
Mauna Loa Observatory (MLO)	Remote site	1973-2015	26-65	
American Samoa Observatory	Remote site	1973-2015	5-20	
South Pole Observatory	Remote site	1973-2015	17-40	
China			34	
Central East China			36	

Beijing–Tianjin–Hebei region	Rural site	2014-2017	39	Dufour et al. (2021)
Yangtze River Delta			35	
Pearl River Delta			31	
North America, Europa and Est Asia (Korea et Japan)	3136 Rural sites	2010-2014	0-56 and more	Gaudel et al. (2018)
North America, Europa and Est Asia	3348 Rural sites and 1453 urban sites	2010-2014	0-100 and more	Fleming et al. (2018)
North America, Europa and Est Asia	Rural site	1996-2005	15-55	Young et al. (2018)
North America, Europa and Est Asia	Rural and urban site	2010-2014	10-60	Schultz et al. (2017)
Eastern North America	Rural site	2000-2014	26-38	Chang et al. (2017)
	Urban site		28-38	

Several sites reported in Table 54 and Fig. 10 are exposed to high O<sub>3</sub> concentrations. These different levels observed in Africa and around the world are in most cases above values displayed in this study, with the exception of sites in southern Africa.

595 Indeed, in Africa particularly, the earlier studies investigated have mentioned high ozone concentrations measured in southern  
Africa. Laban et al. (2018) have observed the elevated surface ozone (O<sub>3</sub>) concentrations over four sites in South Africa  
(Botsalano (2006-2008), Marikana (2008-2010), Welgegund (2010-2015) and Elandsfontein (2009- 2010)) with an annual  
mean ranging around from 5 to 70 ppb. The temporal O<sub>3</sub> patterns observed at the four sites resembled typical trends for O<sub>3</sub> in  
600 continental South Africa, with O<sub>3</sub> concentrations peaking in late winter and early spring (Laban et al., 2018). The assessment  
of long-term seasonal and inter-annual trends of a 21-year ozone passive sampling (monthly means) dataset collected at the  
Cape Point Global Atmosphere Watch (CPT GAW) station indicated that annal mean ozone level at this coastal area is of 26  
ppb (Swartz et al., 2020b) while at Louis Trichardt (1995-2015), Amersfoort (1997-2015) and Skukuza (2000-2015) the level  
ranging from 22 ppb to 31 ppb (Swartz et al., 2020a). Over the sites of Botswana (1999-2001) and the Mpumalanga highveld,  
605 Zunckel et al. (2004) emphasized the springtime maximum of O<sub>3</sub> concentrations is between 40 and 60 ppb, but reached more  
than 90 ppb as a mean in October 2000. At the background stations at Cape Point (2000-2002), in Namibia (2000-2002) and  
areas adjacent to the highveld the maximum concentrations are between 20 and 30 ppb with minimums between 10 and 20  
ppb. Ngoasheng et al. (2021) have investigated on the surface ozone concentrations during the period from 2014 to 2015 and  
2018 to 2019 over ten sites located at North West in South Africa (8 ppb à 48 ppb). In addition, a more intensive campaign  
was conducted in June, July and August 2019 during what, 15 additional sites were also monitored. During the campaign from  
610 September 1999 to June 2001 of the newly established WMO/GAW Urban Research Meteorology and Environment (GURME)  
project, the mean values of ozone concentrations over the sites of Elandsfontein (35.1 ppb), Cape point (24.2 ppb) in South  
Africa, Tamanrasset in Algeria (33.2 ppb), Mt. Kenya (31.5 ppb) were evaluated and indicated high values over many sites  
(Carmichael et al 2003). Over a period of nine to 11-year (1995-2005) at four remote sites: Louis Trichardt (South Africa),  
Cape Point (South Africa), Amersfoort (South Africa) and Okaukuejo (Namibia) in southern Africa, Martins et al. (2007)  
615 exhibited a fairly constant high mean value of ozone about 27 ppb throughout the region except for the Louis Trichardt site,  
with a relatively high 10-year mean of 35 ppb. These values are approximately two times higher compared to Western and  
Central Africa INDAAF ozone data. The main reason ~~for the discrepancies~~ could be the proximity of ~~South Africa~~ these sites  
to O<sub>3</sub> precursor sources. They are generally located close to industrial, commercial and residential areas, not far from road  
traffic, garbage dumps, etc., where precursor emissions are high. Some sites may also be influenced by continental air masses  
620 containing gaseous pollutants. From 2012 to 2015, Hamdun and Arakaki (2015) measured surface ozone levels at three urban  
sites (Mapipa, Ubungo, and Posta) and two suburban sites (Kunduchi and Vijibweni) in the city of Dar es Salaam and in the  
village of Mwetemo, a rural area of Bagamoyo, Tanzania. Ozone levels at suburban (7.9-23.6) ppb sites were generally higher

625 than at urban sites (10.3-18.6) ppb. In the context of the POLCA (Pollution of African Capitals) program, O<sub>3</sub> was measured using a passive sampling technique from Jan. 2008 to Dec. 2009 at Dakar and from Jun. 2008 to Dec. 2009 at Bamako (Adon et al., 2016). The mean annual concentrations of O<sub>3</sub> are 7.7 ppb in Dakar and 5.1 ppb in Bamako, respectively. At Abidjan during an intensive campaign within the dry season (15 December 2015 to 16 February 2016), using INDAAF (International Network to study Deposition and Atmospheric chemistry in Africa) passive samplers exposed in duplicate for 2- week periods (Bahino et al., 2018), the highest O<sub>3</sub> concentration measured is at the two coastal sites of Gonzagueville and Félix-Houphouët-Boigny International Airport located in the southeast of the city, with average concentrations of 19.1 ± 1.7 and 18.8 ± 3.0 ppb, respectively.

630 At urban sites such as Al-Ain, Bamako, Dakar, Abidjan and Cotonou, the low O<sub>3</sub> levels are due to the saturated NO<sub>x</sub> regime observed at these sites, which limits photochemical O<sub>3</sub> production (Adon et al., 2013; Bahino et al., 2018; Salem et al., 2009). At most INDAAF sites, concentrations are lower because of their rural characteristics, generally far from anthropogenic sources, and much more influenced by biogenic activities from soils and vegetation. In the framework of IDAF Program, Adon et al. (2010) analysed ozone concentrations from 2000 to 2007 over the sites of Banizoumbou (Niger), Katibougou and Agoufou (Mali), Djougou (Benin), Lamto (Cote d'Ivoire), Zoetele (Cameroon) and Bomassa (Congo). Annual mean O<sub>3</sub> concentrations are lower for all ecosystems and range from 4.0±0.4 ppb (Bomassa) to 14.0±2.8 ppb (Djougou) and are the same order of magnitude over period 2000-2020 (INDAAF program) where concentrations ranging from 3.9±1.1 ppb (Bomassa) to 14.8±4.3 ppb at Bambey in Western and Central Africa. Results are fairly illustrative of the various mitigation or vigilance measures that need to be adopted to ensure the environmental well-being of each ecosystem. The additional efforts

635 must therefore be made, through projects or programs, to densify monitoring networks for polluting gases in general and O<sub>3</sub> in particular, especially in Africa, where very few long-term monitoring exist.

640

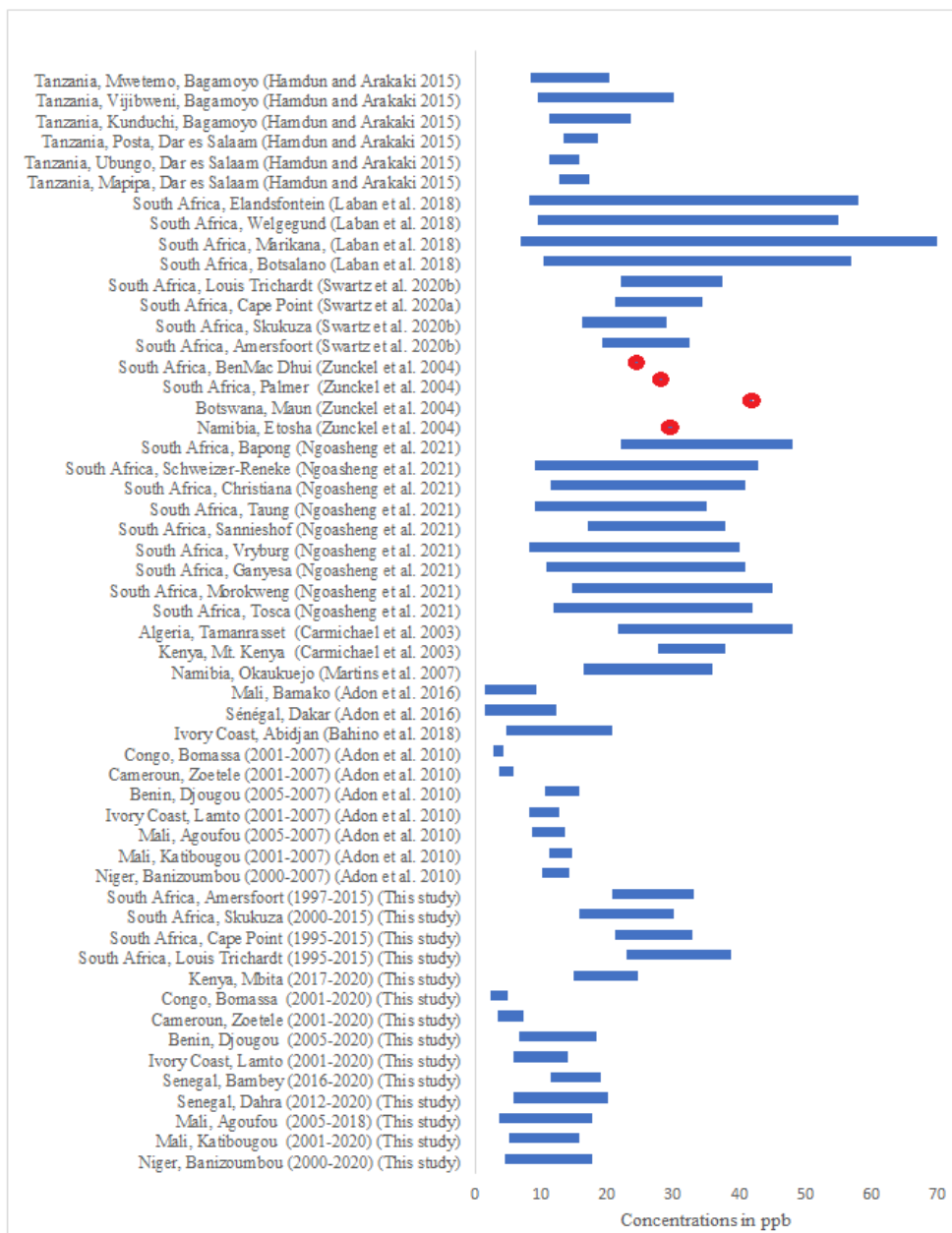


**Figure 13.** Overview of O<sub>3</sub> monitoring studies in Africa. Blue bars represent lower and upper range of means if reported. Red points represent average concentration of O<sub>3</sub>.

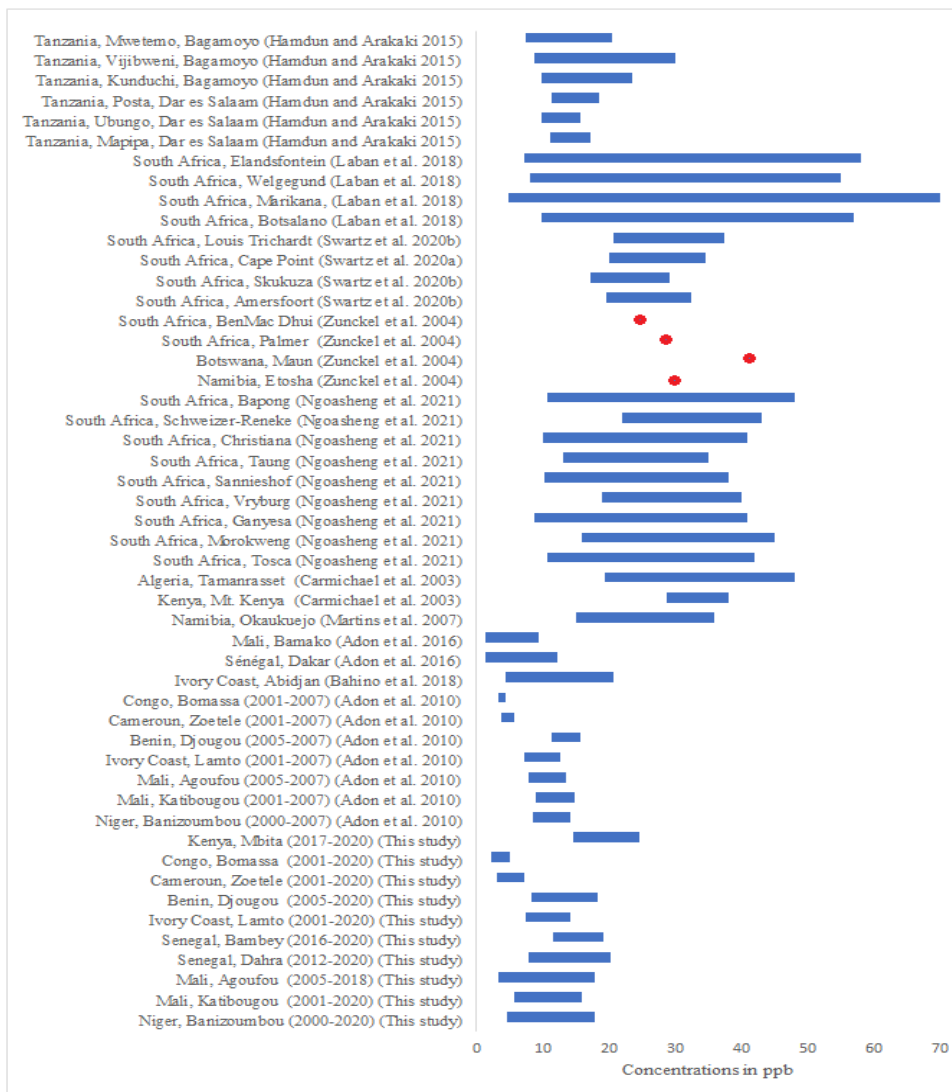


**Figure 10.** Overview of  $O_3$  monitoring studies in Africa. Blue bars represent lower and upper range of means if reported. Red points represent average concentration of  $O_3$ .

650

### 3.3 Monthly variation in $NO_x$ and VOC anthropogenic and natural emissions

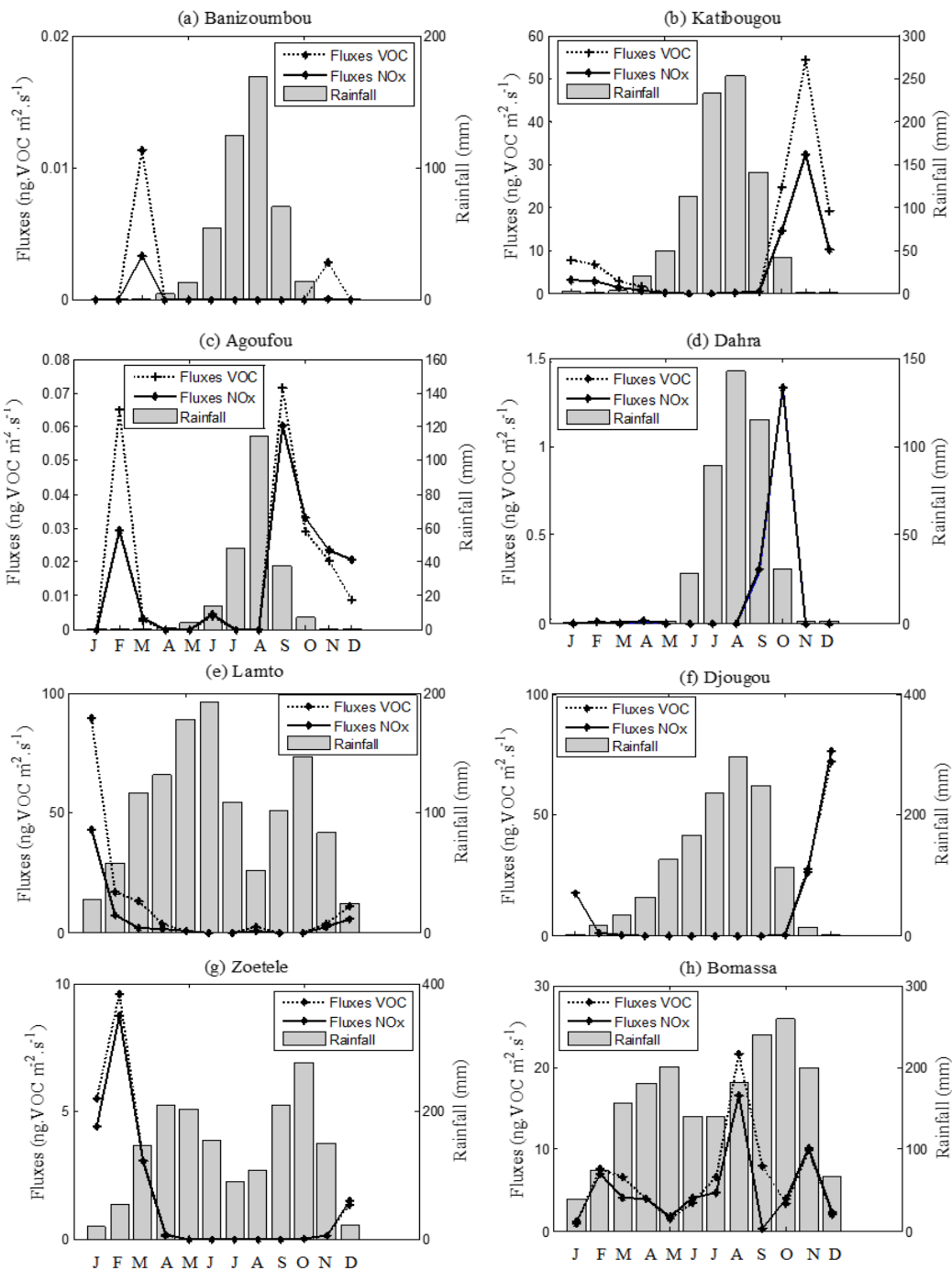
Tropospheric  $O_3$  concentrations result from atmospheric chemistry involving precursors especially  $NO_x$  and VOCs, and from transport (distance and time). Locating the sources of precursors (both biogenic and anthropogenic), and their amplitude, is therefore necessary to explain  $O_3$  levels, on a local and regional scale.

655

660

### 3.3.1 NO<sub>x</sub> and VOC anthropogenic emissions

Monthly variation in anthropogenic NO<sub>x</sub> and VOC emissions are studied at all sites, with the exception of the Bb station, where emission data are not available (Fig. 11). In dry savanna, during the wet season, NO<sub>x</sub> and VOC fluxes are very low. On the other hand, maxima are observed in the dry season with the highest emissions found in Ka. Indeed, the monthly averaged biomass combustion emissions (GFED4) over the 18 year period (1998-2015) in the Sahel show that Ka is significantly affected by the biomass combustion source in November (Ossohou et al., 2019). In wet savannas (La, Dj), and forest (Zo), NO<sub>x</sub> and VOC fluxes reach their maxima during the dry season. The mean flux estimates are respectively 14.5; 24.2; 4.9 ng.m<sup>-2</sup>.s<sup>-1</sup> for NO<sub>x</sub> and 26.8; 29.4; 5.5 ng.m<sup>-2</sup>.s<sup>-1</sup> for anthropogenic VOCs at La, Dj and Zo. High dry season NO<sub>x</sub> emission rates observed are linked to biomass combustion sources (Abbadie, 2006; Adon et al., 2010; Akpo et al., 2015; Ossohou et al., 2019; Swartz et al., 2020b). In Bo, high NO<sub>x</sub> and VOC fluxes are observed in the wet season, unlike in Zo, corroborated by Ossohou et al (2019) over the period 1998-2015. The source of these recorded anthropogenic emissions could be biomass combustion. Indeed, according to the work of Sauvage et al. (2005), the period from August to September corresponds to a peak in biomass burning activity in the southern African countries (Mozambique, Zimbabwe, South Africa). Moving air masses over Central Africa via the northern edge of the continental anticyclone could explain such high emissions at Bo in August-September. NO<sub>x</sub> and VOC fluxes are quantifiable in February (dry season) at Mbita and are thought to be due to the combustion of biomass from agricultural activities and from biomass burning in savannas north of the site (South Sudan, Central African Republic and Democratic Republic of Congo) (Bakayoko et al., 2021; Boiyo et al., 2017b). At the South African sites, the mean fluxes vary from 0.3 ng.m<sup>-2</sup>.s<sup>-1</sup> (LT) to 10.2 ng.m<sup>-2</sup>.s<sup>-1</sup> (Sk) for NO<sub>x</sub> and from 2.9 ng.m<sup>-2</sup>.s<sup>-1</sup> to 11.8 ng.m<sup>-2</sup>.s<sup>-1</sup> (Sk) for VOCs with the maxima recorded in dry season. These values may be explained by significant anthropogenic emissions from domestic biomass burning and solid fuel combustion resulting in high levels of pollutants in South Africa's Highveld region (Kai et al., 2022). By developing an African regional inventory of anthropogenic emissions (wood and charcoal burning, charcoal manufacture, open waste burning etc.), Keita et al. (2021) estimate that Southern Africa is among the highest emitting regions for NO<sub>x</sub>, due to industrial sources and power plants. Using satellite data for NO<sub>2</sub> between 2005 and 2017, Oluleye (2021) has noted that nitrogen dioxide concentrations during the dry season were up to 200% higher than the values observed during the rainy season. The high NO<sub>x</sub> and VOC levels observed at the different sites during the dry season result from these different sources, releasing large quantities of precursors in the atmosphere, and not washed out by rainfall.



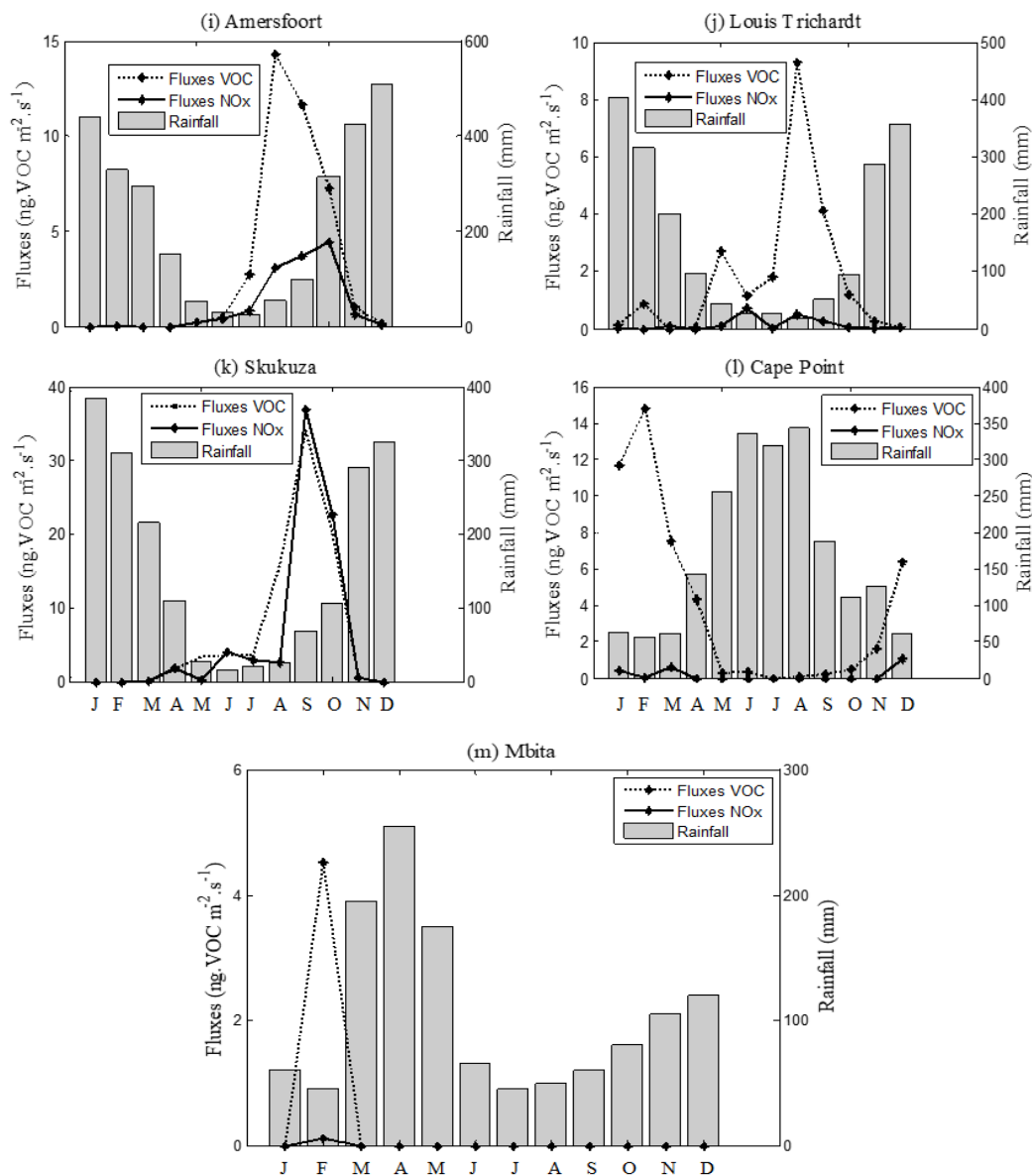


**Figure 11.** Mean monthly fluxes of NO<sub>x</sub> and VOC from biomass combustion estimated by the GFED4 inventory for 0.25° × 0.25° grid cells centered on each of dry savanna, wet savanna, forest and semi-Agricultural/arid savanna sites.

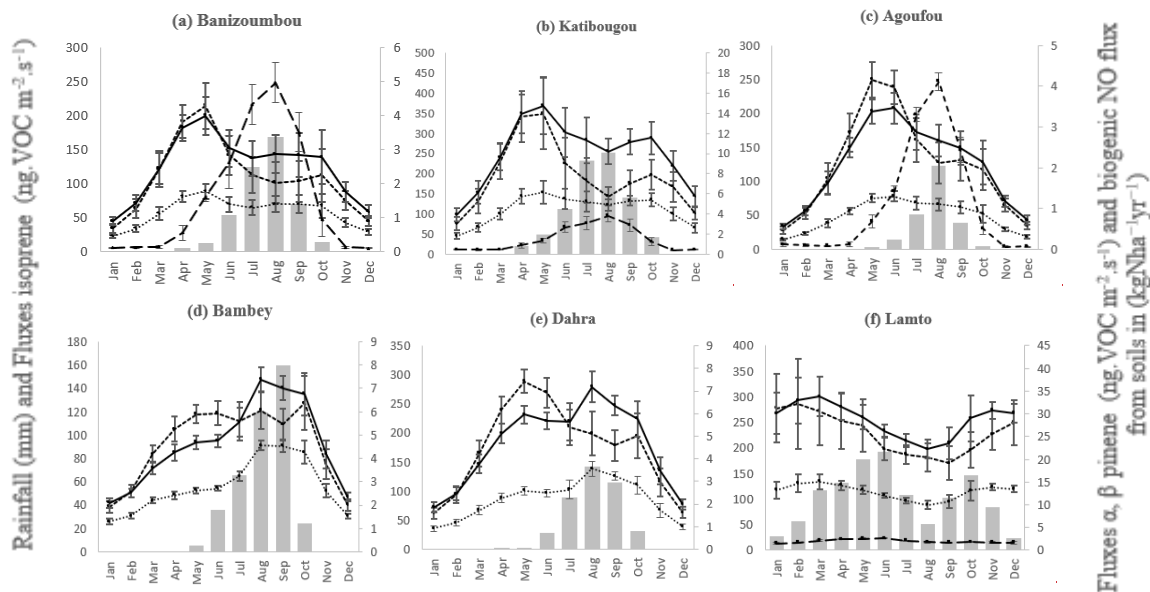
### 695 3.3.2 NO<sub>x</sub> and VOC natural emissions

Monthly variations in VOCs ( $\alpha$  pinene,  $\beta$  pinene and isoprene) and biogenic NO around the studied sites are shown in Fig. 12. ~~Biogenic NO fluxes in dry savanna show a bell-shaped variation, peaking in August (wet season).~~ In wet savanna and forest, the highest values are also recorded during the wet season. Peaks range from  $2.1 \pm 0.1$  (Bo) to  $5.0 \pm 0.6$  kgNha<sup>-1</sup>.year<sup>-1</sup> (Ba) in the three ecosystems. These peaks of emission could be explained by the correlation between soil moisture, NO production in the soil and its release to the atmosphere, as shown in Delon et al., (2010), Galy-Lacaux et al., (2009), Onojeghuo et al. (2017) and as illustrated in Sect. 3.2.1.1. The soil moisture content during the dry season is higher in wet savanna and forest than in

700



dry savanna, which limits the NO pulse in these ecosystems (Delon et al., 2012). Monthly profile of BVOC fluxes (isoprene,  $\alpha$ -pinene and  $\beta$ -pinene) in dry savanna shows a maximum at the end of the dry season/beginning of wet season at Ba, Ka and Ag, or during the wet season at Bb and Da. Isoprene fluxes are more obvious at Da ( $214.2 \pm 30$ )  $\text{ng}\cdot\text{m}^{-2}\cdot\text{s}^{-1}$  whereas  $\alpha$ -pinene, and  $\beta$ -pinene exhibit larger values at Ka site ( $11.2 \pm 1.8$ ;  $5.2 \pm 0.8$   $\text{ng}\cdot\text{m}^{-2}\cdot\text{s}^{-1}$  respectively). In La, Dj, Zo, Bo and Mb, BVOC maxima fluxes are also obtained at the end of the dry season/beginning of the wet season. A drop in these fluxes is then observed during the wet season. From dry savanna to forest, the transect gradient is positive for BVOC emissions, and is due to the abundance of vegetation in wet savanna (La) and forest. At Southern African sites, more specifically LT, Af and Sk, the highest values of BVOC are reached in the wet season:  $189.6 \pm 46.8$   $\text{ng}\cdot\text{m}^{-2}\cdot\text{s}^{-1}$  (isoprene),  $14.2 \pm 2.7$   $\text{ng}\cdot\text{m}^{-2}\cdot\text{s}^{-1}$  ( $\alpha$ -pinene) and  $5.6 \pm 1.0$   $\text{ng}\cdot\text{m}^{-2}\cdot\text{s}^{-1}$  ( $\beta$ -pinene). At CP, the maximum emissions are measured in the dry months of January/February. BVOC emission rates variation is a function of several factors, namely temperature (Guenther et al., 1993), carbon dioxide ( $\text{CO}_2$ ) concentration, precipitation, plant species (Jaars et al., 2016), crops, shrubs (Guenther et al., 1995), modulated on seasonal and interannual time scales by changes in land cover and canopy environment (Chen et al., 2018) as well as by climate change. In dry savanna, the peaks in BVOC observed at the end of the dry season (April/May) could therefore be due to strong radiation and high temperatures which could impact certain woody species (Zwarts et al., 2023), and cause biogenic emissions (Saxton et al., 2007). Indeed, woody species in grasslands are major sources of BVOC emissions (Jaars et al., 2016). Furthermore, positive correlations were obtained between isoprene emissions and air temperature (Jaars et al., 2016; Guenther et al., 1993; Saxton et al., 2007). In the forest, Serça et al. (2001) reported that the average ambient isoprene concentration for a tropical forest in northern Congo was the highest at the start of the rainy season and fell sharply at the end of the rainy season. At the Welgegund site (South Africa), which belongs to the same ecosystem as LT, Af and Sk, Jaars et al. (2016) also measured the highest BVOC concentrations during the rainy season as in this study, and increased BVOC concentrations were associated with high soil moisture. Gradual decrease in BVOC fluxes during the wet season observed at most of the sites is thought to be due to the uptake of VOCs by soils, thanks to the microbial activity that develops during this period. Soils could therefore play an important role as isoprene sinks (Gray et al., 2015).



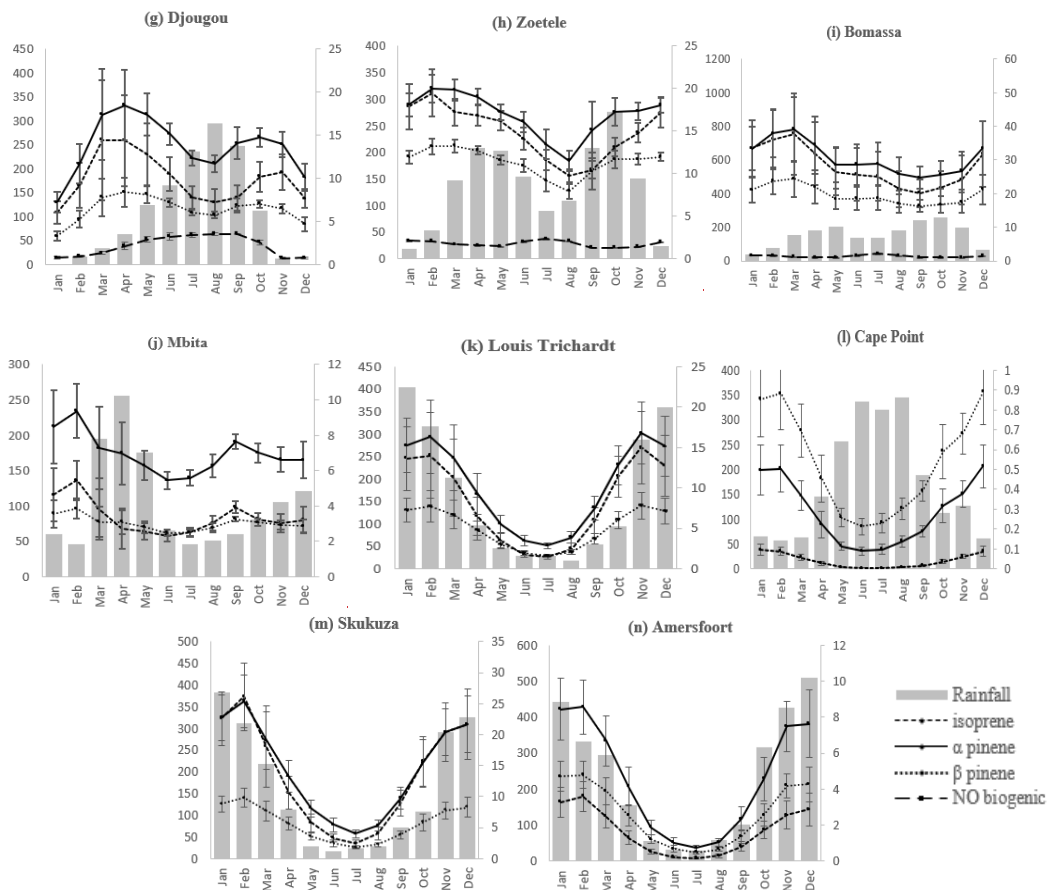


**Figure 12.** Mean monthly fluxes of BVOCs estimated by the MEGAN inventory for  $0.25^\circ \times 0.25^\circ$  centered meshes and biogenic NO in dry savanna, wet savanna, forest and semi Agricultural/arid savanna.

### 3.4. Contributions of meteorological variables, NO<sub>x</sub> and VOC to O<sub>3</sub> production

In this section, we use PCA to estimate the relevant number of axes (Sect. 3.4.1) to identify the major sources of O<sub>3</sub>-precursor emissions at each site, based on their contribution to the construction of the axis and the quality of their representation on the axis (Sect. 3.4.2).

#### 3.4.1. Estimation of the inertia of the studied factors

At all sites, ten to eleven factors (meteorological variables and chemical pollutants) are studied. Each factor could correspond to a given axis. However, the cumulative inertia calculated indicated that the first two axes ranged from 79.9% (Ag) to 95.4% (Af) at all sites (Fig. 13). These values are well above the reference value of 54.2% (Tsuyuzaki et al., 2020). These axes therefore represent the main axes. The high inertia values obtained indicate that the factors studied are not independent and that there are strong links between them. The projection of the dataset onto the factorial plane (with two axes) is therefore a good approximation of the air quality at each site, as it contains most of the available information.

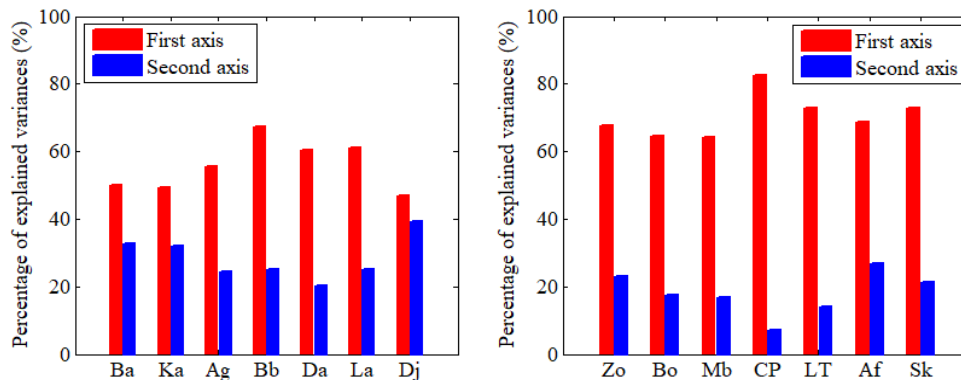


**Figure 13.** Decomposition of the total inertia of  $O_3$ -precursors on the factorial axes.

### 3.4.2. Characterisation of $O_3$ -precursor emission sources and studies of correlations

#### 3.4.2.1 Dry savanna

At the dry savanna sites, two groups of pollutants can be identified through their contribution to the two axes.  $O_3$ ,  $\alpha$  pinene,  $\beta$  pinene, isoprene and  $NO$  are strongly correlated with the first axis ( $0.58 < r^2 < 0.98$ ) and  $NO_x$ , VOCs anthropogenic fluxes correlate well with the second axis ( $0.62 < r^2 < 0.92$ ). These results suggest the presence of two major sources of precursors: biogenic and anthropogenic activities. Calculating the Pearson correlation between the different pollutants, we observe a good dependence of  $O_3$  only with all biogenic precursors ( $0.51 < r < 0.95$ ) at Ba, Ka and Ag in the presence of high relative humidity and precipitation ( $0.64 < r < 0.95$ ) (Table 5). On the other hand, at Bb and Da, isoprene correlates well with  $O_3$  ( $r = 0.79$ ). It appears as a dominant precursor under the influence of temperature and radiation, which are also well correlated with  $O_3$  ( $0.5 < r < 0.76$ ) (Table 5). The main contributions to the formation of the first axis are observed for BVOC (39.5% to 44.6%) with a good quality of representation (0.5 to 0.9) (Fig. 14). The contribution of biogenic  $NO$  is about 10%. The most relevant meteorological variables (humidity, temperature, precipitation, radiation) contribute significantly, ranging from 10.5% to 30.8%. In dry savanna, Ohuleye et al. (2013) estimated that rain was responsible for 62% of the  $O_3$  distribution in the West African region, excluding the precursors  $NO$ ,  $CO$  and hydrocarbons, as also illustrated in our results. Saunois et al. (2009) have shown that soil  $NO_x$  emissions, combined with the northward advection of volatile organic compounds (VOCs), play a key role in  $O_3$  production in dry savanna regions. This large scale impact of biogenic emissions has also been verified by Williams et al. (2009), who estimate that 2–45% of tropospheric  $O_3$  over equatorial Africa may originate from  $NO_x$  emissions from African soils. All these works are in agreement with the results of this study.

#### 3.4.2.2 Wet savanna and forest

In wet savanna and forest, pollutants such as  $O_3$ ,  $\alpha$  pinene,  $\beta$  pinene, isoprene, anthropogenic  $NO_x$  and VOCs (except at Bo and Dj) are positively correlated to the same axis ( $0.62 < r^2 < 0.97$ ), while only  $NO$  is linked to the second axis. The major sources highlighted in this case could be anthropogenic activities and those linked to biogenic vegetation on the one hand, and biogenic soil activities on the other. Strong Pearson correlations are observed between  $O_3$ ,  $NO_x$  and the VOCs ( $0.49 < r < 0.92$ ) (Table 5). Temperature and radiation are also well correlated with  $O_3$  ( $0.54 < r < 0.89$ ) in these two ecosystems. The dominant contributors are then BVOC (31% to 60.8%), temperature (11% to 12.1%), radiation (11.1% to 12.4%) (Fig. 14). Anthropogenic emissions at La and Zo make a significant contribution (5.8% to 10.2%). These results are corroborated by the literature. Indeed, radiation and humidity facilitate the propagation of radical chain reactions and the production of hydroxyl radicals (OH) at these sites (Graedel and Crutzen, 1993). According to several authors,  $O_3$  levels tend to increase under warm, sunny conditions favorable to photochemical  $O_3$  production (Hamdun and Arakaki, 2015; Morakinyo et al., 2020). Moreover,

780 ~~Aghedo et al. (2007), Mari et al. (2011), Saunois et al. (2009) and Saxton et al. (2007) have reported that vegetated areas emit large quantities of biogenic organic compounds that influence O<sub>3</sub> production in the presence of light and temperature.~~

### 3.4.2.3 Agricultural and semi-arid savanna

785 At the South African sites, the major sources of pollutant vary from one site to another. At Af, we identify a first group of pollutants ( $\alpha$  pinene,  $\beta$  pinene, isoprene) strongly dependent on the first axis ( $0.98 < r^2 < 0.99$ ), suggesting the presence of a source linked to biogenic activities originating from vegetation. On the other hand, the second group, comprising O<sub>3</sub>, VOCs and NO<sub>x</sub> anthropogenic, indicates a source from combustion activities ( $0.83 < r^2 < 0.89$ ), which favors O<sub>3</sub>-photochemistry. At CP, LT and Sk sites, the pollutant category in which O<sub>3</sub> is found is linked to biogenic emissions (VOCs) and combustion sources. At these sites, temperature, humidity, precipitation and radiation are anti-correlated with O<sub>3</sub> ( $-0.90 < r < -0.43$ ) (Table 5). High O<sub>3</sub> concentrations are therefore measured at these sites during the driest and coldest months (Swartz et al., 2020b). The main contributions are BVOCs, NO<sub>x</sub> and anthropogenic VOCs, temperature and rainfall at CP, VOCs, humidity, temperature at Sk, NO<sub>x</sub> and anthropogenic VOCs, and radiation at Af and anthropogenic VOCs, radiation, humidity at LT. These factors contribute between 5.1% and 39.4% (Fig. 14) to the formation of the axes, with a good representation quality (0.44 to 0.97) for most of them. Observations made at South African sites are confirmed by several recent studies. Indeed, Swartz et al. (2020b) attributed the decrease in O<sub>3</sub> concentrations from 1995 to 2001 to the decrease in NO<sub>2</sub> concentrations over this period at LT. The importance of humidity and temperature in O<sub>3</sub>-photochemistry observed at almost all South African sites has been highlighted by Balachov et al. (2014), Laban et al. (2018, 2020). Laban et al. (2018) added that emissions from domestic combustion (in winter) and regional biomass combustion (in spring) are also responsible for the increase of O<sub>3</sub> levels. The contribution of VOCs to O<sub>3</sub>-photochemistry in South Africa is confirmed by Jaars et al. (2016). At Mb, neither of the two main axes has a significant relationship with O<sub>3</sub>, with a poor quality of representation on the main axes (0.14). Further studies on other precursors such as biogenic NO and carbon monoxide (CO) should be carried out, and biomass combustion on a continental scale should also be taken into account, in order to better assess the dominant chemical contributions to O<sub>3</sub> production at this site.

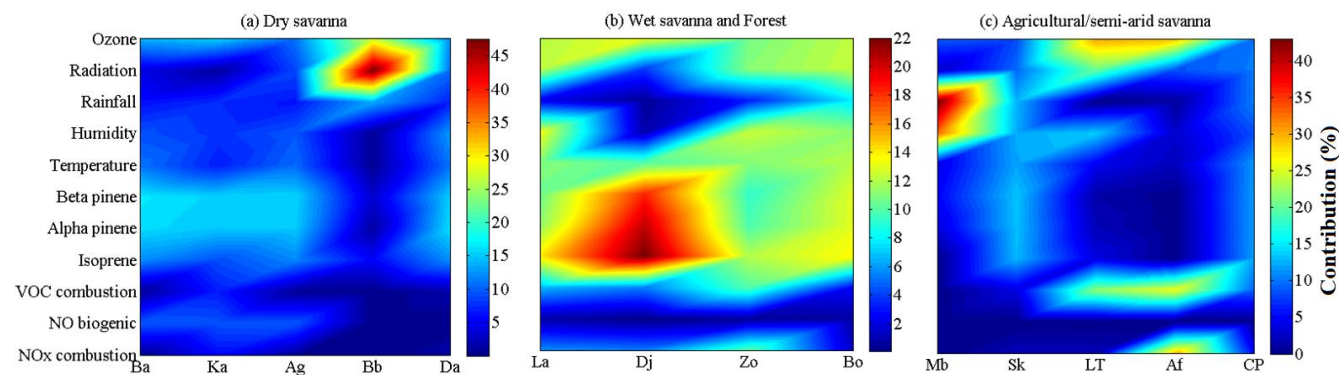


**Figure 14.** Contribution of different variables to photochemical O<sub>3</sub> pollution in (a) Dry savanna (b) West savanna and Forest (c) Agricultural/semi arid savanna.

810

**Table 5.** Correlation r between O<sub>3</sub>, its precursors and meteorological variables at different sites. Blank spaces in the table indicate the absence of data on this site for the precursor concerned over the study period.

Ecosystem	Dry savanna					Wet savanna		Forest		Agricultural/semi-arid savanna				
Sites	Ba	Ka	Ag	Bb	Da	La	Dj	Ze	Be	Mb	LT	CP	Af	Sk
	O <sub>3</sub>													
NO <sub>x</sub> biogenic	0.85	0.73	0.92	-	-	-0.15	-0.24	0.43	-10 <sup>-2</sup>	-	-	-	-	-
NO <sub>x</sub> _C	-0.33	-0.43	0.04	-	0.004	0.49	0.059	0.80	-0.33	0.31	0.37	-0.67	-0.62	0.61
VOC_C	-0.40	-0.47	-0.003	-	-5.10 <sup>-3</sup>	0.54	0.05	0.79	-0.40	0.31	0.60	-0.87	-0.53	0.65
isoprene	0.51	0.54	0.46	0.79	0.78	0.92	0.81	0.80	0.92	0.42	-0.39	-0.91	-0.29	-0.64
α pinene	0.67	0.76	0.66	0.45	0.77	0.74	0.64	0.63	0.90	0.36	-0.45	-0.86	-0.29	-0.67
β pinene	0.70	0.79	0.72	0.34	0.72	0.70	0.56	0.60	0.89	0.33	-0.48	-0.85	0.27	-0.71
Temperature	0.45	0.47	0.42	0.51	0.76	0.72	0.69	0.68	0.89	0.47	-0.46	-0.90	0.49	-0.62
Humidity	0.82	0.64	0.95	0.52	0.70	-0.85	-0.19	-0.89	-0.79	-0.61	-0.79	-0.68	0.1	-0.80
Rainfall	0.74	0.64	0.75	0.15	0.51	-0.48	-0.39	-0.76	-0.54	-0.18	-0.49	0.74	0.53	-0.69
Radiation	0.16	0.15	0.26	0.75	0.69	0.72	0.54	0.65	0.87	0.21	-0.19	-0.76	0.71	-0.43

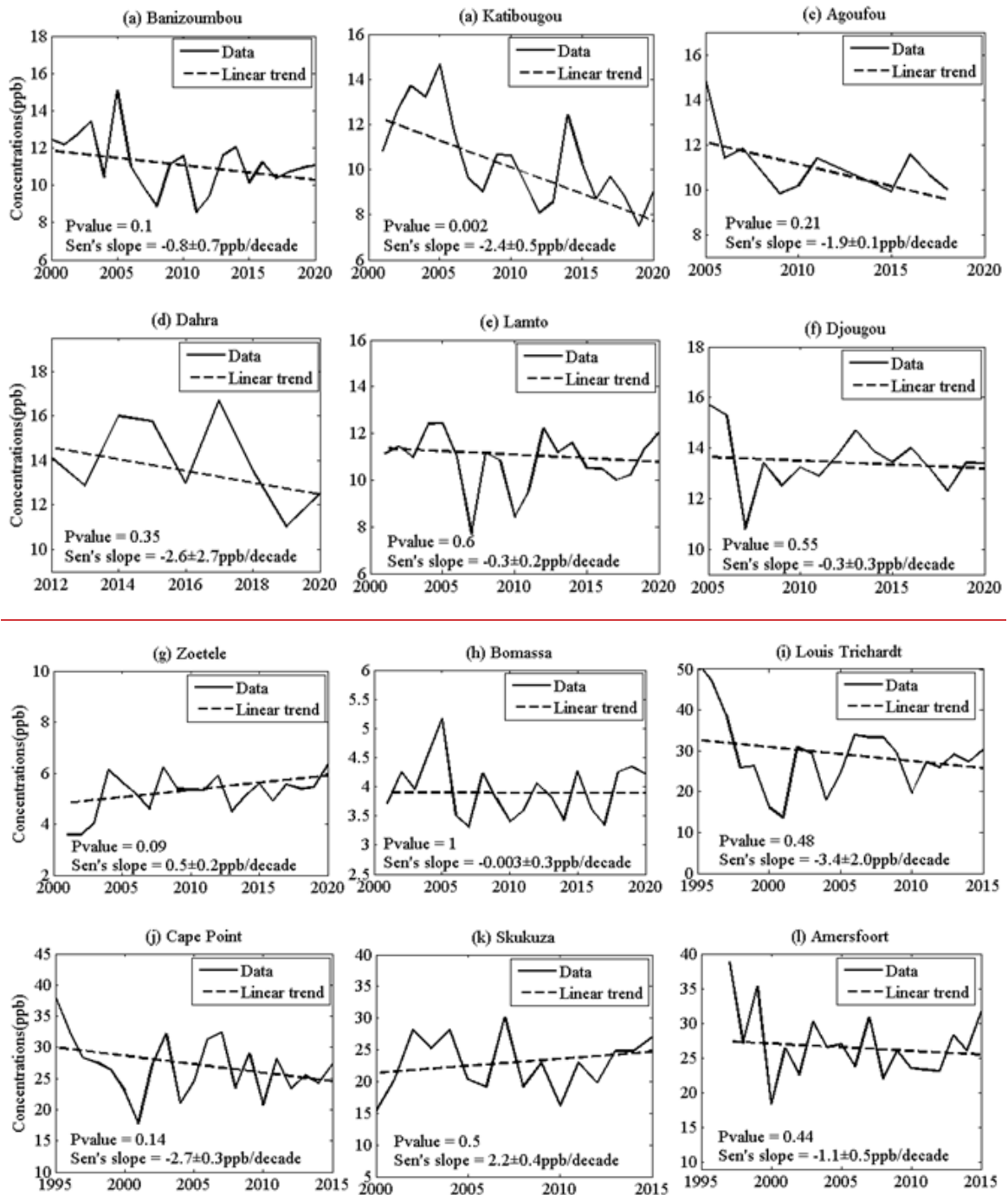
### 3.35 Annual and seasonal trends of O<sub>3</sub> and its precursors

#### 3.35.1 Annual trends

Annual trends in O<sub>3</sub> concentrations were calculated all sites (except Bambe and Mbita which do not have 10 years of measurements) according to -95% confidence intervals in Mann-Kendall test in dry savanna, wet savanna, forest and Agricultural/semi-arid savanna to Mann-Kendall test (Fig. 145). -At the annual scale, Katibougou site in Mali shows a significant decrease in O<sub>3</sub> concentrations around 2.4 ppb decade<sup>-1</sup> -0.24 ppb yr<sup>-1</sup> (-2.3 % yr<sup>-1</sup>) from 2001 to 2020 (pvalue = 0.002) at the 95% confidence level. This At the seasonal scale, this downward trend at Katibougou is confirmed in both the dry and wet seasons. Ozone concentrations decrease by -1.8 ppb decade<sup>-1</sup> -0.18 ppb (-2.1 % yr<sup>-1</sup>; (pvalue = 0.03) per year in the dry season and -3.3 ppb decade<sup>-1</sup> -0.33 ppb (-2.4 % yr<sup>-1</sup>; (pvalue < 0.01) in the wet season. At the same site, the trend in nitrogen oxide (NO<sub>2</sub>) over the 1998-2020 period shows a decline in annual concentrations and annual seasonal means. Osshou et al. (2019) observed a decrease in NO<sub>2</sub> concentrations at Katibougou in the wet season of (-0.4 ppb decade<sup>-1</sup>) -0.04 ppb yr<sup>-1</sup> (-2.4 % yr<sup>-1</sup>) over the period 1998-2015. These downward trends in NO<sub>2</sub> could therefore explain the downward trends in O<sub>3</sub>. At the Banizoumbou site (Niger) a medium certainty for a decrease trend by -0.8 ppb decade<sup>-1</sup> of O<sub>3</sub> concentrations (pvalue = 0.1) is noted at a 95% confidence level. During the dry period, a significant this downward trend is calculated with high certainty recorded, with O<sub>3</sub> decreasing by -1.5 ppb decade<sup>-1</sup> -0.15 ppb yr<sup>-1</sup> (-1.9 % yr<sup>-1</sup>; (pvalue = 0.04). Calculation of trends on biogenic VOCs at Banizoumbou indicate a decrease in biogenic emissions of alpha pinene (τ = -0.37, p value = 0.020) and beta pinene (τ = -0.39, p value = 0.01). Chen et al. (2018) indicated that trends in global tree cover from 2000 to 2015 have led to clear decreases, particularly in West Africa with a reduction of around 10% in regional BVOC emissions due to agricultural expansion. At the sites of Agoufou (Mali) and Bambe (Senegal), a low certainty of the O<sub>3</sub> concentrations decrease is observed (respectively pvalue = 0.21; pvalue = 0.35). In wet savanna and forests, Lamto (Cote d'Ivoire) and Djougou (Benin) sites show a downward trend by -0.3 ppb decade<sup>-1</sup>. At 95% confidence interval, there is very low certainty that this trend will occur. In West Africa generally, we note a decrease in surface ozone concentrations even if this trend is not significant at almost all sites. On these remote sites, this decrease could be partly linked to a large decrease in burned area in tropical savannas in Africa, particularly those with low and intermediate levels of tree density (Andela et al., 2017). At Bomassa site (Congo) (pvalue = 1), we have no trend contrary to Zoetele (Cameroon) where an increase of O<sub>3</sub> concentrations by 0.5 ppb decade<sup>-1</sup> is recorded, with a medium certainty. To explain the trends observed at Zoetele, we apply the Kendall rank correlation between O<sub>3</sub> concentrations and its precursors. We obtain a significant positive rank correlation at the 95% confidence level. For NO<sub>x</sub>

845 and anthropogenic VOCs,  $\tau = 0.7$  (pvalue= 0.03) while with biogenic VOCs, the correlation varies from 0.54 to 0.69 (pvalue <0.01). In addition, we observe increasing trends for biogenic VOCs. Isoprene increases by  $18 \text{ ng.m}^{-2}\text{s}^{-1}$  per decade (pvalue = 0.001), alpha pinene by  $1 \text{ ng.m}^{-2}\text{s}^{-1}$  per decade (pvalue < 0.001) and beta pinene by  $0.4 \text{ ng.m}^{-2}\text{s}^{-1}$  per decade (pvalue = 0.003). Similar trends were also observed in the wet season for alpha pinene and beta pinene, and in the dry season for isoprene. The rise in  $\text{O}_3$  concentrations in Zoetele could therefore be explained by these increasing trends observed in isoprene, alpha pinene and beta pinene from one season to the other and in anthropogenic emissions in African forest regions. These results are corroborated by 18 years of satellite data (1998-2015) by Andela et al. (2017) who noted an increasing trend in burned areas close-canopy forests. In South Africa sites, at Louis Trichardt (pvalue = 0.48) and Amersfoort (pvalue = 0.44), a downward trend is reported with a very low certainty respectively by  $-3.4 \text{ ppb decade}^{-1}$  and  $-1.1 \text{ ppb decade}^{-1}$  at scale confidence of 95%. The same negative trend is recorded at Cape Point (pvalue = 0.14) with a low certainty (by  $-2.7 \text{ ppb decade}^{-1}$ ). At Skukuza (pvalue = 0.49), an increase of  $\text{O}_3$  concentrations by  $2.21 \text{ ppb decade}^{-1}$  with no evidence of trends at a confidence threshold of 95% is observed. At the other sites, no significant trends were observed. The absence of annual trends at South African sites assessed with certainty confirms the results obtained by Swartz et al. (2020a, 2020b) at the Louis Trichardt, Amersfoort, Skukuza and Cape Point sites using multiple linear regression model approach. Indeed, the trend lines for the  $\text{O}_3$  concentrations measured during the entire sampling periods indicate slight negative slopes at Amersfoort and Louis Trichardt and a small positive slope at Skukuza (Swartz et al., 2020a). Gaudel et al. (2020) and Wang et al. (2022) have observed that annual trends of median ozone values have increased in the tropospheric column (950 to 250 hPa) respectively around  $2 \text{ nmol mol}^{-1} \text{ decade}^{-1}$  during 22 years (1994-2016) of measurement and of  $2.61 \pm 0.34 \text{ ppbv per decade}$  (1995-2017) above Gulf of Guinea. These results are contrary to the decrease in ozone observed at the INDAAF sites in the Gulf of Guinea (Lamto and Djougou), which show no trend. To partly explain the increase of ozone in recent decades, Gaudel et al. (2020) pointed out that although  $\text{NO}_x$  emissions from biomass combustion have decreased in the tropics, this decrease has been overcompensated by the increase in fossil fuel emissions. However, we believe that the discrepancy between these studies could be explained by the proximity of the measurement sites to the sources of precursor emissions. Indeed, the data measured from the commercial aircraft monitoring network used in the work of Gaudel et al. (2020) are taken at airports closer to cities, whereas INDAAF sites are rural sites, far from fossil fuel combustion sources. In addition, Gaudel et al. (2018) reported that spatially, global surface ozone trends are highly variable depending on time period, region, elevation and proximity to fresh ozone precursor emissions. The distributions of ozone annual trends in the recent two decades (2000-2019) explored by Hou et al. (2023) over six regions on the world including Africa ( $25^\circ\text{S}-25^\circ\text{N}$ ,  $17^\circ\text{W}-51^\circ\text{E}$ ) showed a significant increase in these six regions of the Tropospheric Column Ozone (OMI/MLS satellite data), with the smallest value of  $\sim 0.07 \text{ DU/yr}$  in the African while with MET+2015EMIS model, the annual trends of ozone over Africa turn to insignificant decreases ( $0.04 \text{ DU/yr}$ ). These trends, which contrast with the changes observed at most INDAAF sites, could support that ozone surface data do not necessarily represent the free troposphere where the radiative forcing effects of ozone are concentrated. We also think that the ozone trends could be estimate more accurately in combining of the soundings and long-term surface observations is necessary. Breaks in the annual concentration data were observed at Ba and Ka in 2006 as a result of the Pettitt test. During the dry and wet seasons, further breaks were recorded in the annual series in 2006 (Ka) and 2007 (Ba) (dry season) and in 2014 at Ka (wet season). However, no trend inversion was induced in these break years. At the other study sites, no breaks were observed.

880



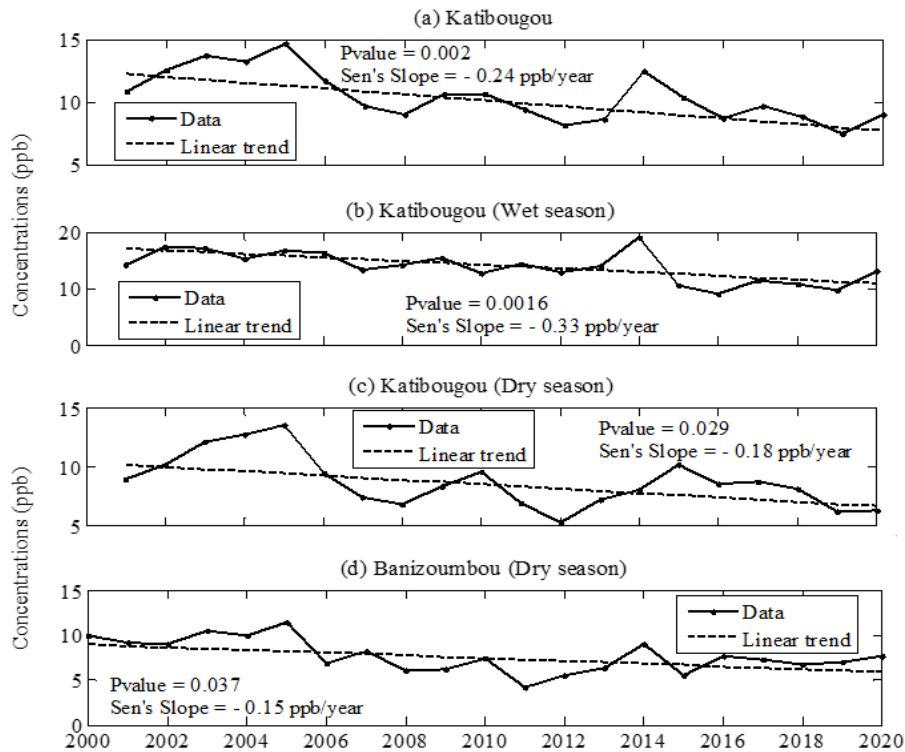


**Figure 145.** Significant long-term annual linear trend of in situ O<sub>3</sub> concentrations over the period 1995-2000-2020 at 95% confidence intervals calculated for 12 measurement sites representative of African dry savanna, wet savanna, forest and agricultural/semi-arid savannas and p-value for each trend.

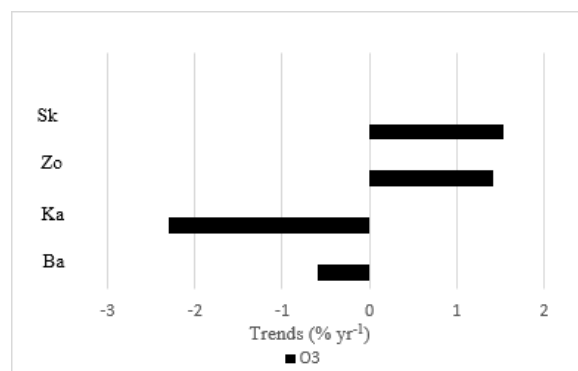
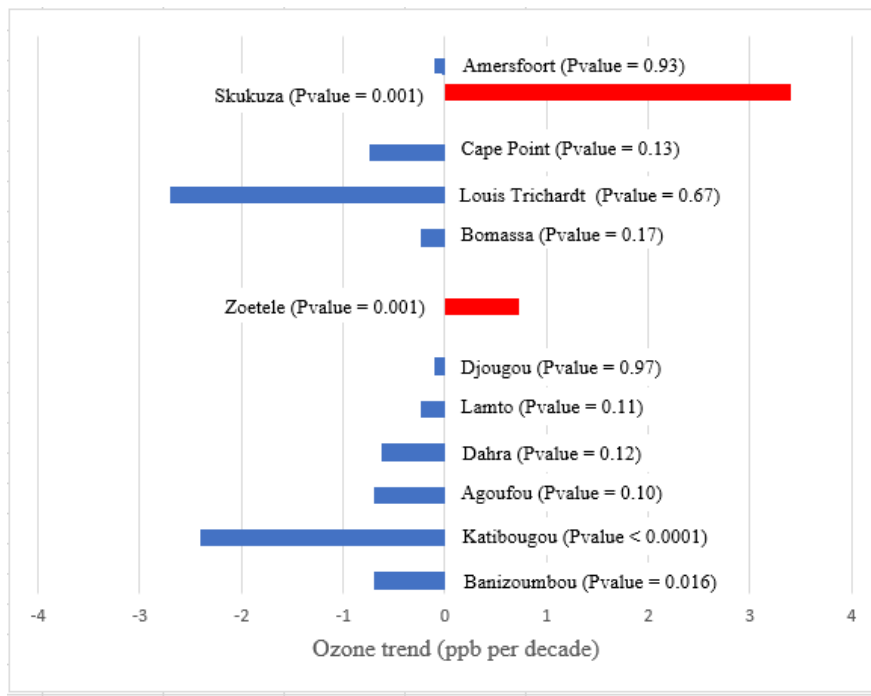
### 3.35.2 Seasonal trends

Trend tests were performed on monthly mean O<sub>3</sub> concentrations using seasonal Kendall test and all significant trend results are presented in Fig. 156. Test reveals a downward trend of  $-0.7 \text{ ppb decade}^{-1}$  at Banizoumbou (pvalue = 0.02), with high certainty at 95% confidence level. At Ka (pvalue < 0.001), O<sub>3</sub> concentrations decrease by  $-2.4 \text{ ppb decade}^{-1}$  with very high certainty. The test reveals downward trends of  $-0.07 \text{ ppb yr}^{-1}$  ( $-0.6 \% \text{ yr}^{-1}$ ; pvalue = 0.02) at Ba and  $-0.24 \text{ ppb yr}^{-1}$  ( $-2.3 \% \text{ yr}^{-1}$ ; pvalue < 0.001) at Ka for a 95% confidence level. At the other sites in West Africa, a downward trend of O<sub>3</sub> of  $-0.7 \text{ ppb decade}^{-1}$  at Agoufou,  $-0.6 \text{ ppb decade}^{-1}$  at Dahra,  $-0.23 \text{ ppb decade}^{-1}$  at Lamto and  $-0.11 \text{ ppb decade}^{-1}$  at Djougou are calculated. However, the certainty is medium at Agoufou, low at Dahra and Lamto and very low at Djougou at 95% confidence interval. The trends in Bomassa (pvalue = 0.17) and Cape Point (pvalue = 0.13), are similar to sites of West Africa with low certainty. At the Louis Trichardt and Amersfoort sites, the results show no ozone trend (pvalue = 0.67 and 0.93) but respectively  $-2.7 \text{ ppb}$  and  $-0.1 \text{ ppb}$  per decade decrease. In contrast, an upward trend with very high certainty is reported. A significant upward trend is reported at Zoetele in Cameroon (Sen slope =  $0.7 \text{ ppb decade}^{-1}$   $0.1 \text{ ppb yr}^{-1}$ ;  $1.4 \% \text{ yr}^{-1}$ ; pvalue = 0.001), and at Skukuza in South Africa (Sen slope =  $3.4 \text{ ppb decade}^{-1}$   $0.3 \text{ ppb yr}^{-1}$ ;  $1.5 \% \text{ yr}^{-1}$ ; pvalue = 0.001) at 95% confidence interval. All the annual trends observed at INDAAF sites are confirmed by Kendall's seasonal trends.

The O<sub>3</sub> mixing ratio in the lower troposphere is slightly higher in central Africa in July than in northern Africa (in January), likely indicating rapid photochemical O<sub>3</sub> production by biomass burning precursors (Singh et al., 1996) during the Southern Hemisphere fires (Tsvilidou et al., 2023). Biomass burning air mass transport from the hemisphere where fires occur (where



910 the highest CO is measured) to the opposite hemisphere is allowed by either the north-easterly Harmattan flow (January) or the southeasterly winds and monsoon flow (July) (Sauvage et al., 2005; Tsvlidou et al., 2023) and could be also explain the upward trend observed at Zoetele. To explain the trends observed at Zo, we apply the Kendall rank correlation between O<sub>3</sub> concentrations and its precursors. We obtain a significant positive rank correlation at the 95% confidence level. For NO<sub>x</sub> and anthropogenic VOCs,  $\tau = 0.7$  (pvalue= 0.03) while with biogenic VOCs, the correlation varies from 0.54 to 0.69 (pvalue <0.01). In addition, we observe increasing trends for biogenic VOCs. Isoprene increases by 1.8 ng.m<sup>-2</sup>s<sup>-1</sup> per year (pvalue = 0.001), alpha pinene by 0.1 ng.m<sup>-2</sup>s<sup>-1</sup> (pvalue < 0.001) and beta pinene by 0.04 ng.m<sup>-2</sup>s<sup>-1</sup> (pvalue = 0.003). Similar trends were also observed in the wet season for alpha pinene and beta pinene, and in the dry season for isoprene. The significant rise in O<sub>3</sub> concentrations in Zo could therefore be explained by these increasing trends observed in isoprene, alpha pinene and beta pinene from one season to the next and in anthropogenic emissions in African forest regions. These results are corroborated by 18 years of satellite data (1998–2015) used by Andela et al. (2017) who noted an increasing trend in burned areas in dense canopy forests. At Skukuza, the upward trend is thought to be due to anthropogenic and biogenic emissions. At the Irene site in the North-eastern interior of South Africa, Bencherif et al. (2020) obtained an upward trend in the tropospheric O<sub>3</sub> column (1998–2017) -at a rate of around 2.4% per decade. At Irene an increase of tropospheric ozone is reported respectively by Thompson et al. (2014) in spring, and Mulumba et al. (2015) in summer, from ozonesonde records (1990 to 2008) and ozone tropospheric columns (1998 à 2013). In addition, an upward trend in NO<sub>2</sub> levels was also evident at Skukuza, signifying the influence of growing rural communities on the Kruger National Park border (Swartz et al., 2020ab). At the South African sites, the high values of NO<sub>x</sub> and COV fluxes are observed at Skukuza (Fig. 11d). This population growth and the associated increase in anthropogenic activities (like domestic biomass burning and solid fuel combustion) result in high levels of pollutants in South Africa's Highveld region (Kai et al., 2022; Keita et al., 2021) and could therefore justify the upward trend obtained. The increase in O<sub>3</sub> in South Africa could be also explained by biomass burning (agriculture reason) and greenhouse (urban-industry reason) activities implemented in Africa during summer and spring seasons (Bencherif et al., 2020; Diab et al., 2004; Sivakumar et al., 2017). Furthermore, pollutants emissions from domestic biofuel, brought by long-range transport of pollution in the Southern Hemisphere have an impact at the continental scale (Thompson et al., 2014). Moreover, Thompson et al. (2021) have observed an increase mean trend of + 1.2% per decade (pvalue = 0.119) from 22-year SHADOZ record (1998–2019) of ozone profiles in the free tropospheric (5–15 km) at Nairobi in East Africa. This trend result is similar with surface ozone change observed in Skukuza. The increase in tropospheric ozone in the tropics, is partly of dynamic origin with the movement of air masses and not solely due to growing anthropogenic emissions (Thompson et al., 2021), could also explain this similarity. Balashov et al. (2014) reported from 1990 to 2007 over the South African Highveld that the sites of Palmer and Makalu exhibit statistically significant negative trends in surface ozone over the spring season and the month of September respectively, whereas Verkykkop and Elandsfontein show no statistically significant change in surface ozone. At most INDAAF sites (remote and rural) we found, as in the work of Balashov et al. (2014), that the surface ozone data still showed no trend. These results confirm however that surface ozone trends in Africa are not uniform regionally or seasonally as mentioned by Thompson et al. (2021).



945

**Figure 156** Significant Kendall's seasonal trend of in situ for O<sub>3</sub> concentrations over the period 1995-2020 at 95% confidence intervals calculated for 12 measurement sites representative of African dry savanna, wet savanna, forest and agricultural/semi-arid savannas and p-value for each trend.

950

#### 4. Conclusion

This work presents an original database of long-term O<sub>3</sub> concentrations at fourteen African sites belonging to the INDAAF program and companion projects. This database gives a better understanding of O<sub>3</sub> concentration levels at remote tropical sites representative of the major African biomes. In this study, we establish a mean annual cycle by site and ecosystem type, and investigate the seasonal variability of O<sub>3</sub> concentrations over the period 1995-2020. Our analysis of the seasonality of anthropogenic and biogenic NO<sub>x</sub> and VOC emissions then highlights the significant factors contributing to O<sub>3</sub> formation. Finally, we calculate the O<sub>3</sub> long-term trends, which provide an insight into the long-term evolution of O<sub>3</sub> levels and the local and regional dynamics of the emission sources of its precursors.

955

The results indicated that O<sub>3</sub> levels are the highest during the rainy season in dry savannas and during the dry season in wet savannas and forests. In agricultural fields, no seasonal variations of O<sub>3</sub> concentrations are observed. In semi-arid savanna (South Africa), dry season O<sub>3</sub> levels are the highest at [Louis Trichardt](#) and [Skukuza](#). At [Cape Point](#) and [Amersfoort](#) sites, maxima occur during the rainy season. Mean annual O<sub>3</sub> concentrations range from 10.5±5.4 to 14.8±4.3 ppb in dry savannas, from 10.8±3.3 to 13.5±4.8 ppb in wet savannas, from 3.9±1.1 to 5.2±2.1 ppb in forest ecosystems and from 19.9±4.7 to 29.1±8.4 ppb in semi-arid/agricultural savannas. BVOC (under the influence of air temperature), NO emissions (in the presence of humidity) and precipitation, are the main contributors to O<sub>3</sub> formation in dry savannas. The seasonality of O<sub>3</sub> measurements and dominant precursors confirm the important role of microbial processes leading to high NO emissions at the beginning of the wet season for O<sub>3</sub> production. Furthermore, the influence of air temperature and solar radiation on woody emissions from shrubs in the Sahel, and the presence of sparse vegetation (short grasses, forbs and dicotyledonous shrubs with perennial ground cover) in this region could be at the origin of BVOC emissions. The photochemical O<sub>3</sub> regime in savannas and rainforests (heavily vegetated areas) is strongly linked to BVOC emissions from vegetation, and to temperature, radiation and humidity. At [Lamto](#) and [Zoetele](#), anthropogenic NO<sub>x</sub> and VOC also contribute to O<sub>3</sub> formation. The most dominant precursor species in southern Africa are mainly [NO<sub>x</sub>VOC](#) emissions (anthropogenic and biogenic), humidity and temperature, as well as anthropogenic [VOCNO<sub>x</sub>](#) at a few sites. They are due of Biomass and fuel combustion, large-scale transport of pollutants, domestic combustion in winter and biogenic emissions from vegetation. At INDAAF sites, which are rural sites far from many anthropogenic sources, O<sub>3</sub> concentrations are below most of the values reported in the literature. [At 95% confidence intervals,](#)

Annual and seasonal Mann-Kendall trends at all sites indicate that the [Katibougou](#) site in Mali and the [Banizoumbou](#) site in Niger experience a [significant](#) decrease in O<sub>3</sub> concentrations (around  $-2.43 \text{ ppb decade}^{-1}$  and  $-0.8 \text{ ppb decade}^{-1}$ ) [with a high certainty](#) over the period 2000 to 2020 justified by downward trends of NO<sub>2</sub> trends observed at [Katibougou](#) and the BVOC emissions at [Banizoumbou](#). In contrast, a significant upward trend is reported at [Zoetele](#) ( $0.7 \text{ ppb decade}^{-1}$ ) and [Skukuza](#) ( $3.4 \text{ ppb decade}^{-1}$ ) in South Africa. These trends could be attributed to the increase in BVOCs in [Zoetele](#) and anthropogenic and biogenic emissions in [Skukuza](#).

This study described in details the O<sub>3</sub> levels in representative African biomes, as well as the photochemical regimes and conditions leading to the observed concentrations. The results presented in this article constitute a robust database showing the importance of developing or maintaining long-term observation projects and observatories. This database could be used to assess the impact of O<sub>3</sub> dry deposition fluxes on African crops and the potential yield losses because of O<sub>3</sub> absorption by crops. An assessment of the various agricultural losses during the growing season will help to better orient actions to improve crop yield and achieve food security. In addition, this documentation is invaluable for modeling chemical processes in the atmosphere and for projecting future changes in tropospheric O<sub>3</sub>. It could limit the uncertainties of these models and facilitate their validation, which is mainly based on data measured in situ.

**Data availability.** [Dataset DOIs of O<sub>3</sub> observations for INDAAF sites \(see complete citation in the reference list\), available in the INDAAF database ~~The INDAAF O<sub>3</sub> observations are available on the program website~~ at <https://indaaf.obs-mip.fr> :](#)

<a href="#">Banizoumbou</a> (Niger)	<a href="#">Katibougou</a> (Mali)	<a href="#">Agoufou</a> (Mali)	<a href="#">Bambey</a> (Senegal)
<a href="https://doi.org/10.25326/608">https://doi.org/10.25326/608</a> <a href="#">Laouali et al. (2023)</a>	<a href="https://doi.org/10.25326/604">https://doi.org/10.25326/604</a> <a href="#">Galy-Lacaux et al. (2023a)</a>	<a href="https://doi.org/10.25326/610">https://doi.org/10.25326/610</a> <a href="#">Galy-Lacaux et al. (2023b)</a>	<a href="https://doi.org/10.25326/609">https://doi.org/10.25326/609</a> <a href="#">Galy-Lacaux et al. (2023c)</a>
<a href="#">Dahra</a> (Senegal)	<a href="#">Lamto</a> (Cote d'Ivoire)	<a href="#">Djougou</a> (Benin)	<a href="#">Zoetele</a> (Cameroon)
<a href="https://doi.org/10.25326/606">https://doi.org/10.25326/606</a> <a href="#">Galy-Lacaux et al. (2023d)</a>	<a href="https://doi.org/10.25326/275">https://doi.org/10.25326/275</a> <a href="#">Galy-Lacaux et al. (2023e)</a>	<a href="https://doi.org/10.25326/605">https://doi.org/10.25326/605</a> <a href="#">Akpo et al. (2023)</a>	<a href="https://doi.org/10.25326/603">https://doi.org/10.25326/603</a> <a href="#">Ouafo-Leumbe et al. (2023)</a>
<a href="#">Bomassa</a>	<a href="#">Mbita</a>	<a href="#">Louis Trichardt</a>	<a href="#">Skukuza</a>

<u>(Congo)</u>	<u>(Kenya)</u>	<u>(South Africa)</u>	<u>(South Africa)</u>
<a href="https://doi.org/10.25326/607">https://doi.org/10.25326/607</a> <u>Galy-Lacaux et al. (2023f)</u>	<a href="https://doi.org/10.25326/642">https://doi.org/10.25326/642</a> <u>Galy-Lacaux et al. (2023g)</u>	<a href="https://doi.org/10.25326/646">https://doi.org/10.25326/646</a> <u>van Zyl et al. (2023a)</u>	<a href="https://doi.org/10.25326/645">https://doi.org/10.25326/645</a> <u>van Zyl et al. (2023b)</u>
<u>Cape Point</u> <u>(South Africa)</u>	<u>Amersfoort</u> <u>(South Africa)</u>		
<a href="https://doi.org/10.25326/644">https://doi.org/10.25326/644</a> <u>van Zyl et al. (2023c)</u>	<a href="https://doi.org/10.25326/647">https://doi.org/10.25326/647</a> <u>van Zyl et al. (2023d)</u>		

~~(<https://doi.org/10.25326/608> ; <https://doi.org/10.25326/604> ; <https://doi.org/10.25326/610> ; <https://doi.org/10.25326/609> ; <https://doi.org/10.25326/606> ; <https://doi.org/10.25326/275> ; <https://doi.org/10.25326/605> ; <https://doi.org/10.25326/603> ; <https://doi.org/10.25326/607> ; <https://doi.org/10.25326/642> ; <https://doi.org/10.25326/646> ; <https://doi.org/10.25326/645> ; <https://doi.org/10.25326/644> ; <https://doi.org/10.25326/647>).~~

GFED4 (NO<sub>x</sub>, COV) and MEGAN-MACC (Isoprene, pinene-a, pinene-b) data are available from <https://eccad.sedoo.fr/#/data>. ERA5 reanalysis data are available from

<https://cds.climate.copernicus.eu/cdsapp#!/dataset/reanalysis-era5-single-levels?tab=overview>.

**Author contributions.** CGL designed the study, wrote the protocol and edited the paper. HEVD conducted data processing, the statistical analysis and wrote the paper. CD made conceptual contributions and edited the paper. ABA and MO contributed at the statistical analysis, assisted in sample collection and edited the paper. VY, DL, MO-L, ON, PGVZ assisted in sample collection and edited the paper. EG and MDA analysed the samples.

**Competing interests.** The contact author has declared that none of the authors has any competing interests.

#### Disclaimer.

**Acknowledgements.** The authors would like to acknowledge the INDAAF project (International Network to study Deposition and Atmospheric chemistry in Africa), and especially all its local technicians for their maintenance and sampling work. We would also like to acknowledge the "Cycle de l'Azote entre la Surface et l'Atmosphère en Afrique" (CASAQUE) project and the Integrated Nitrogen Management system (INMS) for providing us with data on O<sub>3</sub> concentrations at Dahra and Mbita. This study was supported by the INSA (Integrated Nitrogen Studies in Africa) project, which funded the research carried out for this paper at the "Laboratoire d'Aérodynamique de Toulouse". We are indebted to the AMMA-CATCH project, the University of Copenhagen and the Observatoire de recherche en environnement "Bassins versants tropicaux expérimentaux" (SO BVET) for providing us with meteorological data from Niger, Benin, Senegal and Cameroon. We are also grateful to the ECCAD platform and the European Centre for Medium-Range Weather Forecasts (ECMWF) for biogenic and anthropogenic emissions and ERA5 reanalysis data.

**Financial support.** This study has received funding from the European Union's Horizon 2020 research and innovation programme under the Marie Skłodowska-Curie grant agreement no. 871944.

#### Review statement.

#### References

Abbadie, L. (Ed.), Lamto: Structure, Functioning, and Dynamics of a Savanna Ecosystem, Ecological Studies, Springer Science+Business Media, New York, 415pp., ISBN: 9780387948447, 2006.

- 1030 Abiodun, B. J., Ojumu, A. M., Jenner, S., Ojumu, T. V.: The transport of atmospheric NO<sub>x</sub> and HNO<sub>3</sub> over Cape Town, *Atmos. Chem. Phys.*, 14, 559–575, <https://doi.org/10.5194/acp-14-559-2014>, 2014.
- Adon, M., Galy-Lacaux, C., Delon, C., Yoboue, V., Solmon, F., and Kaptue T. A, T.: Dry deposition of nitrogen compounds (NO<sub>2</sub>, NO<sub>3</sub>, NH<sub>3</sub>), sulfur dioxide and ozone in west and central African ecosystems using the inferential method, *Atmos. Chem. Phys.*, 13, 11351–11374, 2013.
- 1035 Adon, M., Galy-Lacaux, C., Yoboué, V., Delon, C., Lacaux, J. P., Castera, P., Gardrat, E., Pienaar, J., Al Ourabi, H., Laouali, D., Diop, B., Sigha-Nkamdjou, L., Akpo, A., Tathy, J. P., Lavenu, F., and Mougine, E.: Long term measurements of sulfur dioxide, nitrogen dioxide, ammonia, nitric acid and ozone in Africa using passive samplers, *Atmos. Chem. Phys.*, 10, 7467–7487, doi:10.5194/acp-10-7467-2010, 2010.
- Adon, M., Yoboue, V., Galy-Lacaux, C., Lioussé, C., Diop, B., Doumbia, E. H. T., Gardrat, E., Ndiaye, S. A., and Jarnot, C.: Measurements of NO<sub>2</sub>, SO<sub>2</sub>, NH<sub>3</sub>, HNO<sub>3</sub> and O<sub>3</sub> in West African urban environments, *Atmos. Environ.*, 135, 31–40, <https://doi.org/10.1016/j.atmosenv.2016.03.050>, 2016
- 1040 Aghedo, A. M., Schultz, M. G., and Rast, S.: The influence of African air pollution on regional and global tropospheric ozone, *Atmos. Chem. Phys.*, 7, 1193–1212, <https://doi.org/10.5194/acp-7-1193-2007>, 2007.
- ~~Ait-Sahalia, Y. and Xiu, D.: Principal Component Analysis of High Frequency Data. *Journal of the American Statistical Association*, 114, 287–303, 2019.~~
- 1045 ~~[Akpo, A., Galy-Lacaux, C., Delon, C., Gardrat, E., Dias Alves, M., Lenoir, O., Halisson, J., Darakpa, C. & Darakpa, D. : Trace gases, Djougou, Benin, \[dataset\], AERIS, <https://doi.org/10.25326/605>, 2023.](https://doi.org/10.25326/605)~~
- Akpo, A. B., Galy-Lacaux, C., Laouali, D., Delon, C., Lioussé, C., Adon, M., Gardrat, E., Mariscal, A., Darakpa, C.: Precipitation chemistry and wet deposition in a remote wet savanna site in West Africa: Djougou (Benin), *Atmospheric Environment*, 115, 110–123, 2015, <http://dx.doi.org/10.1016/j.atmosenv.2015.04.064>
- 1050 Alves, E. G., Jardine, K., Tota, J., Jardine, A., Yáñez-Serrano, A. M., Karl, T., et al. : Seasonality of isoprenoid emissions from a primary rainforest in central Amazonia, *Atmospheric Chemistry and Physics*, 16, 3903–3925. <https://doi.org/10.5194/acp-16-3903-2016>
- Andela, N., Morton, C., Giglio, L., Chen, Y., van Der Werf, G., Kasibhatla, P. S., DeFries, R. S., Collatz, G. J., Hantson, S., Kloster, S., Bachelet, D., Forrest, M., Lasslop, G., Li, F., Mangeon, S., Melton, J. R., Yue, C., Randerson, J. T.: A human-driven decline in global burned area, *Science*, 356, 1356–1362, <https://doi.org/10.1126/science.aal4108>, 2017.
- 1055 Bahino, J., Yoboué, V., Galy-Lacaux, C., Adon, M., Akpo, M., Lioussé, C., Gardrat, E., Chiron, C., Ossouhou, M., Gnamien, S., Keita, S., and Djossou, J.: A pilot study of gaseous pollutants' measurement (NO<sub>2</sub>, HNO<sub>3</sub>, SO<sub>2</sub>, NH<sub>3</sub> and O<sub>3</sub>) in Abidjan, Côte d'Ivoire: contribution to an overview of gaseous pollution in African cities, *Atmos. Chem. Phys.*, 18, 5173–5198, <https://doi.org/10.5194/acp-18-5173-2018>, 2018.
- 1060 ~~[Baglama, J., Reiche, L. and Lewis, B. W.: Fast Truncated Singular Value Decomposition and Principal Components Analysis for Large Dense and Sparse Matrices. R package version 2.3.5, URL: <https://CRAN.Rproject.org/package=irlba>, 2021.](https://CRAN.Rproject.org/package=irlba)~~
- Balashov, N. V., Thompson, A. M., Piketh, S. J., and Langerman, K. E.: Surface ozone variability and trends over the South African Highveld from 1990 to 2007, *J. Geophys. Res.-Atmos.*, 119, 4323–4342, <https://doi.org/10.1002/2013JD020555>, 2014.
- 1065 Baldy, S., Ancellet, G., Bessafi, M., Badr, A., and Luk, D. L. S.: Field observations of the vertical distribution of tropospheric ozone at the island of Reunion (southern tropics), *J. Geophys. Res.-Atmos.*, 101, 23835–23849, doi:10.1029/95jd02929, 1996.
- Bakayoko, A., Galy-Lacaux, C., Véronique Yoboué, V., Hickman, J., E., Roux, F., Gardrat, E., Julien, F., and Delon, C.: Dominant contribution of nitrogen compounds in precipitation chemistry in the Lake Victoria catchment (East Africa), *Environ. Res. Lett.*, 16, 1–20, doi:10.1088/1748-9326/abe25c, 2021.
- Bencherif, H., Tohir, A. M., Mbatha, N., Sivakumar V., Preez, D. J., Bègue, N., and Coetzee, G.: Ozone Variability and Trend Estimates from 20-Years of Ground-Based and Satellite Observations at Irene Station, South Africa, *Atmosphere*, 11, 1216, doi:10.3390/atmos11111216, 2020.
- 1070 Bigaignon, L., Delon, C., Ndiaye, O., Galy-Lacaux, C., Serçea, D., Guérin, F., Talleg, T., Merbold, L., Tagesson, T., Fensholt, R., André, S. and Sylvain Galliau, S.: Understanding N<sub>2</sub>O Emissions in African Ecosystems: Assessments from a Semi-Arid Savanna Grassland in Senegal and Sub-Tropical Agricultural Fields in Kenya, *Sustainability*, MDPI, 12, 1–26, doi:10.3390/su12218875, 2020.
- 1075 ~~[Boiyo, R., Kumar, K. R., Zhao, T. and Bao, Y. : Climatological analysis of aerosol optical properties over East Africa observed from space-borne sensors during 2001–2015, \*Atmos. Environ.\*, 152, 298–313, <https://doi.org/10.1016/j.atmosenv.2016.12.050>, 2017b.](https://doi.org/10.1016/j.atmosenv.2016.12.050)~~
- ~~[Brown, F., Folberth, G. A., Sitch, S., Bauer, S., Batters, M., Boeck, P., Cheesman, A. W., Deushi, M., Dos Santos Vieira, I., Galy-Lacaux, C., Haywood, J., Keeble, J., Mercado, L. M., O'Connor, F. M., Oshima, N., Tsigaridis, K., and Verbeek, H.: The ozone–climate penalty over South America and Africa by 2100, \*Atmos. Chem. Phys.\*, 22, 12331–12352, 2022 <https://doi.org/10.5194/acp-22-12331-2022>, 2022.](https://doi.org/10.5194/acp-22-12331-2022)~~
- 1080 ~~[Bruno, P., Caselli, M., de Gennaro, G. and Traini, A.: Source apportionment of gaseous atmospheric pollutants by means of an absolute principal component scores \(APCS\) receptor model, \*Fresenius J. Anal. Chem.\*, 371, 1119–1123, doi:10.1007/s002160101084, 2001.](https://doi.org/10.1007/s002160101084)~~
- 1085 ~~[Carmichael, G.R., Ferm, M., Thongboonchoo, N., Woo, J.-H., Chan, L., Murano, K., Viet, P.H., Mossberg, C., Bala, R., Boonjawat, J., Upatum, P., Mohan, M., Adhikary, S.P., Shrestha, A.B., Pienaar, J., Brunke, E.B., Chen, T., Jie, T., Guoan, D., Peng, L.C., Dhiharto, S., Harianto,](https://doi.org/10.1016/j.atmosenv.2016.12.050)~~

- H., Jose, A.M., Kimani, W., Kirouane, A., Lacaux, J.-P., Richard, S., Barturen, O., Cerda, J.C., Athayde, A., Tavares, T., Cotrina, J.S., Bilici, E. : Measurements of sulfur dioxide, ozone and ammonia concentrations in Asia, Africa, and South America using passive samplers. *Atmos. Environ.*, 37, 1293–1308. [https://doi.org/10.1016/S1352-2310\(02\)01009-9](https://doi.org/10.1016/S1352-2310(02)01009-9), 2003.
- 1090 Carmichael, G. R., Streets, D. G., Calori, G., Amann, M., Jacobson, M. Z., Hansen, J., and Ueda, H.: Changing trends in sulfur emissions in Asia: Implications for acid deposition, *Environ. Sci. Technol.*, 36, 4707–4713, doi:10.1021/es011509c, 2002.
- Camredon, M. and Aumont, B.: I-L'ozone troposphérique : production/consommation et régimes chimiques, *Pollut. Atmos.*, 193, 51–60 doi:10.4267/pollution-atmospherique.1404, 2007.
- 1095 ~~Carmichael, G.R., Feroz, M., Thongboonchoo, N., Woo, J.-H., Chan, L., Murano, K., Viet, P.H., Mossberg, C., Bala, R., Boonjawat, J., Upatum, P., Mohan, M., Adhikary, S.P., Shrestha, A.B., Pienaar, J., Brunke, E.B., Chen, T., Jie, T., Guoan, D., Peng, L.C., Dhiarto, S., Harjanto, H., Jose, A.M., Kimani, W., Kirouane, A., Lacaux, J.-P., Richard, S., Barturen, O., Cerda, J.C., Athayde, A., Tavares, T., Cotrina, J.S., Bilici, E. : Measurements of sulfur dioxide, ozone and ammonia concentrations in Asia, Africa, and South America using passive samplers. *Atmos. Environ.*, 37, 1293–1308. [https://doi.org/10.1016/S1352-2310\(02\)01009-9](https://doi.org/10.1016/S1352-2310(02)01009-9), 2003.~~
- 1100 Chang, K.-L., Petropavlovskikh, I., Cooper, I. O. R., Schultz, M. G., and Wang, T.: Regional trend analysis of surface ozone observations from monitoring networks in eastern North America, Europe and East Asia, *Elem Sci Anth*, 50, 1–22, doi: <https://doi.org/10.1525/elementa.243>, 2017.
- Chen, W. H., Guenther, A. B., Wang, X. M., Chen, Y. H., Gu, D. S., Chang, M., Zhou, S. Z., Wu, L. L., Zhang, Y. Q.: Regional to global biogenic isoprene emission responses to changes in vegetation from 2000 to 2015, *Journal of Geophysical Research: Atmospheres*, 123, 3757–3771, <https://doi.org/10.1002/2017JD027934>, 2018.
- 1105 Clain, G., Baray, J. L., Delmas, R., Diab, R., Leclair de Bellevue, J., Keckhut, P., Posny, F., Metzger, J. M., and Cammas J. P.: Tropospheric ozone climatology at two Southern Hemisphere tropical/subtropical sites, (Reunion Island and Irene, South Africa) from ozone sondes, LIDAR, and in situ aircraft measurements, *Atmos. Chem. Phys.*, 9, 1723–1734, <https://doi.org/10.5194/acp-9-1723-2009>, 2009.
- Cooper, O. R., Schultz, M. G., Schröder, S., Chang, K.-L., Gaudel, A., Benítez, G. C., Cuevas, E., Fröhlich, M., Galbally, I. E., Molloy, S., Kubistin, D. Lu, X., McClure-Begley, A., Nédélec, P., O'Brien, J., Oltmans, S. J., Petropavlovskikh, I., Ries, L., Senik, I. Sjöberg, K., 1110 Solberg, S., Spain, G. T., Spang, W., Steinbacher, M., Tarasick, D., Thouret V., and Xu, X.: Multi-decadal surface ozone trends at globally distributed remote locations, *Elem Sci Anth*, 8, 1–34, DOI: <https://doi.org/10.1525/elementa.420>, 2020.
- Cooper, O. R., Parrish, D. D., Ziemke, J., Balashov, N. V., Cupeiro, M., Galbally, I. E., Gilge, S., Horowitz, L., Jensen, N. R., Lamarque, J.-F., Naik, V., Oltmans, S. J., Schwab, J., Shindell, D. T., Thompson, A. M., Thouret, V., Wang, Y., Zbinden, R. M.: Global distribution and trends of tropospheric ozone: An observation-based review, *Elementa*, 2, 1–28, DOI: <https://doi.org/10.12952/journal.elementa.000029>, 2014.
- 1115 Conradie, E. H., Van Zyl, P. G., Pienaar, J. J., Beukes, J. P., Galy-Lacaux, C., Venter, A. D., and Mkhathswa, G. V.: The chemical composition and fluxes of atmospheric wet deposition at four sites in South Africa, *Atmos. Environ.*, 146, 113–131, <https://doi.org/10.1016/j.atmosenv.2016.07.033>, 2016.
- 1120 Cros, B., Fontan, J., Minga, A., Helas, G., Nganga, D., Delmas, R., Chapuis, A., Benech, B., Druilhet, A., and Andreae, M. O.: Vertical profiles of ozones between 0 and 400 meters in and above the African equatorial Forest, *J. Geophys. Res.*, 97, 12877–12887, 1992.
- Darras, S., Granier, C., Lioussé, C., Doumbia, T., Keita, S., Soulie, A.: The ECCAD database: Access to a variety of inventories of emissions for greenhouse gases and air pollutants, 35ème colloque annuel de l'Association Internationale de Climatologie – AIC, France, 6–9 July 2022, 1–6, 2022.
- 1125 Debaje, S. B., Jeyakumar, S. J., Ganesan, K., Jadhav, D. B., and Seetaramayya, P.: Surface ozone measurements at tropical rural coastal station Tranquebar, India, *Atmos. Environ.*, 37, 4911–4916, <https://doi.org/10.1016/j.atmosenv.2003.08.005>, 2003.
- Delon, C., Galy-Lacaux, C., Adon, M., Lioussé, C., Serça, D., Diop, B., and Akpo, A.: Nitrogen compounds emission and deposition in West African ecosystems: comparison between wet and dry savanna *Biogeosciences*, 9, 385–402, 2012. doi:10.5194/bg-9-385-2012, 2012.
- 1130 ~~Delon, C., Galy-Lacaux, C., Barret, B., Ndiaye, O., Serça, D., Guérin, F., Gardrat, E., Mougín, E., Agbohessou, Y. F., Probst, A.: Nitrogen budget and critical load determination at a Sahelian grazed grassland site, *Nutr Cycl Agroecosyst*, 124, 17–34, <https://doi.org/10.1007/s10705-022-10220-6>, 2022.~~
- Delon, C., Galy-Lacaux, C., Boone, A., Lioussé, C., Serça, D., Adon, M., Diop, B., Akpo, A., Lavenu, F., Mougín, E., and Timouk, F.: Atmospheric nitrogen budget in Sahelian dry savannas, *Atmos. Chem. Phys.*, 10, 2691–2708, <https://doi.org/10.5194/acp-10-2691-2010>, 2010.
- 1135 Delon, C., Mougín, E., Serça, D., Grippa, M., Hiernaux, P., Diawara, M., Galy-Lacaux, C., Kergoat, L.: Modelling the effect of soil moisture and organic matter degradation on biogenic NO emissions from soils in Sahel rangeland (Mali), *Biogeosciences*, 12, 3253–3272. <https://doi.org/10.5194/bg-12-3253-2015>, 2015.
- Diab, R. D., Raghunandan, A., Thompson, A. M., and V. Thouret, V.: Classification of tropospheric ozone profiles over Johannesburg based on mozaic aircraft data, *Atmos. Chem. Phys.*, 3, 713–723, <https://doi.org/10.5194/acp-3-713-2003>, 2003.
- 1140 Diab, R. D., Thompson, A. M., Mari, K., Ramsay, L., and Coetzee, G. J. R.: Tropospheric ozone climatology over Irene, South Africa, from 1990 to 1994 and 1998 to 2002, *Journal of geophysical research*, 109, 20301-203012, doi:10.1029/2004JD004793, 2004.

- 1145 Dufour, G., Hauglustaine, D., Zhang, Y., Eremenko, M., Cohen, Y., Siour, G., Lachatre, M., Bense, A., Bessagnet, B., Cuesta, J., Thouret, V.,  
and Zheng, B., Gaudel, A., Ziemke, J.: Recent ozone trends in the Chinese free troposphere: role of the local emission reductions and  
meteorology. *Atmos. Chem. Phys.*, 21, 16001–16025, <https://doi.org/10.5194/acp-21-16001-2021>, 2021.
- ~~Duriš, V., Bartková, R., Tírpáková, A.: Principal Component Analysis and Factor Analysis for an Atanassov IF Data Set. *Mathematics*, 9, 1–  
12. <https://doi.org/10.3390/math9172067>, 2021.~~
- 1150 Ferm, M.: A Sensitive Diffusional Sampler, IVL Report L91, Göteborg, Swedish Environmental Research Institute, Sweden, 12pp, ISSN  
0283-877X, 1991.
- Ferm, M., Rodhe, H.: Measurements of Air Concentrations of SO<sub>2</sub>, NO<sub>2</sub> and NH<sub>3</sub> at Rural and Remote Sites in Asia, *Journal of atmospheric  
chemistry*, 27, 17–29, <http://dx.doi.org/10.1023/A:1005816621522>, 1997.
- Ferreira, J., Reeves, C. E., Murphy, J. G., Garcia-Carreras, L., Parker, D. J., and Oram, D. E.: Isoprene emissions modelling for West Africa:  
MEGAN model evaluation and sensitivity analysis, *Atmos. Chem. Phys.*, 10, 8453–8467, [https://doi.org/10.5194/acp-10-8453-  
2010](https://doi.org/10.5194/acp-10-8453-2010), 2010
- 1155 Fleming, Z. L., Doherty, R. M., von Schneidmesser, E., Malley, C. S., Cooper, O. R., Pinto, J. P., Colette, A., Xu, X., Simpson, D., Schultz,  
M. G., Lefohn, A. S., Hamad, S., Moolla, R. Solberg, S., and Feng, Z.: Tropospheric Ozone Assessment Report: Present-day ozone  
distribution and trends relevant to human health, *Elem Sci Anth*, 6, 1–41 DOI: <https://doi.org/10.1525/elementa.273>, 2018.
- 1160 Fowler, D., Pilegaard, K., Sutton, M.A., Ambus, P., Raivonen, M., Duyzer, J., Simpson, D., Fagerli, H., Fuzzi, S., Schjoerring, J.K., Granier,  
C., Neftel, A., Isaksen, I.S.A., Laj, P., Maione, M., Monks, P.S., Burkhardt, J., Daemmgen, U., Neiryneck, J., Personne, E., Wichink-  
Kruit, R., Butterbach-Bahl, K., Flechard, C., Tuovinen, J.P., Coyle, M., Gerosa, G., Loubet, B., Altimir, N., Gruenhage, L., Ammann,  
C., Cieslik, S., Paoletti, E., Mikkelsen, T.N., Ro-Poulsen, H., Cellier, P., Cape, J.N., Horvath, L., Loreto, F., Niinemets, Ü., Palmer, P.I.,  
Rinne, J., Misztal, P., Nemitz, E., Nilsson, D., Pryor, S., Gallagher, M.W., Vesala, T., Skiba, U., Brüggemann, N.,  
Zechmeister-Boltenstern, S., Williams, J., O’ Dowd, C., Facchini, M.C., De Leeuw, G., Flossman, A., Chaumerliac, N., Erisman, J.W. :  
1165 Atmospheric composition change: ecosystems-Atmosphere interactions, *Atmos. Environ.* 43, 5193–5267. [https://doi.  
org/10.1016/j.atmosenv.2009.07.068](https://doi.org/10.1016/j.atmosenv.2009.07.068), 2009.
- Frimpong, B. F., Koranteng, A., and Molkenthin, F.: Analysis of temperature variability utilising Mann–Kendall and Sen’s slope estimator  
tests in the Accra and Kumasi Metropolises in Ghana. *Environmental Systems Research*, 11, 1–13, [https://doi.org/10.1186/s40068-022-  
00269-1](https://doi.org/10.1186/s40068-022-00269-1), 2022.
- 1170 Galanter, M., Levy I. I., H., and Carmichael, G. R.: Impacts of biomass burning on tropospheric CO, NO<sub>x</sub>, and O<sub>3</sub>, *J. Geophys. Res.*, 105,  
6633–6653, doi: 10.1029/1999JD901113, 2000.
- ~~Galy-Lacaux, C., Delon, C., Bakayoko, A., Gardrat, E., Dias Alves, M. & Okumu, S.: Trace gases, Mbita, Kenya. [dataset], Aeris.  
<https://doi.org/10.25326/642>, 2023g.~~
- ~~Galy-Lacaux, C., Diop, B., Orange, D., Sanogo, S., Soumaguel, N., Kanouté, C.O., Gardrat, E., Dias Alves, M., Lenoir, O., Ossohou, M.,  
1175 Adon, M. & Al-Ourabi, H.: Trace gases, Katigoubou, Mali. [dataset], Aeris. <https://doi.org/10.25326/604>, 2023a.~~
- ~~Galy-Lacaux, C., Dorego, G.S., Gardrat, E., Dias Alves, M., Lenoir, O., Der Ba, S., N’Diaye, G.R., Séné, M., Thiam, A., Féron, A. & Ossohou,  
M.: Trace gases, Bambey, Senegal. [dataset], Aeris. <https://doi.org/10.25326/609>, 2023c.~~
- Galy-Lacaux, C., Laouali, D., Descroix, L., Gobron, N., Lioussé, C.: Long term precipitation chemistry and wet deposition in a remote dry  
savanna site in Africa (Niger). *Atmos. Chem. Phys.*, 9, 1579–1595, <https://doi.org/10.5194/acp-9-1579-2009>, 2009.
- 1180 Galy-Lacaux, C. and Modi, A.I.: Precipitation Chemistry in the Sahelian Savanna of Niger, Africa, *Journal of Atmospheric Chemistry*,  
30, 319–343, 1998.
- ~~Galy-Lacaux, C., Mougin, E., Maïga, H., Soumaguel, N., Delon, C., Gardrat, E., Dias Alves, M., Lenoir, O. & Lavenu, F.: Trace gases,  
Agoufou, Mali. [dataset], Aeris. <https://doi.org/10.25326/610>, 2023b.~~
- ~~Galy-Lacaux, C., N’Diaye, O., Guiro, I., Ba, D., Delon, C., Gardrat, E., Dias Alves, M., Lenoir, O. & Ossohou, M.: Trace gases, Dahra,  
1185 Senegal. [dataset], Aeris. <https://doi.org/10.25326/606>, 2023d.~~
- ~~Galy-Lacaux, C., Tathy, J.-P., Opepa, C.K., Brncic, T., Gardrat, E., Dias Alves, M. & Lenoir, O.: Trace gases, Bomassa, Congo. [dataset],  
Aeris. <https://doi.org/10.25326/607>, 2023f.~~
- ~~Galy-Lacaux, C., Yoboué, V., Ossohou, M., Gardrat, E., Dias Alves, M., Lenoir, O., Konaté, I., Ki, A.F., Ouattara, A., Adon, M., Al-Ourabi,  
H. & Zouzou, R.: Trace gases, Lamto, Côte d’Ivoire. [dataset], Aeris. <https://doi.org/10.25326/275>, 2323e.~~
- 1190 García-Lázaro, J., Moreno-Ruiz, J., Riaño, D., Arbelo, M.: Estimation of burned area in the northeastern siberian boreal forest from a long-  
term data record (LTDR) 1982–2015 time series. *Rem. Sens.* 10, 1–15, <https://doi.org/10.3390/rs10060940>, 2018.
- Gaudel, A., Cooper, O. R., Ancellet, G., Barret, B., Boynard, A., Burrows, J. P., Clerbaux, C., Coheur, P.-F., Cuesta, Cuevas, J. E., Doniki, S.,  
Dufour, Ebojite, G. F., Foret, Garcia, G. O., Granados-Muñoz, M. J., Hannigan, J. W., Hase, F., Hassler, B., Huang, G., Hurtmans, D.,  
Jaffe, D., Jones, N., Kalabokas, P., Kerridge, B., Kulawik, S., Latter, B., Leblanc, T., Le Flochmoën, E., Lin, W., Liu, J., Liu, X., Mahieu,  
1195 E., McClure-Begley, A., Neu, J. L., Osman, M., Palm, M., Petetin, H., Petropavlovskikh, I., Querel, R., Rappoe, R. N., Rozanov, A.,  
Schultz, M. G., Schwab, J., Siddans, R., Smale, D., Steinbacher, M., Tanimoto, H., Tarasick, D. W., Thouret, V., Thompson, A. M.,

- Trick, T., Weatherhead, E., Wespes, C., Worden, H. M., Vigouroux, C., Xu, X., Zeng, G., Ziemke, J.: Tropospheric Ozone Assessment Report: Present-day ozone distribution and trends relevant to climate and model evaluation, *Elem Sci Anth*, 6, 1–58, DOI: <https://doi.org/10.1525/elementa.291>, 2018.
- 1200 Gaudel, A., Cooper, O. R., Chang, K.-L., Bourgeois, I., Ziemke, J. R., Strode, S. A., Oman, L. D., Sellitto, P., Nédélec, P., Blot, R., Thouret, V., Granier, C.: Aircraft observations since the 1990s reveal increases of tropospheric ozone at multiple locations across the Northern Hemisphere, *Sci. Adv.*, 6, 1–11, DOI: 10.1126/sciadv.aba8272, 2020.
- Graedel, T. E., and P. J.: Crutzen.: *Atmospheric Change: An Earth System Perspective*, NY: W. H. Freeman and Company, New York, 446 pp, ISBN 0716723344, 1993.
- 1205 ~~Gray, C. M., Helmig, D., Fierer, N.: Bacteria and fungi associated with isoprene consumption in soil. *Elementa: Science of the Anthropocene*, 3, 1–10, doi: 10.12953/journal.elementa.000053, 2015.~~  
~~Guenther, A., Hewitt, C.N., Erickson, D., Fall, R., Geron, C., Graedel, T., Harley, P., Klinger, L., Lerdau, M., McKay, W.A., Pierce, T., Scholes, B., Steinbrecher, R., Tallamraju, R., Taylor, J., Zimmerman, P.A.: Global model of natural volatile organic compound emissions, *J. Geophys. Res.* 100, 8873–8892. <https://doi.org/10.1029/94JD02950>, 1995.~~
- 1210 Guenther, A., Karl, T., Harley, P., Wiedinmyer, C., Palmer, P. I., and Geron, C.: Estimates of global terrestrial isoprene emissions using MEGAN (Model of Emissions of Gases and Aerosols from Nature), *Atmos. Chem. Phys.*, 6, 3181–3210, doi:10.5194/acp-6-3181, 2006  
~~Guenther, A. B., Zimmerman, P. R., Harley, P. C., Monson, R. K., & Fall, R.: Isoprene and monoterpene emission rate variability: Model evaluations and sensitivity analyses, *Journal of Geophysical Research*, 98, 12609–12617. <https://doi.org/10.1029/93jd00527>, 1993~~
- Hagenbjörk, A., Malmqvist, E., Mattisson, K., Sommar, N. J., Modig, L.: The spatial variation of O<sub>3</sub>, NO, NO<sub>2</sub> and NO<sub>x</sub> and the relation between them in two Swedish cities, *Environ. Monit. Assess.* 189, 161–172, <https://doi.org/10.1007/s10661-017-5872-z>, 2017.
- 1215 Hamdun, A. M., and Arakaki T.: Analysis of Ground Level Ozone and Nitrogen Oxides in the City of Dar es Salaam and the Rural Area of Bagamoyo, Tanzania, *Open Journal of Air Pollution*, 4, 224–238, DOI: 10.4236/ojap.2015.44019, 2015.
- Heue, K.-P., Coldewey-Egbers, M., Delcloo, A., Lerot, C., Loyola, D., Valks, P., and van Roozendaal, M., : Trends of tropical tropospheric ozone from 20 years of European satellite measurements and perspectives for the Sentinel-5 Precursor, *Atmos. Meas. Tech.*, 9, 5037–5051, 2016.
- 1220 Hirsch, R. M., Slack, J. R., Smith, R. A.: Techniques of trend analysis for monthly water quality data, *Water Resour. Res.* 18, 107–121. <https://doi.org/10.1029/WR018i001p00107>, 1982.
- Homyak P. M., Sickman, J. O., Miller, A. E., Melack, J. M., and Schimel, J. P., : Assessing N saturation in a seasonally dry chaparral watershed: Limitations of traditional indicators of N saturation, *Ecosystems*, 17: 1286–1305, <https://doi.org/10.1007/s10021-014-9792-2>, 2014.
- 1225 ~~Hou, X.; Zhang, Y.; Lv, X.; Lee, J.: The Impact of Meteorological Conditions and Emissions on Tropospheric Column Ozone Trends in Recent Years. *Remote Sens.* 15, 5293-5305. <https://doi.org/10.3390/rs15225293>, 2023.~~
- Ihedeke, C., Mooney, J. D., Fulton, J., and Ling, J.: Evaluation of real-time monitored ozone concentration from Abuja, Nigeria, *BMC Public Health*, 23, 1–7, <https://doi.org/10.1186/s12889-023-15327-1>, 2023.
- 1230 Jaars, K., van Zyl, P. G., Beukes, J. P., Hellén, H., Vakkari, V., Josipovic, M., Venter, A. D., Räsänen, M., Knoetze, L., Cilliers, D. P., Siebert, S. J., Kulmala, M., Rinne, J., Guenther, A., Laakso, L., and Hakola, H.: Measurements of biogenic volatile organic compounds at a grazed savannah grassland agricultural landscape in South Africa, *Atmos. Chem. Phys.*, 16, 15665–15688, 2016.
- Jaegle, L., Martin, R. V., Chance, K., Steinberger, L., Kurosu, T. P., Jacob, D. J., Modi, A. I., Yoboue, V., Sigha-Nkamdjou, L., and Galy-Lacaux, C.: Satellite mapping of rain-induced nitric oxide emissions from soils, *J. Geophys. Res.*, 109, 1–10, doi:10.1029/2004JD004787, 2004.
- 1235 ~~Jolliffe, I. T.: *Principal component analysis*. Springer New York, État de New York, 488p, <https://doi.org/10.1007/b98835>, 1986.~~
- Josipovic, M., Annegarn, H. J., Kneen, M. A., Pienaar, J. J. and Piketh, S. J.,: Concentrations, distributions and critical level exceedance assessment of SO<sub>2</sub>, NO<sub>2</sub> and O<sub>3</sub> in South Africa, *Environmental Monitoring and Assessment*, 171, 181–196, DOI: 10.1007/s10661-009-1270-5, 2010.
- 1240 Kai, R. F., Scholes, M. C., Piketh, S. J., Scholes, R. J.: Analysis of the first surface nitrogen dioxide concentration observations over the South African Highveld derived from the Pandora-2s instrument, *Clean air journal*, 32, 1–11, <http://dx.doi.org/10.17159/caj/2022/32/1.13242>, 2022.
- Kendall, M.G.: *Rank Correlation Methods*, fourth ed. Charles Griffin, 4th Edition, Charles Griffin, London, 1975.
- 1245 Keita, S., Liousse, C., Assamoi, E.-M., Doumbia, T., N'Datchoh, E. T., Gnamien, S., Elguindi, N., Granier, C. and Yoboué, V., : African anthropogenic emissions inventory for gases and particles from 1990 to 2015, *Earth Syst. Sci. Data*, 13, 3691–3705, <https://doi.org/10.5194/essd-13-3691-2021>, 2021.
- Khoder, M. I., Diurnal, Seasonal and Weekdays-Weekends Variations of Ground Level Ozone Concentrations in an Urban Area in Greater Cairo. *Environmental Monitoring and Assessment*, 149, 349–362, <https://doi.org/10.1007/s10661-008-0208-7>, 2009.
- Kimayu, J. M., Gikuma-Njuru, P., and Musembi, D. K., : Temporal and Spatial Variability of Tropospheric Ozone in Nairobi City, Kenya, *Physical Science International Journal*, 13, 1–12, DOI: 10.9734/PSIJ/2017/31452, 2017.
- 1250



- Kiros F., Shakya K. M., Rupakheti M., Regmi R. P., Maharjan R., Byanju R. M., Naja M., Mahata K., Kathayat B., Peltier E. R., : *Variability of Anthropogenic Gases: Nitrogen Oxides, Sulfur Dioxide, Ozone and Ammonia in Kathmandu Valley, Nepal, Aerosol and Air Quality Research*, 16: 3088–3101, <https://doi.org/10.7275/9997447>, 2016.
- 1255 Laakso, L., Vakkari, V., Virkkula, A., Laakso, H., Backman, J., Kulmala, M., Beukes, J. P., van Zyl, P. G., Tiitta, P., Josipovic, M., Pienaar, J. J., Chiloane, K., Gilardoni, S., Vignati, E., Wiedensohler, A., Tuch, T., Birmili, W., Piketh, S., Collett, K., Fourie, G. D., Komppula, M., Lihavainen, H., de Leeuw, G., and Kerminen, V.-M.: South African EUCAARI measurements: seasonal variation of trace gases and aerosol optical properties, *Atmos. Chem. Phys.*, 12, 1847–1864, <https://doi.org/10.5194/acp12-1847-2012>, 2012.
- 1260 Laakso, L., Laakso, H., Aalto, P. P., Keronen, P., Petäjä, T., Nieminen, T., Pohja, T., Siivola, E., Kulmala, M., Kgabi, N., Molefe, M., Mabaso, D., Phalatsé, D., Pienaar, K., and Kerminen, V.-M.: Basic characteristics of atmospheric particles, trace gases and meteorology in a relatively clean Southern African Savannah environment, *Atmos. Chem. Phys.*, 8, 4823–4839, <https://doi.org/10.5194/acp-8-4823-2008>, 2008.
- Laban, T. L., Van Zyl, P. G., Beukes, J. P., Mikkonen, S., Santana, L., Josipovic, M., Vakkari, Thompson, A. M., Kulmala, M. and Laakso L.: Statistical analysis of factors driving surface ozone variability over continental South Africa, *Journal of Integrative Environmental Sciences*, pp; 1–28, DOI:10.1080/1943815X.2020.1768550, 2020.
- 1265 Laban, T. L., Van Zyl, P. G., Beukes, J. P., Vakkari, V., Jaars, K., Borduas-Dedekind, N., Josipovic, M., Thompson, A. M., Kulmala, M., Laakso, L., : Seasonal influences on surface ozone variability in continental South Africa and implications for air quality, *Atmos. Chem. Phys.*, 15491–15514. <https://doi.org/10.5194/acp-18-15491-2018>, 2018.
- Lacaux, J. P., Tathy, J. P., and Sigha, L.: Acid wet deposition in the tropics: two case studies using DEBITS measurements, *IGACTivities Newsletter of the International Global Atmospheric Chemistry Project, DEBITS Special 2*, 13–18, 2003.
- 1270 Lanz, V. A., Alfara, M. R., Baltensperger, U., Buchmann, B., Hueglin, C. and Prévôt, A. S. H.: *Source apportionment of submicron organic aerosols at an urban site by factor analytical modelling of aerosol mass spectra*, *Atmospheric Chem. Phys.*, 7, 1503–1522, doi: , 2007.
- Lannuque, V., Sauvage, B., Barret, B., Clark, H., Athier, G., Boulanger, D., Cammas, J.-P., Cousin, J.-M., Fontaine, A., Le Flochmoën, E., Nédélec, P., Petetin, H., Pfaffenzeller, I., Rohs, S., Smit, H. G. J., Wolff, P., and Thouret, V.: *Origins and characterization of CO and O<sub>3</sub> in the African upper troposphere*, *Atmos. Chem. Phys.*, 21, 14535–14555, <https://doi.org/10.5194/acp-21-14535-2021>, 2021.
- 1275 Laouali, D., Galy-Lacaux, C., Gardrat, E., Dias Alves, M., Lenoir, O., Zakou, A., Ossouhou, M., Adon, M. & Al-Ourabi, H.: *Trace gases, Banizoumbou, Niger, [dataset], Aeris*, <https://doi.org/10.25326/608>, 2023.
- Laville, P., Henault, C., Gabrielle, B., and Serca, D.: Measurement and modelling of NO fluxes over maize and wheat crops during their growing seasons: effect of crop management, *Nutr. Cycl. Agroecosyst.* 72, 159–171, doi: 10.1007/s10705-005-0510-5, 2005.
- 1280 Lee, J. D., Squires, F. A., Sherwen, T., Wilde, S. E., Cliff, S. J., Carpenter, L. J., Hopkins, J. R., Bauguitte, S. J., Reed, C., Barker, P., Allen, G., Bannan, T. J., Matthews, E., Mehra, A., Percival, C., Heard, D. E., Whalley, L. K., Ronnie, G. V., Seldon, S., Ingham, T., Keller, C. A., Knowland, K. E., Nisbet, J. E. G., and Andrews, S. S.: Ozone production and precursor emission from wildfires in Africa, *Environ. Sci.: Atmos.*, 1, 524–542., doi: 10.1039/D1EA00041A, 2021.
- Lefohn, A. S., Malley, C. S., Smith, L., Wells, B., and Hazucha, M., : *Tropospheric Ozone Assessment Report: Global ozone metrics for climate change, human health, and crop/ecosystem research*, *Elem Sci Anth*, 6, 1–39 DOI: <https://doi.org/10.1525/elementa.279>, 2018.
- 1285 Lelieveld, J., Evans, J. S., Fnais, M., Giannadaki, D., and Pozzer, A.: The contribution of outdoor air pollution sources to premature mortality on a global scale, *Nature*, 525, 367–371, <https://doi.org/10.1038/nature15371>, 2015.
- Lin, M., Horowitz, L. W., Cooper, O. R., Tarasick, D., Conley, S., Iraci, L. T., Johnson, B., Leblanc, T., Petropavlovskikh, I., and Yates, E. L.: Revisiting the evidence of increasing springtime ozone mixing ratios in the free troposphere over western North America., *Geophys Res Lett* 42, 8719–8728. DOI: <https://doi.org/10.1002/2015GL065311>, 2015.
- 1290 Liu, Y., Schallhart, S., Taipale, D., Tykkä, T., Räsänen, M., Merbold, L., Hellén, H., and Pellikka, P.: Seasonal and diurnal variations in biogenic volatile organic compounds in highland and lowland ecosystems in southern Kenya, *Atmospheric Chemistry and Physics* , 21, 14761–14787, <https://doi.org/10.5194/acp-21-14761-2021>, 2021.
- Lourens, A. S., Beukes, J. P., Van Zyl, P. G., Fourie, G. D., Burger, J. W., Pienaar, J. J., Read, C. E., and Jordaan, J. H.: Spatial and temporal assessment of gaseous pollutants in the Highveld of South Africa, *S. Afr. J. Sci.*, 107, 1–8, doi: 10.4102/sajs.v107i1/2.269, 2011.
- 1295 Lu, X., Zhang, L., Zhao, Y., Jacob, D. J., Hu, Y., Hu, L., Gao, M., Liu, X., Petropavlovskikh, I., McClure-Begley, A., Querel, R.: Surface and tropospheric ozone trends in the Southern Hemisphere since 1990: possible linkages to poleward expansion of the Hadley circulation, *Science Bulletin*, 64, 400–409, <https://doi.org/10.1016/j.scib.2018.12.021>, 2019.
- Ludwig, J., Meixner, F. X., Vogel, B., and Forstner, J.: Soil-air exchange of nitric oxide: An overview of processes, environmental factors, and modelling studies, *Biogeochemistry*, 52, 225–257, DOI: 10.1023/A:1006424330555, 2001.
- 1300 Mari, C. H., Reeves, C. E., Law, K. S., Ancellet, G., Andres-Hernandez, M. D., Barret, B., Bechara, J., Borbon, A., Bouarar, I., Cairo, F., Commane, R., Delon, C., Evans, M. J., Fierli, F., Floquet, C., Galy-Lacaux, C., Heard, D. E., Homan, C. D., Ingham, T., Larsen, N., Lewis, A. C., Lioussé, C., Murphy, J. G., Orlandi, E., Oram, D. E., Saunio, M., Serçe, D., Stewart, D. J., Stone, D., Thouret, V., van Velthoven, P., and Williams, J. E.: Atmospheric composition of West Africa: highlights from the AMMA international program, *Atmos. Sci. Lett.* 12, 13–18, <https://doi.org/10.1002/asl.289>, 2011.

- 1305 Martins, J. J., Dhammapala, R. S., Lachmann, G., Galy-Lacaux, C., and Pienaar, J. J.: Long-term measurements of sulphur dioxide, nitrogen dioxide, ammonia, nitric acid and ozone in southern Africa using passive samplers, *S. Afr. J. Sci.*, 103, 336–342, <https://hdl.handle.net/10520/EJC96693>, 2007.
- Mayaux, P., Bartholomé, E., Fritz, S., and Belward, A.: A new land-cover map of Africa for the year 2000: New land-cover map of Africa. *J. Biogeogr.*, 31, 861–877, <https://doi.org/10.1111/j.1365-2699.2004.01073.x>, 2004.
- 1310 Merabtene, T., Siddique, M., Shanableh, A.: Assessment of seasonal and annual rainfall trends and variability in sharjah city, UAE. *Adv. Meteorol.*, 2016, 1–13, <https://doi.org/10.1155/2016/6206238>, 2016.
- Mills, G., Pleijel, H., Malley, C. S., Sinha, B., Cooper, O. R., Schultz, M. G., Neufeld, H. S., Simpson, D., Sharps, K., Feng, Z., Gerosa, G., Harmens, H., Kobayashi, K., Saxena, P., Paoletti, E., Sinha, V., and Xu, X.: Tropospheric Ozone Assessment Report: Present-day tropospheric ozone distribution and trends relevant to vegetation. *Elem Sci Anth*, 6, 1–46, DOI: <https://doi.org/10.1525/elementa.302>, 2018.
- 1315 Morakinyo, O. M., Mukhola M. S., and Mokgobu. M. I.: Ambient Gaseous Pollutants in an Urban Area in South Africa: Levels and Potential Human Health Risk. *Atmosphere*, 11, 1–14, doi:10.3390/atmos11070751, 2020.
- ~~Mouissi, S., Alayat, H.: (2016) Use of the Principal Component Analysis (PCA) for Physico-Chemical Characterization of an Aquatic Ecosystem Waters: Case of Oubeira Lake (Extreme Northeastern Algeria), *J. Mater. Environ. Sci.* 7, 2214–2220, 2016.~~
- 1320 Monks, P. S., Archibald, A. T., Colette, A., Cooper, O., Coyle, M., Derwent, R., Fowler, D., Granier, C., Law, K. S., Mills, G. E., Stevenson, D. S., Tarasova, O., Thouret, V., von Schneidmesser, E., Sommariva, R., Wild, O., and Williams, M. L.: Tropospheric ozone and its precursors from the urban to the global scale from air quality to short-lived climate forcer, *Atmos. Chem. Phys.*, 15, 8889–8973, <https://doi.org/10.5194/acp-15-8889-2015>, 2015.
- Monks, P., Leigh, R.: Tropospheric chemistry and air pollution. In: Hewitt, C.N., Jackson, A.V. (Eds.), *Atmospheric Science for Environmental Scientists*. Wiley-Blackwell, Oxford, UK, 300 pp, ISBN 978140518542-4, 2009.
- 1325 ~~Mulumba, J.-P., Venkataraman, S., Thomas, J. O.: Modeling Tropospheric Ozone Climatology over Irene (South Africa) Using Retrieved Remote Sensing and Ground-Based Measurement Data, *J. Remote Sens. GIS*, 4, 151, DOI:10.4172/2469-4134.1000151, 2015.~~
- Ngoasheng, M., Beukes, J. P., van Zyl, P. G., Swartz, J.-S., Loate, V., Krisjan, P., Mpambani, S., Kulmala, M., Vakkari, V., and Laakso, L.: Assessing SO<sub>2</sub>, NO<sub>2</sub> and O<sub>3</sub> in rural areas of the North West Provinc. *Clean air journal*, 31, 1–14, <http://dx.doi.org/10.17159/caj/2021/31/1.9087>, 2021.
- 1330 Ojumu, A.M.: Transport of Nitrogen Oxides and Nitric Acid Pollutants over South Africa and Air Pollution in Cape Town. MSc, University of South Africa, 68 pp, 2013.
- Oltmans, S. J., Lefohn, A. S., Shadwick, D., Harris, J. M., Scheel, H. E., Galbally, I., Tarasick, D. W., Johnson, B. J., Brunke, E. G., Claude, H., Zeng, G., Nichol, S., Schmidlin, F., Davies, J., Cuevas, E., Redondas, A., Naoe, H., Nakano, T., and Kawasato, T.: Recent tropospheric ozone changes-A pattern dominated by slow or no growth, *Atmos. Environ.*, 67, 331–351, <https://doi.org/10.1016/j.atmosenv.2012.10.057>, 2013.
- 1335 ~~Oluleye, A.: Satellite Observation of Spatio-temporal Variations in Nitrogen Dioxide over West Africa and Implications for Regional Air Quality, *Journal of Health & Pollution*, 11, 1–16, DOI: 10.5696/2156-9614.11.31.210913, 2021.~~
- Oluleye, A., and Okogbue, E. C.: Analysis of temporal and spatial variability of total column ozone over West Africa using daily TOMS measurements, *Atmospheric Pollution Research*, 4, 387–397, <https://doi.org/10.5094/APR.2013.044>, 2013.
- ~~Onojeghuo, A. R., Balzter, H., Monks, P. S.: Tropospheric NO<sub>2</sub> concentrations over West Africa are influenced by climate zone and soil moisture variability., *Atmos. Chem. Phys. Discuss.*, doi:10.5194/acp-2016-1128, 2017.~~
- 1345 Osohou M., C. Galy-Lacaux, C., V. Yoboué, V., Hickman, J. E., Gardrat, E., Adona, M., Darrasi, S., Laoualie, D., Akpod, A., Ouafo, M., Diop, B., Opepah, C.: Trends and seasonal variability of atmospheric NO and HNO concentrations across three major African biomes inferred from long-term series of ground-based and satellite measurements, *Atmos. Environ.* 207, 148–66, <https://doi.org/10.1016/j.atmosenv.2019.03.027>, 2019.
- ~~Ouafo-Leumbe, M.-R., Galy-Lacaux, C., Sigha-Nkamdjou, L., Gardrat, E., Dias Alves, M., Lenoir, O., Meka, M.Z. & Amougou, M.: Trace gases, Zoétélé, Cameroon, [dataset]. AERIS, <https://doi.org/10.25326/603>, 2023.~~
- 1350 Petäjä, T., Vakkari, V., Pohja, T., Nieminen, T., Laakso, H., Aalto, P. P., Keronen, P., Siivola, E., Kerminen, V.-M., Kulmala, M., and Laakso, L.: Transportable Aerosol Characterization Trailer with Trace Gas Chemistry: Design, Instruments and Verification, *Aerosol Air Qual. Res.*, 13, 421–435, <https://doi.org/10.4209/aaqr.2012.08.0207>, 2013.
- Petetin, H., Bowdalo, D., Bretonnière, P.-A., Guevara, M., Armengol, J. M., Cabre, M. S., Serradell, K., Jorba, O., Soret, A., and Garcia-Pando, C. P.: Model output statistics (MOS) applied to Copernicus Atmospheric Monitoring Service (CAMS) O<sub>3</sub> forecasts: trade-offs between continuous and categorical skill scores, *Atmos. Chem. Phys.*, 22, 11603–11630, <https://doi.org/10.5194/acp-22-11603-2022>, 2022.
- 1355 Rummel, U., Ammann, C., Kirkman, G. A., Moura, M. A. L., Foken, T., Andreae, M. O., and Meixner, F. X.: Seasonal variation of ozone deposition to a tropical rain forest in southwest Amazonia, *Atmos. Chem. Phys.*, 7, 5415–5435, doi:10.5194/acp-7-5415-2007, 2007.

- 1360 Sadiq, M., Tai, A. P. K., Lombardozzi, D., and Martin, M. V.: Effects of O<sub>3</sub>-vegetation coupling on surface O<sub>3</sub> air quality via biogeochemical and meteorological feedbacks, *Atmos. Chem. Phys.*, 17, 3055–3066. <https://doi.org/10.5194/acp-17-3055-2017>, 2017.
- Salem, A. A., Soliman, A. A., El-Haty, I. A.: Determination of nitrogen dioxide, sulfur dioxide, ozone, and ammonia in ambient air using the passive sampling method associated with ion chromatographic and potentiometric analyses, *Air Qual Atmos Health*, 2, 133–145, doi: 10.1007/s11869-009-0040-4, 2009.
- 1365 Saunois, M., Reeves, C. E., Mari, C., Murphy, J. G., Stewart, D. J., Mills, G. P., Oram, D. E., and Purvis, R. M.: Ozone budget in the West African lower troposphere during the African Monsoon Multidisciplinary Analysis (AMMA) campaign, *Atmos. Chem. and Phys.*, 9, 6135–6155, doi:10.5194/acp-9-6135-2009, 2009.
- [Sauvage, B., Gheusi, F., Thouret, V., Cammas, J.-P., Duron, J., Escobar, J., Mari, C., Mascart, P., and Pont, V.: Medium-range mid-tropospheric transport of ozone and precursors over Africa: two numerical case studies in dry and wet seasons, \*Atmos. Chem. Phys.\*, 7, 5357–5370, <https://doi.org/10.5194/acp-7-5357-2007>, 2007.](https://doi.org/10.5194/acp-7-5357-2007)
- 1370 Sauvage, B., Thouret, V., Cammas, J.-P., Gheusi, F., Athier, G., and Nédélec, P.: Tropospheric ozone over Equatorial Africa: regional aspects from the MOZIC data, *Atmos. Chem. Phys.*, 5, 311–335, <https://doi.org/10.5194/acp-5-311-2005>, 2005.
- Saxton, J. E., Lewis, A. C., Kettlewell, J. H., Ozel, M. Z., Gogus, F., Boni, Y., Korogone, S. O. U., and Serca. D.: Isoprene and monoterpene measurements in a secondary forest in northern Benin, *Atmos. Chem. Phys.*, 7, 4095–4106, <https://doi.org/10.5194/acp-7-4095-2007>, 2007.
- 1375 Schultz, M. G., et al.: Tropospheric Ozone Assessment Report: Database and metrics data of global surface ozone observations, *Elem Sci Anth*, 5, 1–26, DOI: <https://doi.org/10.1525/elementa.244>, 2017.
- Sen P., K.: Estimates of the regression coefficient based on Kendall's tau, *J. Am. Stat. Assoc.* 63, 1379–1389, <https://doi.org/10.2307/2285891>, 1968.
- 1380 Serca, D., Guenther, A., Klinger, L., Vierling, L., Harley, P., Druilhet, A., Greenberg, J., Baker, B., Baugh, W., Bouka-Biona, C., and Loemba-Ndembi, J.: EXPRESSO flux measurements at upland and lowland Congo tropical forest site, *Tellus B*, 53, 220–234, <https://doi.org/10.3402/tellusb.v53i3.16593>, 2001.
- Silva, S. J., & Heald, C. L.: Investigating Dry Deposition of O<sub>3</sub> to Vegetation, *J. Geophys. Res. Atmos.*, 123, 559–573. <https://doi.org/10.1002/2017JD027278>, 2018.
- 1385 Sindelarova, K., Granier, C., Bouarar, I., Guenther, A., Tilmes, S., Stavrou, T., Müller, J.-F., U. Kuhn, U., P. Stefani, P., and W. Knorr, W.: Global data set of biogenic VOC emissions calculated by the MEGAN model over the last 30 years, *Atmos. Chem. Phys.*, 14, 9317–9341, <https://doi.org/10.5194/acp-14-9317-2014>, 2014.
- [Singh, H. B., Herlth, D., Kolyer, R., Chatfield, R., Viezee, W., Salas, L. J., Chen, Y., Bradshaw, J. D., Sandholm, S. T., Talbot, R., Gregory, G. L., Anderson, B., Sachse, G. W., Browell, E., Bachmeier, A. S., Blake, D. R., Heikes, B., Jacob, D., and Fuelberg, H. E.: Impact of biomass burning emissions on the composition of the South Atlantic troposphere: Reactive nitrogen and ozone, \*J. Geophys. Res.-Atmos.\*, 101, 24203–24219, <https://doi.org/10.1029/96JD01018>, 1996.](https://doi.org/10.1029/96JD01018)
- 1390 [Sivakumar, V., Ogunniyi, J.: Ozone climatology and variability over Irene, South Africa determined by ground based and satellite observations. Part I: Vertical variations in the troposphere and stratosphere. \*Atmósfera\*. 30, 337–353, <https://doi.org/10.20937/atm.2017.30.04.05>, 2017.](https://doi.org/10.20937/atm.2017.30.04.05)
- 1395 Sofen, E. D., Bowdalo, D., and Evans, M. J., How to most effectively expand the global surface ozone observing network, *Atmos Chem Phys* 16, 1445–1457. DOI: <https://doi.org/10.5194/acp-16-1445-2016>, 2016.
- [Stauffer, R. M., Thompson, A. M., Kollonige, D. E., Komala, N., Al-Ghazali, H. K., Risdianto, D. Y., Dindang, A., bin Jamaluddin, A. F., Sammathuria, M. K., Zakaria, N. B., Johnson, B. J., Cullis, P. D.: Dynamical drivers of free-tropospheric ozone increases over equatorial Southeast Asia, \*Atmos. Chem. Phys.\*, <https://doi.org/10.5194/acp-24-5221-2024>, 2024.](https://doi.org/10.5194/acp-24-5221-2024)
- 1400 Stewart, D. J., Taylor, C. M., Reeves, C. E., and McQuaid, J. B.: Biogenic nitrogen oxide emissions from soils: impact on NO<sub>x</sub> and ozone over west Africa during AMMA (African Monsoon Multidisciplinary Analysis): observational study, *Atmos. Chem. Phys.*, 8, 2285–2297, doi:10.5194/acp-8-2285-2008, 2008.
- Swap, R. J., Annegarn, H. J., Suttles, J. T., King, M. D., Platnick, S., Privette, J. L., Scholes, R. J.: Africa burning: a thematic analysis of the southern African regional science initiative (SAFARI 2000), *J. Geophys. Res.* 108, 1–15, <https://doi.org/10.1029/2003JD003747>, 2003
- 1405 Swartz, J.-S., van Zyl, P. G., Beukes, J. P., Galy-Lacaux, C., Ramandh, A., and Pienaar, J. J.: Measurement report: Statistical modelling of long-term trends of atmospheric inorganic gaseous species within proximity of the pollution hotspot in South Africa, *Atmos. Chem. Phys.*, 20, 10637–10665, <https://doi.org/10.5194/acp-20-10637-2020>, 2020a.
- Swartz, J.-S., Van Zyl, P. G., Beukes, J. P., Labuschagne, C., Brunke, E.-G., Galy-Lacaux, C., Pienaar, J. J., Portafaix, T.: Twenty-one years of passive sampling monitoring of SO<sub>2</sub>, NO<sub>2</sub> and O<sub>3</sub> at the Cape Point GAW station, South Africa, *Atmospheric Environment* 222, 1–17, <https://doi.org/10.1016/j.atmosenv.2019.117128>, 2020b.
- 1410 Tarasick, D., Galball, I. E., Cooper, O. R., Schultz, M. G., Ancellet, G., Leblanc, T., Wallington, T. J., Ziemke, J., Liu, X., Steinbacher, M., Staehelin, J., Vigouroux, C., Hannigan, J. W., Garcia, O., Foret, G., Zanis, P., Weatherhead, E., Petropavlovskikh, I., Worden, H., Osman, M., Liu, J., Chang, K.-L., Gaudel, A., Lin, M., Granados-Muñoz, M., Thompson, A. M., Oltmans, S. J., Cuesta, J., Dufour, G., Thouret,

- V., Hassler, B., Trick T., and Neu, J. L.: Tropospheric Ozone Assessment Report: Tropospheric ozone from 1877 to 2016, observed levels, trends and uncertainties, *Elem Sci Anth*, 7, 1–72. DOI: <https://doi.org/10.1525/elementa.376>, 2019.
- 1415 [Thompson, A. M., Balashov, N. V., Witte, J. C., Coetzee, J. G. R., Thouret, V., and Posny, F.: Tropospheric ozone increases over the southern Africa region: Bellwether for rapid growth in Southern Hemisphere pollution? \*Atmospheric Chemistry and Physics\*, 14, 9855–9869. <https://doi.org/10.5194/acp-14-9855-2014>, 2014.](https://doi.org/10.5194/acp-14-9855-2014)
- 1420 [Thompson, A. M., Stauffer, R. M., Wargan, K., Witte, J. C., Kollonige, D. E., Ziemke, J. R.: Regional and seasonal trends in tropical ozone from SHADOZ profiles: Reference for models and satellite products. \*J. Geophys. Res.\*, <https://agupubs.onlinelibrary.wiley.com/doi/10.1029/2021JD034691>, 2021.](https://agupubs.onlinelibrary.wiley.com/doi/10.1029/2021JD034691)
- 1425 [Thompson, A. M., Witte, J. C., Oltmans, S. J., Schmidlin, F. J., Logan, J. A., Fujiwara, M., Kirchhoff, V. W. J. H., Posny, F., Coetzee, G. J. R., Hoegger, B., Kawakami, S., Ogawa, T., Fortuin, J. P. F., and Kelder H. M.: Southern Hemisphere Additional Ozonesondes \(SHADOZ\) 1998–2000 tropical ozone climatology. 2. Tropospheric variability and the zonal wave-one. \*Journal of Geophysical Research\*, 108\(D2\), 1–21, <https://doi.org/10.1029/2002JD002241>, 2003b.](https://doi.org/10.1029/2002JD002241)
- Tiitta, P., Vakkari, V., Croteau, P., Beukes, J.P., Zyl, P.G.V., Josipovic, M., Venter, A.D., Jaars, K., Pienaar, J.J., Ng, N.L., Canagaratna, M.R., Jayne, J.T., Kerminen, V.M., Kokkola, H., Kulmala, M., Laaksonen, A., Worsnop, D.R., Laakso, L., Chemical composition, main sources and temporal variability of PM1 aerosols in southern African grassland. *Atmos. Chem. Phys.* 14, 1909–1927. <https://doi.org/10.5194/acp-14-1909-2014>, 2014.
- 1430 [Tsvilidou, M., Sauvage, B., Bennouna, Y., Blot, R., Boulanger, D., Clark, H., Le Flochmoën, E., Nédélec, P., Thouret, V., Wolff, P., and Barret, B.: Tropical tropospheric ozone and carbon monoxide distributions: characteristics, origins, and control factors, as seen by IAGOS and IASI. \*Atmos. Chem. Phys.\*, 23, 14039–14063, 2023 <https://doi.org/10.5194/acp-23-14039-2023>, 2023.](https://doi.org/10.5194/acp-23-14039-2023)
- [Tsuuzaki, K., Sato, H., Sato, K. and Nikaide, I.: Benchmarking principal component analysis for large scale single-cell RNA sequencing. \*Genome Biology\*, 21, 1–17, <https://doi.org/10.1186/s13059-019-1900-3>, 2020.](https://doi.org/10.1186/s13059-019-1900-3)
- 1435 Vakkari, V., Beukes, J.P., Laakso, H., Mabaso, D., Pienaar, J.J., Kulmala, M., Laakso, L., 2013. Long-term observations of aerosol size distributions in semi-clean and polluted savannah in South Africa. *Atmos. Chem. Phys.* 13, 1751–1770. <https://doi.org/10.5194/acp-13-1751-2013>, 2013.
- Vet, R., Artx, R. S., Carou, S., Shaw, M., Ro, C., Aas, W., Baker, A., Bowersox, V. C., Dentener, F., Galy-Lacaux, C., Hou, A., Pienaar, J.J., Gillet, R., Forti, M. C., Gromov, S., Hara, H., Khodzher, T., Mahowald, N. M., Nickovic, S., Rao, P. S. P., Reid, N. W.: A global assessment of precipitation chemistry and deposition of sulfur, nitrogen, sea salt, base cations, organic acids, acidity and pH, and phosphorus, *Atmos. Environ.* 93, 3–100, <https://doi.org/10.1016/j.atmosenv.2013.10.060>, 2014.
- 1440 Vitolo, C., Di Giuseppe, F., D'Andrea, M.: Caliver: an R package for CALibration and VERification of forest fire gridded model outputs, *PLoS ONE*, 13, 1–18, <https://doi.org/10.1371/journal.pone.0189419>, 2018.
- 1445 [Wang, H., Lu, X., Jacob, D. J., Cooper, O. R., Chang, K.-L., Li, K., Gao, M., Liu, Y., Sheng, B., Wu, K., Wu, T., Zhang, J., Sauvage, B., Nédélec, Blot, P. R., and Fan, S.: Global tropospheric ozone trends, attributions, and radiative impacts in 1995–2017: an integrated analysis using aircraft \(IAGOS\) observations, ozonesonde, and multi-decadal chemical model simulations. \*Atmos. Chem. Phys.\*, 22, 13753–13782, 2022 <https://doi.org/10.5194/acp-22-13753-2022>, 2022.](https://doi.org/10.5194/acp-22-13753-2022)
- Williams, J. E., Scheele, M. P., van Velthoven P. F. J., Cammas, J-P., Thouret V., Galy-Lacaux, C., Volz-Thomas, A.: The influence of biogenic emissions from Africa on tropical tropospheric ozone during 2006: a global modeling study, *Atmos. Chem. Phys.*, 9, 5729–5749, <https://doi.org/10.5194/acp-9-5729-2009>, 2009.
- 1450 Young, P. J., Archibald, A. T., Bowman, K. W., Lamarque, J.-F., Naik, V., Stevenson, D.S., Tilmes, S., Voulgarakis, A., Wild, O., Bergmann, D., Cameron-Smith, P., Cionni, I., Collins, W. J., Dalsøren, S. B., Doherty, R. M., Eyring, V., Faluvegi, G., Horowitz, L. W., Josse, B., Lee, Y. H., MacKenzie, I. A., Nagashima, T., Plummer, D. A., Righi, M., Rumbold, S. T., Skeie, R. B., Shindell, D. T., Strode, S. A., Sudo, K., Szopa, S. and Zeng, G.: Corrigendum to “Pre-industrial to end 21st century projections of tropospheric ozone from the Atmospheric Chemistry and Climate Model Intercomparison Project (ACCMIP)”, *Atmos. Chem. Phys.*, 13, 2063–2090, *Atmos. Chem. Phys.*, 13, 5401–5402. DOI: <https://doi.org/10.5194/acp-13-5401-2013>, 2013.
- 1455 Young, P. J., Naik, V., Fiore, A. M., Gaudel, A., Guo, J., Lin, M. Y., Neu, J. L., Parrish, D. D., Rieder, H. E., Schnell, J. L., Tilmes, S., Wild, O., Zhang, L., Ziemke, J., Brandt, J., Delcloo, A., Doherty, R. M., Geels, C., Hegglin, M. I., Hu, L., Im, U., Kumar, R., Luhar, A., Murray, L., Plummer, D., Rodriguez, J., Saiz-Lopez, A., Schultz, M. G., Woodhouse M. T., and Zeng G.: Tropospheric Ozone Assessment Report: Assessment of global-scale model performance for global and regional ozone distributions, variability, and trends, *Elem Sci Anth*, 6, 1–49, DOI: <https://doi.org/10.1525/elementa.265>, 2018.
- 1460 Zhang, Y., Cooper, O. R., Gaudel, A., Thompson, A. M., Nédélec, P., Ogino, S.-Y. and West, J. J.: Tropospheric ozone change from 1980 to 2010 dominated by equatorward redistribution of emissions. *Nature Geoscience* 9, 875–879, DOI: <https://doi.org/10.1038/ngeo2827>, 2016.
- 1465 Zunckel M., Venjonoka K., Pienaar J. J., Brunke E. G., Pretorius O., Koosiale A., Raghunandan A., van Tienhoven A. M., Surface ozone over southern Africa: synthesis of monitoring results during the cross-border air pollution impact assessment project. *Atmos Environ.* 38:6139–6147. doi:10.1016/j.atmosenv.2004.07.029, 2004.
- [Zwarts, L., Bijlsma, R. G., and Kamp, J.: Selection by Birds of Shrub and Tree Species in the Sahel, \*Ardea\*, 111, 143–174, <https://doi.org/10.5253/arde.2022.a20>, 2023.](https://doi.org/10.5253/arde.2022.a20) van Zyl, P.G., Jaars, K., Beukes, J.P., Pienaar, J.J., Fourie, G.D., van der Walt, H.J.,

- 1470 Mkhatshwa, G.V., van der Merwe, C. & Deacon, M.: Trace gases, Amersfoort, South Africa, [dataset], Aeris, <https://doi.org/10.25326/647>, 2024d.
- van Zyl, P.G., Jaars, K., Beukes, J.P., Pienaar, J.J., Fourie, G.D., van der Walt, H.J., Mkhatshwa, G.V., van der Merwe, C. & James, C.: Trace gases, Louis Trichardt, South Africa, [dataset], Aeris, <https://doi.org/10.25326/646>, 2024a.
- van Zyl, P.G., Jaars, K., Beukes, J.P., Pienaar, J.J., Fourie, G.D., van der Walt, H.J., Mkhatshwa, G.V., van der Merwe, C., Govender, N., Kubheka, W., Gardiner, E. & Tleane, J.: Trace gases, Skukuza, South Africa, [dataset], Aeris, <https://doi.org/10.25326/645>, 2024b.
- 1475 van Zyl, P.G., Jaars, K., Beukes, J.P., Pienaar, J.J., Labuschagne, C., Mkololo, T., Brunke, E.-G. & Joubert, W.: Trace gases, Cape Point, South Africa, [dataset], Aeris, <https://doi.org/10.25326/644>, 2024c.